DEPARTMENT OF DEFENCE
DEFENCE SCIENCE & TECHNOLOGY ORGANISATION
DSTO

Review of F-111 Structural Materials

T. Mills, G. Clark, C. Loader,
P.K. Sharp and R. Schmidt

DSTO-TR-1118

Review of F-111 Structural Materials

T. Mills, G. Clark, C. Loader, P.K. Sharp and R. Schmidt*

***Aerostructures Technologies, Pty. Ltd.**

Airframes and Engines Division
Aeronautical and Maritime Research Laboratory

DSTO-TR-1118

ABSTRACT

The RAAF is now the sole operator of the F-111 and current plans for the fleet will keep the aircraft in service until 2020. The F-111 is a structurally complex aircraft, and its swing-wing geometry in particular requires materials of ultra high strength to handle expected loadings. In particular, the D6ac steel used in most of the critical components in the aircraft was subjected to rigorous research efforts in the early 1970s to better characterise material performance in fatigue. This report summarises many of these efforts to characterise the main alloys in the airframe, namely: D6ac steel and aluminium alloys 2024-T851, 7079-T651, and 7075-T6. The major goal is to study the available data for these critical F-111 materials, evaluate the completeness of the existing data sets and make recommendations for research efforts necessary to ensure that the F-111 fleet is operated as safely and economically as possible until retired. Particular attention is payed to the fact that the RAAF now uses JP-8 fuel rather than the original JP-4 fuel. Short crack behaviour from corrosion damage will likely be a concern for the F-111, particularly in the D6ac steel. Stress corrosion cracking is likely to continue to be the biggest problem for the 7xxx-series aluminium alloy components and will have to be monitored carefully.

RELEASE LIMITATION

Approved for public release

DEPARTMENT OF DEFENCE
DEFENCE SCIENCE & TECHNOLOGY ORGANISATION
DSTO

Published by

DSTO Aeronautical and Maritime Research Laboratory
506 Lorimer St
Fishermans Bend Vic 3207 Australia

Telephone: (03) 9626 7000
Fax: (03) 9626 7999

AR-011-800
March 2001

APPROVED FOR PUBLIC RELEASE

Review of F-111 Structural Materials

Executive Summary

Safety by inspection has been the key to protecting the F-111 fleet since the early 1970s. The ageing of the F-111 fleet in conjunction with a significant increase in planned retirement date has presented a new challenge to the RAAF, namely: maintaining the level of safety from catastrophic failure while still being able to economically operate the fleet. Such a goal requires an in-depth understanding of the structure, materials, and possible failure modes. For instance, structural optimisation aimed to increase inspection intervals for critical structure (which will reduce the maintenance burden) should only be practiced if time-dependant failure modes, such as corrosion, will not become the new life-limiting scenario for that location. With this example in mind, it was imperative to review the literature and assess the state-of-knowledge associated with the F-111 structural materials and make recommendations as to what new information the RAAF may need to continue to meet safety and economic goals.

This report gives an overview of the more prominent structural materials in the F-111 aircraft. The most important materials are D6ac steel and 2024-T851 aluminium, in that all the fracture critical components are made from one of these two materials—mostly D6ac. Alloy 7079-T651 has also been included as it is widely used in bulkheads and is very susceptible to stress corrosion cracking.

One of the main objectives was to look at available literature data and compare it with the data used by Lockheed to perform the F-111 durability and damage tolerance analysis (DADTA). In some cases, literature data was so sparse that it was essentially limited to the same data sources used by Lockheed. The following observations were made from the review of the D6ac steel data:

- The long crack propagation data in the literature seems to agree well with that used by Lockheed.
- Crack nucleation studies are woefully deficient, mainly corrosion influences on fatigue. DSTO/AMRL has important programs in place to address this lack of useful data.
- Fatigue crack growth from corrosion pits is the area of primary concern because pitting is the most threatening form of corrosion to D6ac.
- Discrepancies between material models and laboratory behaviour of D6ac coupons indicate possible problems with either the near-threshold crack growth data, the validity of the stress intensity solution for small crack sizes, or both. It

may be necessary to revisit the material models and threshold crack growth data for D6ac if corrosion is to be accurately incorporated into life predictions.

- Particularly damaging to D6ac is the possibility of pitting leading to SCC before transitioning to fatigue or corrosion fatigue. Service examples of this scenario have been uncovered, and the unpredictable nature of SCC makes the situation potentially dangerous.
- In the F-111, stress corrosion cracks have been found perpendicular to the primary load axis, an orientation where interaction with fatigue is of significant risk. Locations where this could occur should be treated very carefully as inspection intervals in such areas could be rendered unconservative.
- Fatigue data for D6ac steel covers a variety of chemical environments including laboratory air, humid air, and JP-4 fuel. The F-111 now uses JP-8 fuel, which has different composition and additives, so it may be worth looking at crack propagation, SCC and threshold behaviour in this new chemical environment. The same could be said for aluminium alloy 2024-T851, the wing skin material.

No major concerns were raised about available fatigue data for the aluminium alloys found in the F-111. Aluminium alloys are much more widespread in the aircraft industry than D6ac steel; unfortunately, the aluminium alloys used in the F-111 are an exception.

- Alloy 7079-T651 is avoided in new aircraft. The alloy is no longer made, and as such is no longer included in most references for material property and selection.
- Alloy 2024 in the T851 temper used on the F-111 is relatively uncommon. Not much literature data was uncovered on this material, but what was found seems to be sufficient for managing the F-111.
- Aluminium alloy 2024-T851 has greatly increased stress corrosion and corrosion fatigue performance. However, the artificially aged variant is very susceptible to corrosion damage. Because of this, it is also vulnerable to fatigue originating from this type of damage.
- Programs at DSTO/AMRL and around the world are focused on finding ways to model corrosion damage as an engineering parameter for life prediction. DSTO/AMRL has several programs looking at different types of corrosion damage in various aircraft aluminium alloys. This should provide enough information without starting anything new specifically for the F-111.
- The same concerns for SCC in D6ac apply to the aluminium alloys, particularly the 7xxx-T6xx materials.
- Lockheed data in the fatigue crack growth threshold, as compared with literature data elsewhere, shows that the Lockheed values are conservative.

By better understanding the behaviour of the critical materials in the F-111, the safety of the fleet will be maintained or even improved. The informed decisions surrounding dealing with failure modes such as corrosion will allow the F-111 to be managed more economically. The ultimate benefit for the RAAF will be reduced aircraft down time and increased availability.

Authors

T. Mills
Aerostructures Technologies, Pty. Ltd.

Thomas Mills, Principal Engineer--Aerostructures, graduated from the University of Missouri in 1991 with a Bachelor of Science in Mechanical Engineering. Graduate studies earned him Master of Science and PhD degrees in Mechanical Engineering from the University of Utah, ending in 1997. From there, he joined the Air Force Research Laboratory, Wright-Patterson AFB Ohio, where for three years he researched both corrosion/fatigue interactions in aluminium and bonded composite repairs of aluminium aircraft structure. In April 2000, he moved to Australia to work for Aerostructures located at AMRL, Fishermans Bend where his primary responsibility is to incorporate corrosion into the damage tolerance assessment of the F-111 strike aircraft as part of the Sole Operator Program.

G. Clark
Airframes & Engines Division

Graham Clark, Principal Research Scientist, graduated from University of Cambridge in 1972 in natural Sciences. After completing research for a PhD on the growth of fatigue cracks at notches, undertook post-doctoral research at Cambridge on the detection and growth of cracks in submarine nuclear pressure vessels. In 1977 he commenced work at DSTO in Maribrynong, leading research on cracking in thick-walled pressure vessels, which developed a comprehensive fracture control plan for Australian manufactured ordnance and a capability of prediction ordnance fatigue lives. In 1984 he moved to Fishermans Bend, where he established a research program on the damage tolerance of thick carbon-fibre composite materials, involving modelling and experimental investigation of impact damage in aircraft materials. In his present position, he leads tasks which support defect assessment in ADF aircraft, NDI evaluation and fatigue crack growth research. He is also chairperson of the AMRL Accident Investigation Committee.

C. Loader
Airframes & Engines Division

Christopher Loader, Professional Officer, graduated from Monash University in 1998 with a Bachelor of Science majoring in Materials Science and Chemistry and a Bachelor of Engineering with Honours in Materials Engineering. Since arriving at Fishermans Bend two years ago, he has worked several programs aimed at better understanding corrosion-initiated fatigue in a variety of aluminium and steel alloys used in the aircraft industry.

P. Khan Sharp
Airframes & Engines Division

Khan Sharp, Research Scientist. Graduated from Monash University in 1987 having obtained a Materials Engineering Degree with Honours. In 1990, he completed a Masters of Engineering Science degree and commenced work in the Fatigue and Fracture Detection and Assessment area at Fishermans Bend. Over the past 10 years he has been involved in the metallurgical investigation of aircraft structures and components, fractographic analysis of fatigue surfaces and research into fatigue crack growth and fracture of aircraft materials. During that time he has published over 40 reports and papers. He has completed extensive research into novel methods of retarding crack growth and innovative NDI methods. In 1999, he was awarded a Research Scientist Fellowship to study at the US Air Force Research Laboratory. He presently manages the Structural Implications of Corrosion task and conducts research on fatigue and fracture.

Contents

1. Introduction: Design Implications on Material Selection

The F-111 aircraft was conceived as a low-level flight supersonic strike aircraft capable of terrain-following flight in all weather and visibility conditions. This in turn required some unique characteristics of the design, such as the variable sweep wings, which would provide the aerodynamic performance for low-altitude supersonic flight while allowing for take off and landing with a very high weapon load.

The design of the aircraft meant that all wing loads were transferred into the fuselage through the wing pivot mechanism. Furthermore, with the wing at a fully swept back position, the elevators in the empennage control not only the pitch of the aircraft, but also its roll. This means that rear fuselage of the aircraft has to withstand twisting as well as bending loads. The whole concept of the aircraft called for high strength materials in the airframe with high strength/weight and strength/volume ratios in the critical structural areas.

Early on in the design stage, it was decided to utilise ultra-high strength (UHS) steel for the structure-critical components, since it had better strength to weight properties than the aluminium alloys used traditionally (until then) [Wilson 1964]. Titanium alloys were considered for a brief period, but it was decided against their extensive use, due to their prohibitive cost and, at the time, limited manufacturers' experience. The steel that was selected was a medium-carbon low alloy Ladish Corporation steel designated D6ac.

Other common UHS steels were considered as well, including H11 and 4340V. However, D6ac showed comparable mechanical properties to the other candidates with the added benefits of better weldability, greater fracture toughness (although some hard lessons were learned on this subject later), stress corrosion resistance, and impact resistance at -54°C (-65°F) [McHenry and Key 1968]. The rest of the airframe was mostly made from 2024, 7075 and 7079 aluminium alloys, with only very limited use of more exotic alloys, such as titanium, or composite materials.

The wing skin material, in particular, received a lot of attention because of the high operating speeds and, therefore, temperatures of the F-111. Alloy 2024-T851 (which starts life as T351 and is then stress relieved and artificially aged to the T8 temper) showed lower strength at room temperature than 7075-T651 and 7079-T651, but the 2xxx-series alloy actually performed better at the higher temperatures encountered in F-111 operations. For components that experience their peak loading at lower temperature, General Dynamics (GD) used 7xxx-series alloys [McHenry and Key 1968].

The F-111 did not have particularly happy start to its service life, due to several structural failures both in-flight and during ground fatigue testing [Gunston 1987].

The cause of the failures was ultimately attributed to a large variation in fracture toughness of the D6ac steel, with the lower limit of the toughness values being unacceptably low. The initial defects were created, almost universally, during manufacture of the steel components. The low toughness of some components or even in some specific locations on individual components meant that only relatively short fatigue crack growth had to occur before the crack reached catastrophic length. In practice, the fatigue life of the aircraft was limited to several hundred flight hours.

The defects and sub-standard properties of the UHS D6ac steel prompted one of the most comprehensive metallurgical and crack growth investigations ever performed. During the course of the investigation, the causes of the failures were identified and new testing and inspection methods were developed to limit the extent of the initial flaws. The success of the recovery measures may be gauged from the fact that no more in-flight structural failures occurred.

As the F-111 aircraft stay longer in service, the airframe degradation from environmental attack takes on more significance. Furthermore, the interaction between corrosion and fatigue in airframe components is not well understood. The present method of dealing with corrosion defects, especially in critical areas, is their complete removal upon detection, but this approach is limited in several aspects. There is an obvious limit on how much material can be removed before the part's static strength is affected, and this approach is both time consuming and expensive. Therefore, if a better method of dealing with corrosion in the airframe components can be found, there is potential for considerable financial and time savings.

This report evaluates the metallic material data for the F-111 as well as the operational environment and service induced defects. One of the spin-offs of the very concentrated research effort was that large amount of data was generated. A part of this research was performed by DSTO at AMRL, but most of it was performed by, or on behalf of, General Dynamics, the manufacturer of the F-111 aircraft. However, as the structural problems were resolved, the research effort ceased, with the result that the most recent General Dynamics research data date from 1972. Likewise, the research activity at AMRL finished in 1978. Most of this data was never brought together in a single report or compared as to its accuracy and validity.

This report creates an overview of F-111 metallic material data and evaluates data originating from different sources. In the intervening years, our knowledge and understanding has also increased, which may require re-evaluation of some of the data in the light of the latest findings. The most recent material data comes from service and defect reports for individual aircraft. However, most of the data from the USAF is inaccessible, plus what data is available must be treated with caution due to different F-111 types operated by the USAF, and also different usage patterns and operating environments.

2. F-111 Materials

2.1 List of F-111 Metallic Materials

Lockheed Martin Tactical Aircraft Systems (LMTAS) identified 13 different materials in the critical locations in the F-111 structure [Ball and Doerfler 1996]. These materials are listed in Table 1. This report only covers D6ac steel and 2024-T8xx, 7079-T6xx and, to a lesser degree, 7075-T6xx aluminium alloys.

Table 1. List of F-111 metallic materials [Ball and Doerfler 1996].

Material Designation and heat treatment	Material
4330V	Steel
4340 200-220† HT	Steel
D6ac 220-240 HT	Steel
D6ac 260-280 HT	Steel
PH13-8Mo H1000	Stainless Steel
15-5 PH H925	Stainless Steel
PH15-7Mo Th1050	Stainless Steel
17-4PH H900	Stainless Steel
2014-T6	Aluminium
2024-T62	Aluminium
2024-T851	Aluminium
2024-T852	Aluminium
2124-T851	Aluminium
7075-T6	Aluminium
7075-T651	Aluminium
7079-T651	Aluminium
6Al-4V STA	Titanium

2.2 Classification of F-111 Structure

Critical parts of the airframe structure have been identified and graded, with Class I being the most critical. These definitions, taken from a General Dynamics (1970) report, are as follows:

- Class I: Parts whose failure in flight would most probably be catastrophic, resulting in a loss of an aircraft.
- Class IIA: Those Class II parts that are borderline between Class I and Class II and can be considered more serious than Class IIB.

† Refers to Ultimate Tensile Strength (UTS) range in ksi. Due to the large amount of data supplied by the USA, English units will be used in most cases.

- Class IIB: Parts whose failure in flight would be serious but most probably would not be catastrophic.
- Class III: Parts whose failure in flight is not considered to be catastrophic. (Landing Gear, High Lift and Secondary Structural Parts)

The Class I parts (26 in all) are identified in Tables 2 and 3. The nineteen Class IIA parts are shown in Table 4.

Table 2. Class I: Fifteen critical forgings, all D6ac Steel [General Dynamics 1970].

	Wing Pivot Fitting	
1	220-240ksi D6ac	12W475 Upper Plate
2	220-240ksi D6ac	12W476 Lower Plate - Pt 1. Fuel Flow Hole - Pt 2. Splice Bolt Hole - Pt 3. Surface - Pt 4. Surface - Pt 5. Surface
3	220-240ksi D6ac	12W477-21 Forward Web
4	220-240ksi D6ac	12W412 Shear Lug
5	260-280ksi D6ac	12W415 Wing Pivot Pin
	Wing Pivot Support Assembly	
6	220-240ksi D6ac	12B7313 CTB Outboard Bulkhead
7	220-240ksi D6ac	12B7314 CTB Aft Web
8	220-240ksi D6ac	12B7315 CTB Forward Outboard Web - Pt 1 Surface (upper) - Pt 2 Surface (lower)
	Station 496 Bulkhead	
9	220-240ksi D6ac	12B2910 Bulkhead Post
	Upper Longeron	
10	220-240ksi D6ac	12B1891 Upper Longeron
	Station 770 Bulkhead	
11	220-240ksi D6ac	12B10521 Outboard Bulkhead (Pistol Fitting)
12	220-240ksi D6ac	12B10520 Centre Bulkhead
13	220-240ksi D6ac	12B10523 Upper Frame
	Empennage	
14	220-240ksi D6ac	12T9600 Horizontal Tail Horn
15	220-240ksi D6ac	12T406 Rudder Torque Tube

Table 3: Class I: Eleven critical parts, other than forgings [General Dynamics 1970].

	Wing Pivot Fitting	
16	260-280ksi D6ac	12W472 Flanges, Shear Ring - (1) Front Spar Flange - (2) Rear Spar Flange - (3) Centre Spar Flange
17	220-240ksi D6ac	12W472 Webs, Welded - (1) Front Spar Web - (2) Rear Spar Web
18	220-240ksi D6ac	12W491 Plate, Front Spar
19	220-240ksi D6ac	12W492 Web, Aft Spar
20	220-240ksi D6ac	12W478 Shear Ring
	Wing Carry Through Box	
21	220-240ksi D6ac	12B7311 Upper Plate
22	220-240ksi D6ac	12B7312 Lower Plate
23	220-240ksi D6ac	12B7318 Actuator Support Bulkhead
24	220-240ksi D6ac	12B7331 Forward Access Door
	Wing Skin	
25	2024-T851	12W950 Upper Surface
26	2024-T851	12W951 Lower Surface

Table 4. Class IIA: Nineteen critical parts [General Dynamics 1970]

1	220-240 ksi D6ac	12B10503 Station 561 Lower Longeron Splice
2	260-280 ksi	12B1831 Station 459-571 Lower Longeron
3	220-240 ksi D6ac	12B2908 Station 496 Outboard Nacelle Former
4	220-240 ksi D6ac	12B2909 Station 496 Lower Nacelle Former
5	220-240 ksi D6ac	12B7319 CTB Truss
6	260-280 ksi	12B7351 CTB Forward Post
7	2024-T851	12W905 Wing Rear Spar
8	2024-T851	12W985 Web Forward Aux Spar
9	2024-T851	12W982 Splice Forward Aux Spar
10	2024-T851	12W961 Pivot Pylon Housing
11	2024-T6 forging	12W963 Pylon Housing
12	2024-T851	12W911 Wing Bulkhead 1.0
13	7075-T651	12B7333 CTB Aft Centre Door
14	2024-T851	12B2685 Station 460 Bulkhead
15	2024-T851 or 2024-T852 forging	12B10529 Aft Upper Longeron Cap
16	7079-T651	12B2760 Station 448 Bulkhead
17	6Al 4V Ti 160ksi	12W490 WPF Centre Spar
18	6Al 4V Ti 160ksi	12W984 Bracket Centre Spar
19	6Al 4V Ti 160ksi	12B3801 Shear Panel

3. D6ac Steel

The steel selection for structure critical components of the F-111 was made during 1964. Ladish Corporation D6ac steel was selected for the combination of mechanical properties, weldability, fatigue strength, toughness and stress corrosion resistance when heat-treated to 220 to 240 ksi strength range [Wilson 1964]. This steel was one of three candidate materials considered by General Dynamics at that time; the other two steels were 4330V high strength steel and H11 tool steel. The 4330V steel (which is a modified 4330 steel) was cleared for use in components whose thickness does not exceed 1½ inch; however, it is used only to a limited extent.

The composition of D6ac classes it into the same group as the commonly used high-strength low alloy (HSLA) 4340 steel. The differences in composition between D6ac, 4330V, 4340 and H11 steels are outlined in Table 5.

*Table 5. Composition of various high-strength steels considered for the F-111 [*Wilson 1964, **RAAF 1975].*

Element	D6ac* Wt%	4330V* Wt%	4340** Wt%	H11* Wt%
Carbon	0.42-0.48	0.28-0.33	0.38-0.40	0.38-0.43
Manganese	0.60-0.90	0.80-1.00	0.60-0.80	0.20-0.40
Silicon	0.15-0.30	0.20-0.35	0.20-0.35	0.80-1.00
Phosphorus	0.010 max.	0.015 max.	0.040 max.	0.015 max.
Sulphur	0.010 max.	0.015 max.	0.040 max	0.015 max.
Chromium	0.90-1.20	0.75-0.95	0.70-0.90	4.75-5.25
Molybdenum	0.90-1.10	0.35-0.50	0.20-0.30	1.20-1.40
Vanadium	0.07-0.15	0.05-0.10	-	0.40-0.60
Nickel	0.40-0.70	1.65-2.00	1.65-2.00	-
Iron	balance	balance	balance	balance

3.1 Heat Treatment

D6ac is used in the F-111 in parts fabricated from welded or bolted plate or in forgings. One of the reasons for the selection of this steel was its ability to through-harden in relatively thick sections; this also would minimise distortion during the heat treatment. During the development of the steel, it was noted that after austenitising at 900°C (1650°F), the steel might be held in the temperature interval of 482-579°C (900-1075°F) for extended periods of time without transformation. Therefore, a two-step quenching process was developed, which GD dubbed the 'Aus-Bay' treatment. The 'bay' refers to the unusually deep austenite bay in the TTT diagram for the steel, which allows a prolonged holding time prior to transformation. The intermediate temperature step allows effective reduction in the quench rates, which led to reduced

distortion of the steel. The original heat-treatment schedule specified by GD is outlined below [Wilson 1964]:

1. Austenitise at 1650 ° ± 25 °F (900 ° ± 13 °C)
2. Transfer immediately to a furnace at 950 °F (510 °C) (this is the Aus-Bay step) and hold until the temperature stabilises.
3. Quench into molten salt at 375 °F (190 °C) or hot oil at 140 °F (60 °C).
4. Air cool to 150 °F (66 °C).
5. Stress-relieve at 375 °F (190 °C) to 550 °F (288 °C) for two hours if there is to be any delay prior to tempering.
6. Double temper for two hours and air cool between tempers.

The D6ac was specified in two different tensile strength levels: 220-240 ksi (1516-1655 MPa) or 260-280 ksi (1793-1931 MPa), which were determined by the tempering temperature (Table 6).

Table 6. Tempering conditions and properties for D6ac steel [Little 1971].

1st Temper Temp. °F	2nd Temper Temp. °F	UTS ksi	YS ksi	Percent Elongation	Hardness Rc	Fracture Toughness @ 75 °F (ksi √in)
1000 min	1015 - 1060	220-240	190	12	46 - 49	80
550 min	550 - 700	260-280	215	7.5	50.5 - 53	58

In practice, the relatively complex heat treatment led to non-uniform microstructure, which resulted in a toughness values varying by a factor of three for the relatively narrow 220-240 ksi strength range [Ryan 1974]. The low toughness of some parts of the structure meant that only very small flaws could be tolerated. General Dynamics did not at first realise the serious implications of the large variation in toughness on the structural integrity of the D6ac components.

3.2 Chronology of Failures of D6ac Components

When the F-111 entered service with the USAF in the late 60s, a number of structural failures occurred in the D6ac components both during service and during full-scale fatigue testing. The first set of failures occurred from manufacturing flaws present in the components, with most of the cracks originating in boltholes for Taper-Lok fasteners. The failures occurred in the most critical components of the aircraft manufactured from the D6ac steel, namely in the Wing Carry Through Box (WCTB) and in the in the Wing Pivot Fittings (WPF). However, as the length of service of the F-111s increased, the failures originating from manufacturing flaws were replaced by failures caused by degradation of the material in service.

Difficulties with inspecting the WCTB, WPFs, and horizontal tails in the F-111, largely because of very small critical crack sizes, resulted in the development of the cold proof load test (CPLT) to prevent in-flight failures. The CPLT program has been through several phases to date and has induced failures in eleven aircraft on the ground (rather than in the air).

In its latest form, the CPLT involves maximum negative and positive g excursions at both minimum and maximum wing sweep at a temperature of -40°C. The principle of the CPLT is simple enough—the steel's toughness is significantly reduced at low temperatures, and, therefore, any failure should occur during the cold-proof load test rather than in service. The test thus allows a "safe" period in service before re-test, this period being based on the time required to grow a crack which just passes the CPLT to the size required to cause failure in service. General Dynamics also hoped that the proof load test would cause crack tip blunting and thus improve the load bearing capacity of the cracked component. However, Gunderson (1970) showed that crack tip blunting does not occur at room temperature, and it will certainly not occur at the reduced temperature of the cold proof load test.

In addition to the CPLT, Susans et al. (1982) reported that aircraft were subjected to a dummy CPLT test before being officially checked at the reduced temperature. This dummy test may have caused compressive yielding at room temperature, leading to several failures (discussed below). In terms of service problems related to plastic deformation, the room temperature test is more critical in this respect, because the yield stress increases with decreasing temperature.

Some of the more well documented failures and defects found in D6ac components are listed below. Many of these failures occurred during CPLT, some happened during the early airframe fatigue tests, and others—the ones that made the CPLT an absolute necessity—happened in flight. Dates and aircraft tail numbers are given where available.

3.2.1 In-flight Failures

The first documented in-flight failure for the F-111 was early in 1968. In this accident, an F111-A crashed during deployment in Vietnam due to a sudden catastrophic failure in the tailplane system. The origin of the failure was traced to a fatigue fracture of a welded joint in the power unit of the left tailplane [Gunston 1987]. This misfortune was repeated on 8 May 1968 when another aircraft was lost near Nellis AFB in the US for exactly the same reason. Unfortunately, it is not clear from the reference whether this component was made from D6ac steel.

The most familiar of all F-111 in-flight failures involved aircraft 67-049. Reaction to this accident was widespread throughout the US Air Force, the airframe contractor, and subcontractors alike. Fallout from the loss of this one aircraft shaped several programs in flight safety that continue today including, for the F-111 specifically, the

CPLT, and for USAF aircraft in general, the adoption of the damage tolerance design philosophy. The accident aircraft was an F-111A, which had accumulated just over 100 flight hours; it crashed on the Nellis AFB range on 22 December 1969.

During pull-up from a rocket-firing pass, a fatigue crack in the wing pivot fitting reached a catastrophic length, and the left wing separated from the aircraft. The crack formed in the 7.26 mm thick lower plate of the WPF from an initial manufacturing flaw 5.72 mm deep. The crack then grew a mere 0.44 mm by fatigue to a critical depth of 6.16 mm during the span of 104.6 flight hours [Buntin 1971]. At the time of failure, the crack had a total surface length of 23.6 mm. Of great concern in this catastrophic failure was both the very small depth of the critical flaw and the extremely short time of fatigue crack growth. The metallurgical investigation of the crack determined that the initial flaw was present in the steel from manufacture as evidenced by remnants of iron oxides and a decarburised zone on the flaw surface. The flaw most likely originated as a cooling crack that formed after the final forging cycle [Hinders 1970].

The failure of WPF on this aircraft resulted in the fleet being grounded. Aircraft were released for flight after being subjected to NDI as well as the CPLT. This process was known as the Recovery Program, and it involved testing at –40°C under two load conditions, -2.4 *g* and +7.33 *g*, at 56 degrees of wing sweep. Two other aircraft experienced failures under the Recovery Program; these will be discussed later.

3.2.2 Fatigue Test Failures

A fatigue test of the full aircraft was started in Fort Worth, Texas in August 1968. The WCTB of test article A4 failed after just 400 hours of testing, foreshadowing the in-flight failure with uncanny accuracy. The failure originated from a bolthole in the aft surface of the WCTB near the junction with the bottom plate. The failure was traced to poor manufacturing processes. First, the part suffered an arc burn from the electrode used to cadmium brush plate the steel. This generated a spot of locally high hardness that was abusively machined when an attempt was made to put a hole in the affected zone. The high heat generated by this machining created untempered martensite that subsequently cracked during the insertion of a Taper-Lok fastener [Hinders 1970]. General Dynamics concluded that the crack originated at manufacture because fuel sealant was observed to penetrate the first 1.02 mm of the fracture. This means that a crack of at least this length was present during application of the sealant. The untempered martensite was found to a depth of 127 μm from the hole surface with a region of higher hardness extending to a depth of 1.27 mm. The first 3 mm of crack growth was intergranular, and the final crack length was small, only 19 mm [General Dynamics 1968].

During a subsequent inspection of the WCTB A4, another crack was found in the attachment of the closure panel to the rear spar. To counter this hot spot, a gusset plate was installed to reduce the strains at this location in future test articles, and this modification also was retrofitted to in-service aircraft [Hinders 1970].

The WCTB continued to be no stranger to failures with the start of the next test. This test article, FW-1, developed a critical crack after 2800 hours [Sutherland]. While this was a grand improvement over 400 hours, it was by no means adequate. This failure originated from a hole placed at the junction of a chord-wise and span-wise stiffening element in the lower plate. The hole was used to mount a hydraulic line, and the surface of the hole contained sharp indentations from grit blasting. Again, the crack was quite small, only 8.9 mm deep by 15.2 mm long (including the hole diameter). To solve this problem, Taper-Loks were installed on existing aircraft, and future aircraft had the holes removed altogether. In view of the superior performance of Taper-Loks, virtually every hole below the neutral axis of the WCTB was refitted with these fasteners [Hinders 1970].

Trouble continued with article FW-2. In June 1969, at 7800 hours, this WCTB suffered a catastrophic failure in the outboard closure bulkhead. The final crack size was a mere 1.77 mm deep by 19.05 mm long. The crack originated from the return flange of the bulkhead at the rear spar. Strain surveys of the area on the static test vehicle showed very high gradients at the ends of the flange where it connected to the front and rear spars. This problem was solved by simply removing two bolts at the spars, which allowed the upper plate to flex slightly relative to the box [Hinders 1970].

A fourth WCTB was pressed into service shortly after, and it incorporated all the changes that resulted from the first three experiences. At the time of Hinders' writing, the box had successfully completed 20 000 spectrum hours, the goal being 24 000 [Hinders 1970].

3.2.3 Proof Test Failures

The Cold Proof Load Tests (CPLT) mentioned earlier has been used extensively to ensure the flight safety of the F-111. Starting with the Recovery Program after the 1969 aircraft crash, the CPLT system has moved through several iterations. The idea of the proof test is to subject the WCTB and the empennage to high loads at low temperature to ensure that gross flaws do not exist in the critical structure. By testing at low temperature, the critical crack size is reduced, so if the structure survives the CPLT, then it is very unlikely to fail at service temperature.

As mentioned earlier, General Dynamics initiated the Recovery Program to clear grounded aircraft for flight. Two aircraft suffered failures during this phase of CPLT.

The first was an F-111E in 1970 [Laffe and Sutherland 1994]. The left hand horizontal tail pivot shaft failed at 88% of the maximum load applied in the Cold Proof Load Test (CPLT) at the Fort Worth test facility [Buntin 1971]. Post failure investigation revealed a local area that was improperly heat-treated.

Shortly thereafter in 1971, another Recovery Program aircraft suffered catastrophic failure, this time in the lower plate of the WCTB. This failure occurred in an F-111A at the Sacramento Air Logistics Center (SM-ALC). The crack completely ruptured the lower plate along with the front and rear spars. This failure emanated from a stress corrosion crack at a Taper-Lok hole that most likely resulted from improper cleaning during assembly [Laffe and Sutherland 1994]. The failure occurred at 57.5% of the maximum +7.3 *g* load [Buntin 1971].

Along with the Recovery Program, General Dynamics also started the Production Proof Test Program that affected every aircraft produced after the 1969 grounding. None of these aircraft suffered failures during the program, but more failures started showing up after the start of the Phase II Structural Inspection Program (II-SIP). The II-SIP effort marked the second application of proof testing to the F-111 fleet. It started in 1973 and ended a decade later. This program was essentially the same as the Recovery Program, but a third test condition was added over the original two. In II-SIP, in addition to the 56-degree sweep angle, the maximum +7.33 *g* load was repeated at minimum wing sweep, 26 degrees. This was done to induce still higher stresses in the WCTB lower plate. The failures are described below.

In 1973, USAF F-111A 66-023 suffered a non-catastrophic failure in the horizontal stabiliser pivot shaft fitting [Findley and Sutherland 1982]. The fatigue crack started from a lap created during hammer peening of the shaft fitting. In an attempt to avoid repeat failures of this component during CPLT, mandatory pre-test inspections were put into place [Laffe and Sutherland 1994].

In May 1978, another non-catastrophic failure occurred, this time in the upper WCTB plate of USAF FB-111A 68-292 [Findley and Sutherland 1982]. Several small fatigue cracks formed at a sealant injection hole in the plate. The hole had been damaged when a drill bit broke off during manufacture. More damage had been created during attempts to remove the detached portion of the drill bit. Again, a mandatory pre-CPLT NDI scheme was put into place for all such holes in highly stressed areas of the WCTB [Laffe and Sutherland 1994].

As part of the F-111A to F-111C Conversion Program for the RAAF, four ex-USAF aircraft were subjected to the CPLT. The first aircraft tested served in the USAF as 67-112 and entered RAAF service as A8-112; the upper plate of the WPF catastrophically failed during the 1981 test [Laffe and Sutherland 1994]. The failure originated at fatigue cracks in number 2 stiffener runout. Since the upper plate is a compression-dominated component during all but negative *g* flight manoeuvres, the failure was quite unusual. Findley and Sutherland postulated that the initial damage occurred upon application of high positive *g* loads, which resulted in localised compressive yielding in the upper plate at the stiffener runout. This damage generated a residual tensile stress in the surface region of the stiffener runout, which led to fatigue cracking. This failure resulted in fleet-wide inspections followed by regularly scheduled inspections in depot [Findley and Sutherland 1982].

In August 1982, a repeat failure of the upper WPF plate occurred in A8-129 during CPLT [Cox *et al.* 1983]. The crack propagation was associated with positive *g* excursions when the upper plate was under net compressive loading. Negative *g* load excursions were observed to mark the fracture surface, but did not significantly contribute towards the crack growth. This failure resulted in revisions to the inspection process developed after the first WPF failure. In addition, the RAAF elected to install boron doubler reinforcements on their remaining F-111C aircraft.

Phase III of the Structural Inspection Program (III-SIP) began in 1986 and marked the third round of CPLT cycles on the F-111 fleet. The original three load cases from the Recovery and II-SIP Programs were used in III-SIP with the addition of a -3.0 *g* load case at 26 degrees of wing sweep. This test condition evolved from the CPLT failures of RAAF aircraft a few years earlier. This case was added to cover increased compressive load in the upper plate of the WPF during high-*g* manoeuvres.

The III-SIP operation proved busy with five major component failures. During this third phase, an EF-111A from the USAF suffered a horizontal stabiliser pivot shaft fitting failure. This occurred in 1987 and happened to come from an area just outside the region normally inspected prior to CPLT. The configuration of this component was unique to early production EF-111A aircraft [Laffe and Sutherland 1994].

The next aircraft failed in 1988. Again the culprit was a horizontal stabiliser pivot shaft fitting; this time the aircraft was an F-111E, and the cause was a stress corrosion crack. The damage formed at a tooling hole in the top of the fitting. This location was added to the inspection package for future programmed depot maintenance (PDM) [Laffe and Sutherland 1994].

Also in 1988, an F-111A lost a WCTB upper plate after catastrophic failure of a fatigue crack emanating from a sealant injection hole. The crack had been found during the pre-CPLT inspection, but the information was lost due to an administrative error, so no repair was ever completed [Laffe and Sutherland 1994].

The next failure in III-SIP did not occur until 1991, this time in a RAAF aircraft. An F-111C horizontal stabiliser pivot shaft fitting failed from a fatigue crack located at the same upper tooling hole that contained the SCC crack in the 1988 F-111E failure. This location had been inspected using mag-rubber before the CPLT, but the configuration of the hole and some machining marks not only contributed to the presence of the crack, but masked its presence as well. The holes have since been reworked to increase inspectability [Laffe and Sutherland 1994].

The last failure under III-SIP occurred in 1991. This time, an EF-111A experienced catastrophic failure of the WCTB. The failure was unusual and only affected the EF-111A configuration. In this case, a fatigue crack formed in a lower plate stiffener at an area of mechanical damage. The damage resulted from impact with a bolt head

located on the upper surface of the upper inlet structure. This most likely occurred during production [Laffe and Sutherland 1994].

3.2.4 Other Cases and Observations

The previous discussions focused on incidents that resulted in substantial failures. The host of inspection programs that came from trouble shooting these major failures did successfully prevent some other serious accidents or, at least, CPLT failures. For instance, cracks were found in the now-familiar No. 2 stiffener runout in the upper WPF of two Australian F-111Cs (A8-148 and A8-109) [Cox 1985]. In both cases the cracks initiated from corrosion pits and the initial fracture was intergranular before developing into a more typical striated fatigue crack. However, the extent of the intergranular fracture was only one grain deep and did not contribute significantly to the overall crack length. The intergranular crack growth probably occurred by a SCC mechanism. The fracture in A8-109 started from three separate pits, and the cracks initially grew at approximately the same rate before joining together to form one large crack.

In a similar incident, an examination of USAF F-111E (68-043) WCTB in 1991 revealed two cracks in the upper plate. These cracks originated from pitting corrosion in Taper-Lok holes [Nguyen 1991]. The fracture mode was predominantly intergranular and was attributed to stress corrosion cracking. In some regions of the crack front there was no evidence of fatigue crack growth, and where present, the fatigue region was still extremely short (~40 μm long). In this instance, the cracks were found during a teardown inspection of the WCTB after 4239 flight hours. The same WCTB also contained tears in the threads Sealant Injection Holes located in the lower plate. The tears originated from a poor machining practice, which resulted in a local overheating and created untempered (white) martensite. However, the tears were not observed to develop into fatigue cracks.

A clearer picture as to the origin and mode of cracking observed in the critical D6ac components is emerging. Up to the 1980s, the failures and cracks originated from flaws generated or left over from the manufacture of the components. A number of these failures occurred in the CPLT, thus preventing almost certain in-flight catastrophic structural failures. Some of the internal reports generated by General Dynamics are very critical of the manufacturing methods employed in construction of the F-111. The Australian F-111C certainly were not immune to the manufacturing difficulties, and their WCTBs were 'manufactured when production standards were poor and quality control even worse [General Dynamics 1968]'. It is not likely that so long after commissioning of the plane the manufacturing defects should play a role in being the primary cause of failure, but they may initiate other defects. The progressive breakdown of the protective schemes may allow environmental attack in places that were previously protected and initiate, for example, stress corrosion cracking.

Since the early 1980s, most of the cracks were observed to originate from damage sustained in service, either in the form of pitting corrosion or compressive overload. Intergranular SCC sometimes followed the pitting corrosion, before developing into a fatigue crack. The presence and extent of SCC most likely depended on the local stress distribution, and whether the static loading was higher than the dynamic or vice versa. Another cracking mechanism originated from the compressive overload, which resulted in localised compressive yielding. Upon removal of the compressive load, the yielded areas contained residual tensile stresses of sufficient magnitude to initiate and propagate SCC and/or fatigue cracks.

3.3 Rectification of Structural D6ac Problems

Through the course of failure investigations on the F-111, it became apparent that significant changes in design, manufacture, and inspection would be necessary if the safety of the fleet was to be assured. These changes took the form of tightened quality control in manufacture, use of Taper-Lok fasteners, supplementary research and testing programs, improved NDI inspection methods, such as magnetic rubber, and the use of the cold proof load test, which was ideally an NDI technique, but occasionally proved to be otherwise. The CPLT and its associated advantages and disadvantages have already been discussed above and will not be covered further in this section.

3.3.1 NDI of D6ac

During the investigation of the loss of aircraft 67-049, it was discovered that the NDI processes used during manufacture were woefully inadequate, as they allowed a WCTB structure to enter service that contained a severe manufacturing defect. The procedures involved pulse echo ultrasound, magnaflux, as well as x-ray of weldments [Hinders 1970].

The first problem was that the ultrasound was not designed to pick up a flaw in the orientation of the one that caused the crash of 67-049. From this shortcoming came delta-scan ultrasonic that, using both a transmitting and receiving transducer, was able to pick up flaws similar to the one in the accident aircraft regardless of orientation [Hinders 1970].

Secondly, the magnaflux technique used originally did not have a powerful enough magnetic field to cause migration of the iron particles to flaws [Hinders 1970]. Again, this was addressed, and a modified process, using magnetic rubber particle inspection, is now the standard NDI technique for some 50 directed inspection locations on the F-111. It can find cracks as small as 0.020 inch (0.5 mm), and can also point out scratches, tool marks, and corrosion pits [Sutherland].

3.3.2 Taper-Lok Fasteners

Better NDI evaluation of the existing structure was merely the first line of defence in protecting the F-111s. Enhanced structural modifications, such as expanded use of Taper-Lok bolts, were implemented.

Taper-Lok bolts were common in the assembly of the WCTB and other D6ac components. They were originally developed for use in fuel sealing applications, but their beneficial effect on fatigue life, a result of reduced stress concentration through complete hole-fill, was soon realised. The bolts were installed with a predetermined amount of interference, which required a very high degree of accuracy for the hole. Too little interference, and the fatigue benefit diminished, too much interference caused tensile stresses that could lead to stress corrosion cracking from the hole [Smith].

Several early structural failures were linked in some way with hole preparation in the WCTB, some from Taper-Lok bolt holes. Still, other holes were problematic as well, and the fatigue benefit of using Taper-Loks was applied to these other locations. So successful were the Taper-Loks, it was decided to use these fasteners in virtually every hole below the neutral axis in the WCTB [Hinders 1970].

As alluded to above, the fatigue benefits were only realised if utmost care was used during assembly or modification, so their use came with a price. Many bolts, especially in the WCTB, were incorrectly assembled, with many bolt heads protruding too far from the surface. Recommended actions to remedy this problem and others included 100% inspection of Taper-Lok holes and rework of damaged holes where necessary [General Dynamics 1968]. The new and reworked holes underwent numerous tests and observations. First, holes were prestressed with a Taper-Lok bolt for 12 hours. Then the holes were inspected using assisted visual NDI (10x magnification) for evidence of tool marks and discolouration, and smoothness was established using a profilometer. Finally, NDI was used to check for cracks, and all questionable holes were further examined with a wax film. Together with the improved inspection procedures, better training was given to production and inspection personnel.

Obviously, the aircraft to receive the most benefit from this inspection program were the ones not yet built. The WCTB is the heart of the F-111's structure; it was not designed with safety-by-inspection in mind. By no means was this structure ever envisioned to require such heavy rework, and so this was not easily accomplished short of complete teardown. As such, since the Australian F-111Cs were already assembled, it appears that only 80 of the 286 Taper-Lok holes were re-inspected or repaired in those aircraft [General Dynamics 1968]. The reasons cited by General Dynamics were:

- The 80 holes were the only ones available for inspection without major disassembly of the aircraft.
- The inspection was based on the failure of the A4 test article, and the failure was confined to the highest stressed area.
- General Dynamics (intuitively) predicted that there is less likelihood of production errors in making Taper-Lok holes in thicker sections.

3.3.3 Cadmium Plating

Most of the D6ac surfaces open to environment are cadmium plated and usually painted with an undercoat and sometimes topcoat. The only exceptions are mating surfaces, where the presence of the coating would interfere with the operation of the part and probably wear away very quickly.

While this system is highly effective in protecting the metal from corrosion, it can also degrade the steel if applied incorrectly, through hydrogen embrittlement. Certain process settings in cadmium plating can generate hydrogen, which enters the steel and weakens lattice bonds. Fortunately, the high diffusivity of hydrogen, combined with the permeability of the cadmium plating allow the hydrogen to diffuse out of the steel if sufficient time is allowed. The diffusion process and corresponding loss of hydrogen is faster at higher temperatures.

The protection offered by Cd plating is vulnerable to local breakdown of the coating. D6ac becomes especially prone to corrosion pitting where the cadmium plating has been damaged, as evidenced by discovery of this damage on several F-111 aircraft [Cox 1985, Nguyen 1991]. In fact, corrosion pits are driven to a much deeper, structurally threatening depth when they occur from degraded local areas of the plating than when they occur in an unprotected component.

In past cases where the plating had broken down, repairs to the cadmium plating were achieved by "brush plating" method. Service experience also indicates that the brush plating is not as effective as the original plating, and corrosion recurs. This may not be related to any deficiencies in the plating process, but perhaps to the difficulties associated with the removal of corrosion product and cleaning of the surface. Some corrosion occurs in very inaccessible locations, where complete removal of the corrosion and its products is very hard to verify [General Dynamics 1968].

3.3.4 The "Humphries" Specimens

In another project to better understand the behaviour of D6ac steel, General Dynamics instituted a testing program using structural 'Humphries' specimen, which simulated D6ac assemblies with Taper-Lok bolts. The Humphries specimens essentially consisted of a central H-profile girder made from the D6ac steel and side-plates or 'doors' made from 7075-T6 aluminium alloy [Nankivell 1972]. The Al plates were attached to the central section by 37 Taper-Lok bolts.

During the testing of the Humphries specimens at AMRL, a number of foreign substances were found in the boltholes. These were thought to originate during manufacture from the breakdown of various coolants and cutting fluids. General Dynamics/Convair Aerospace Division in the U.S. manufactured the Humphries specimens using the same procedures used in the manufacture of the F-111. It was feared that the boltholes in the aircraft also contained remnants of similar foreign substances that may negatively affect fatigue life. An attempt was made to analyse the remnants of foreign substances in Taper-Lok holes in the Australian F-111, but due to limitation of the detection techniques, no conclusive results were obtained [Wilson 1973].

The substances that were found in the boltholes of the Humphries specimens included water, phosphine, trichlorethylene (C_2HCl_3) and some other polychlorinated hydrocarbons such as $C_4H_2Cl_4$, $C_5H_5Cl_5$ and C_4Cl_6. These substances led to corrosion fatigue originating from the boltholes, which substantially reduced the fatigue life.

Water was deemed to be the most serious substance detected in the holes, due to its deleterious effect on fatigue life [Nankivell 1972]. It was retained in the holes two years after assembly, but gradual drying out of the Humphries specimens occurred over the two-year testing period. It is unlikely that any of the foreign substances originating from the aircraft manufacture would be present in the F-111s after 25 years of service.

3.4 Toughness of D6ac Steel

The toughness of the D6ac steel was found to vary by a factor of three without a corresponding variation in tensile strength [Ryan 1974]. The variation in toughness arose from the different martensitic structures obtained from different quench rates. The effect of quenching on the final toughness of the D6ac steel was first observed by Gunderson (1970), who studied the effect of quenching on the mechanical properties of the WCTB. Gunderson determined that the quench bath used in the production of the WCTB was too small and could not deliver the desired cooling rate from the austenitising temperature.

Ryan (1984) performed a more detailed study of the quench medium on toughness and microstructure. Ryan studied quenching from the austenitising temperature into oil at 60°C (140°F), hot salt bath at 210°C (410°F), and air-cooling. The different quenching rates resulted in a different form of martensite being present in each case. The fine scale microstructural differences could be only resolved by electron microscopy; optical microscopy proved to have insufficient resolution. In the air-cooled samples, the martensite was lath-type, with carbides forming a continuous layer on the lath boundaries. This microstructure had the lowest toughness, presumably because the brittle carbide provided continuous crack paths. The oil quenching produced plate-type micro-twinned martensite with discrete carbide

particles much more uniformly dispersed throughout the microstructure. Correspondingly, the oil-quenched steel had the highest toughness. The salt bath quench resulted in an intermediate cooling rate, and the toughness was distributed between the two extremes provided by oil quenching and air-cooling. Unfortunately, General Dynamics originally specified either oil quench or a heated salt bath quench as an acceptable practice [Wilson 1964], and, therefore, many parts displayed large variation in toughness.

General Dynamics detected similar variation in toughness in large (2'x 3') quenched plates, and associated it to variation in quench rates between the edges and centre of the plate. However, Feddersen et al. (1972), who studied additional plates, found that the results were not as consistent as originally thought, due to a high inter-plate variability in toughness. Figure 1 shows the hypothesised isotoughness lines in the plate superimposed with actual toughness values from tests. They attributed the variation in toughness to three factors:

- inherent material variations,
- within-the-part quenching variations, and
- thickness effects.

However, no attempt was made to link the toughness variation to the microstructure.

To rectify the problem with variation in toughness, an improved heat treatment procedure was developed, where the austenitisation temperature was increased from 1650°F to 1700°F and only oil quench was used [Morrow and Hales 1973].

It may be concluded that the variation in toughness detected in many of the D6ac components resulted from a combination of insufficient quench rate provided by the hot salt quench and quenching of large components where the quench rate varied between the edges and centre. Once the large variation in toughness became known, General Dynamics discontinued the use of the salt bath quench, and oil quenching became the only acceptable practice. However, very little could be done about quenching large components with resulting edge to centre quench rate variation.

Feddersen et al. (1972) also studied the effect of test temperature on the fracture toughness. The toughness generally increases with temperature up to 38-66°C (100-150°F) for high toughness plate and forgings, from where it levels off. In low toughness plate, the toughness becomes constant at temperature >66°C (150°F), and in low toughness forgings the levelling off was not observed at all up to 149°C (300°F) (the maximum test temperature reported). The effect of temperature on toughness of plates of various fracture toughness is illustrated in Figure 2. Additional data on the variation in toughness with temperature may be found in Feddersen's report. The decrease in fracture toughness with decreasing temperature was also utilised in the Cold Proof Load Test, where the critical fracture toughness is reached at smaller crack sizes than would be required in normal service, therefore ensuring that surviving cracks are innocuous.

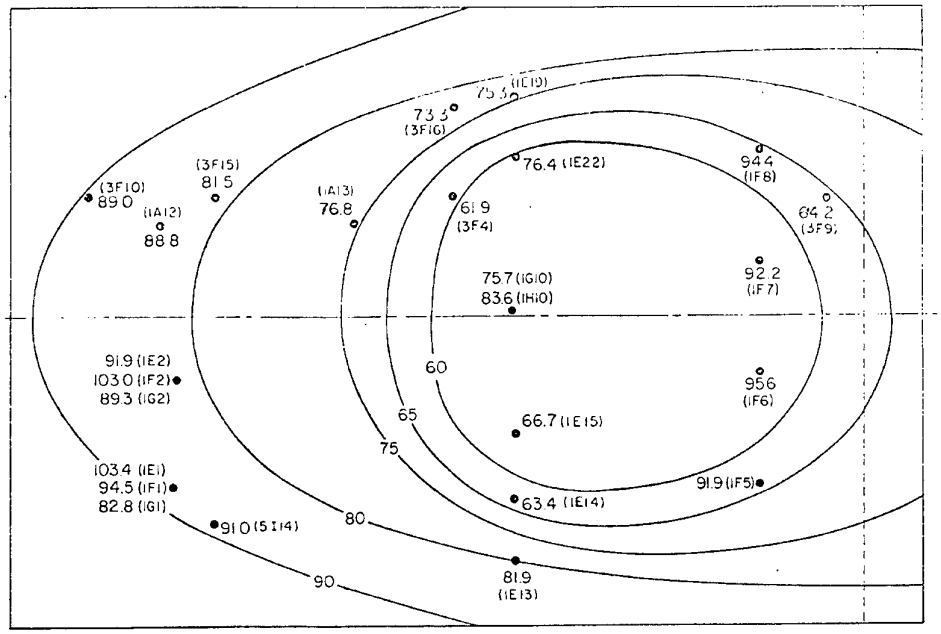

Figure 1. Iso-toughness map of 2'x3' plate generated by General Dynamics with extra toughness measurements, after Feddersen et al. (1972).

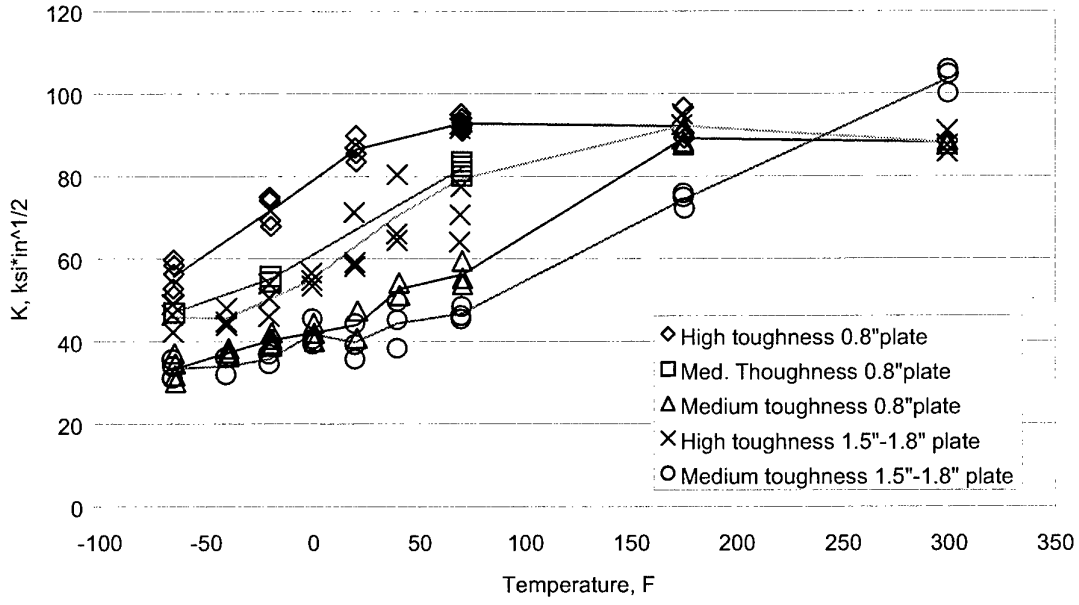

Figure 2. Variation in fracture toughness with test temperature for plates of medium and high toughness at two different thicknesses [Feddersen et al. 1972].

3.5 Fatigue Crack Nucleation and Corrosion Pitting

The failure of the WPFs on the Australian F-111 from fatigue cracks that originated at corrosion pits indicates that pitting creates a significant initial flaw. Information on pitting in D6ac appears to be sparse, particularly in conjunction with effects on fatigue. Considering this, it is imperative that methods for assessing the impact of pitting corrosion on fatigue life be developed. Fortunately, DSTO is well positioned to provide a wealth of useful information in this topic, as several programs are already established to address this failure mode.

Kendall (1971) observed pitting behaviour of D6ac in distilled water and in 3.5%NaCl solution. In distilled water, the pits grew to a maximum depth of approximately 30 μm in 24 hours before general corrosion set in. In 3.5% NaCl solution, the pits grew to a maximum depth of approximately 4 μm in less than 8 hours before general corrosion started. In this respect, the distilled water is a more dangerous environment because it generates larger pits. All environments that created pitting corrosion also generated crevice corrosion.

D6ac self passivates in a 0.05% $Na_2Cr_2O_7$ inhibitor and Oaklite Fleetline JC-5. Even though these two inhibitors prevented general corrosion, they allowed crevice corrosion. The taper-reamed holes were slightly more susceptible to crevice corrosion than drilled holes.

Kendall (1971) examined the general corrosion of four-hole D6ac steel specimens with different surface finishes on the specimen top surface and in the holes. He found that the polished top surface was more susceptible to corrosion than the holes. The surface finish of the holes (taper-reamed *versus* drilled) did not have any effect on general corrosion; however, the taper-reamed holes were slightly more susceptible to crevice corrosion. Presence of water created the most aggressive corrosive environment. Isopropyl alcohol, WD-40, Texaco Clear Tex 140 and ethyl acetate were found to be inert.

Distilled water and 3.5%NaCl solution formed pits in a shape of "circular holes" [Kendall 1971]. The "circular hole" terminology is somewhat unfortunate, because it does not adequately describe the shape of the pits. However, the description of the pitting is consistent with a recent observation of laboratory-generated pits, which were cylindrical with flat bottom [Loader 2000]. These flat-bottom pits were grown during corrosion protocol development for an on-going AMRL research program investigating pitting and fatigue interactions in D6ac. The unexpected shape was attributed to a particularly high corrosion current under galvanic conditions. Subsequent refinement of the procedure produced pits with more conventional elliptical or hemi-spherical shapes as shown in Figure 3.

The electrochemical process used by AMRL developed pits up to 70 μm deep in D6ac without causing general attack damage to the rest of the material. The electrochemical

technique was necessary because the specimens being used in this program were not cadmium plated. If corrosion was allowed to develop naturally in the unplated material, it would be more general in nature with minimal pit depths.

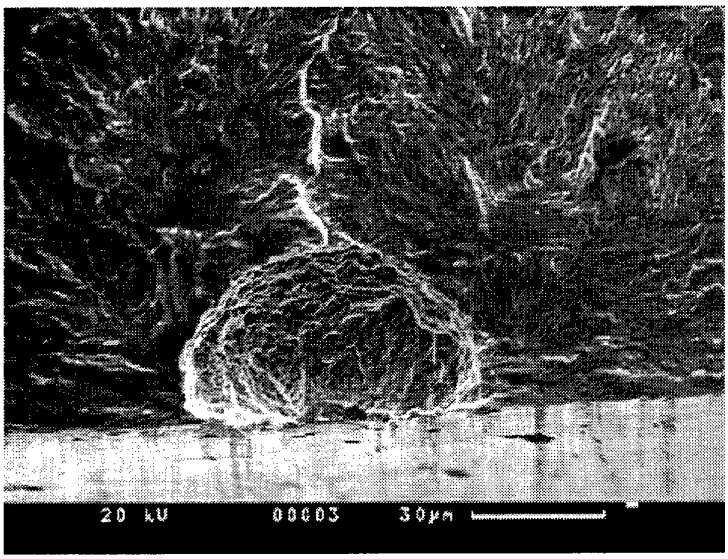

Figure 3. Typical electrochemically grown corrosion pit in D6ac Steel (AMRL fractograph).

The damage created electrochemically represents a morphology associated with local breakdown in cadmium protection as would happen on the F-111 structure. This latter type of damage morphology has been seen in service [Cox 1985].

Service experience shows that pits can develop stress corrosion and/or fatigue cracks. The limited amount of research into such mechanisms in D6ac steel requires intensive measures to ensure safety. The present practice adopted by the RAAF whenever pitting is detected in any D6ac components is to remove it completely, or, where the extent of corrosion is too large, replace the component. This approach is both time consuming and costly, and may lead to damage generated by the removal process itself. Secondly, there is a practical limit to material rework before reduced section thickness infringes on the required load bearing capacity of the structure and further removal becomes untenable.

As mentioned earlier, AMRL and the RAAF recognise the potential seriousness of pitting corrosion in this material and are actively acquiring a better understanding of pitting corrosion and its impact on stress-based failure modes, such as fatigue and SCC.

3.6 Fatigue Crack Growth Behaviour

The initial flight-critical component failures that occurred much earlier in the life of the F-111 prompted one of the most comprehensive fatigue crack investigations in history [Feddersen *et al.* 1972] and provided a significant database on D6ac fatigue properties. That data forms an important input to this report, since it is essential that the crack growth data be only obtained from the steel processed in a same manner as the steel that was used in the F-111s. [D6ac steel is still used in aerospace applications, most notably in the space shuttle, but the processing methods and the properties of the steel have changed, and the data is most likely not directly applicable.]

All data presented in this section were obtained from constant amplitude tests. Three major influences on crack growth behaviour in D6ac have been characterised, namely: variations in material properties, load profile (stress ratio and frequency), and environment (both chemical and temperature).

Many variable amplitude fatigue tests also were performed during the initial material evaluation and when the early failures in D6ac occurred. However, the crack rate is generally lower in variable amplitude tests, and, therefore, the constant amplitude tests present the worst-case scenario.

3.6.1 Impact of Toughness and Material Form on FCG Behaviour

The major material variable affecting the D6ac fatigue was its fracture toughness. The effect of fracture toughness on crack growth rate is portrayed in Figure 4. The toughness does not have any effect on the steady state (Stage II) crack propagation rate, but it affects the onset of catastrophic failure (indicated by arrows in Fig. 4). For a low toughness material, the catastrophic crack growth occurs either at shorter crack length or at a lower stress intensity for a given crack length. This is one of the reasons why some of the catastrophic failures in the F-111 D6ac components occurred at very low flight hours from very small initial defects.

The form of the D6ac, i.e. forging *versus* rolled plate, had very little effect on the crack growth rate. Feddersen *et al.* (1972) observed slightly better performance from forgings than from the plate in a few instances.

3.6.2 Impact of Variations in Load and Environment on FCG Behaviour

Fatigue crack growth rate in dry/laboratory air constitutes the baseline data against which the accelerating effect of a more aggressive environment may be compared. The crack growth rate for different stress ratios is plotted in Figure 5 [Ball and Doerfler 1996]. The upper and lower limits encompassing all the data are also plotted in the figure (as well as Figures 6-7 and Figures 9-15). These limits are subsequently reproduced in all following da/dN vs. ΔK plots to portray the fit of the data and to highlight the effect of the test or environmental variables on the crack growth rate.

Further crack growth data in dry air (from a different source) are plotted in Figure 6 [Paris *et al.* 1972].

The crack growth rate for a high humidity air is plotted in Figure 7. The data for humid air and dry air for two different stress ratios are compared in Figure 8. The humid air does not seem to have any noticeable effect on the rate of crack propagation.

The effect of JP-4 fuel on crack propagation may be seen in Figure 9. Despite the considerable scatter contained in the data, no clear evidence indicates that water saturated JP-4 fuel accelerates the crack growth over the crack growth observed in a dry air environment.

Figures 10, 11 and 12 portray the effect of distilled water on crack growth for R equal to 0.1, 0.3 and 0.5 respectively. Most of the data falls within the limits provided by dry environment, but remain near the upper boundary. The effect of loading frequency is seen clearly in these graphs. The lowest frequency, 0.1 Hz, which allows the longest time for the environmental attack to occur during each loading cycle, always results in the fastest crack growth rate.

Figures 13, 14 and 15 portray the effect of temperature on crack growth rate in 50% R.H. air, 3.5% NaCl solution, water-saturated JP-4 fuel and distilled water respectively. Temperature does not have any effect on crack growth rate in the 50 % R.H. air, but the growth rate is significantly increased in high temperature (79°C, 175°F) 3.5%NaCl solution. There is some effect of temperature on the crack growth in water-saturated JP-4 fuel, but it is not very pronounced. In distilled water, the growth is faster at high (79°C, 175°F) temperature.

The fatigue crack growth rates for plate and forgings in various environments and under various test conditions as measured by Feddersen *et al.* (1972) are summarised in a somewhat different format in Figure 16. The crack growth is slowest in the inert environment (dry air) and independent of test frequency. The stress ratio has some influence on the crack growth rate, but its effect is not very pronounced. The growth rate is about the same in laboratory air and in the water saturated JP-4 fuel, but greater than it was in the inert dry air environment.

The lack of difference between the laboratory air and JP-4 fuel environments implies that the water saturated JP-4 fuel does not significantly enhance corrosion fatigue. However, the RAAF presently uses JP-8 fuel instead of JP-4 fuel. No tests have been conducted in water saturated JP-8 fuel environment to determine its effect on fatigue crack growth rates. The JP-8 fuel has different composition and additives than JP-4, some of which are likely to be highly surface-active and hence significant in terms of potential corrosion mechanisms. Some tests should be performed to determine if JP-8 has an effect on corrosion fatigue in UHS D6ac steel.

3.6.3 Fatigue Crack Growth Threshold and Short Cracks

This region of crack growth is best described as problematic when trying to do engineering assessments. A few programs have investigated FCG threshold in D6ac, and they do not necessarily agree. Perhaps the best explanation is that the data are very difficult and time consuming to obtain, despite the presence of standard test practices.

Table 7 lists threshold values used by Lockheed when analysing structure to determine inspection intervals for the F-111. For this data, the threshold stress intensity (ΔK_{TH}) at which fatigue cracks propagate varies between 1.88 and 7.0 ksi$\sqrt{in}$ depending on the environment and stress ratio. Data from another source [Ryan 1976] show a curve fit that would indicate that ΔK_{th} lies much higher, between 10 and 15 ksi$\sqrt{inch}$. However, the data probably do not extend to low enough values of ΔK for the ΔK_{th} to be determined more accurately.

Table 7. Threshold stress intensity for D6ac heat treated to 220-240 ksi range [Ball and Doerfler, 1996].

Dry/Lab Air		JP-4 Fuel		High Humidity Air	
R	ΔK_{TH} (ksi $\sqrt{in}$)	R	ΔK_{TH} (ksi $\sqrt{in}$	R	ΔK_{TH} (ksi $\sqrt{in}$)
-0.5	7.00	-0.5	7.00	-	-
0.1	3.47	0.1	5.00	0.1	4.00
-	-	0.3	3.45	0.3	3.10
0.5	3.01	0.5	3.17	0.5	2.30
-	-	0.65	2.89	-	-
0.8	2.40	0.8	1.88	-	-

The subject of crack growth threshold is particularly important for D6ac steel because of the criticality of the components made from it. As mentioned before, threshold data are hard to obtain, so not much exists. From looking at the Lockheed data, it should be apparent that the crack growth threshold is very sensitive to chemical environment. That the more corrosive humid air typically lowers the threshold behaviour is no surprise. This is a well-established corrosion fatigue reaction, and it applies to aluminium alloys as well. Since corrosion fatigue lowers the energy required for fracture, it seems natural to assume that in the more aggressive environment, cracks would propagate at lower stress intensities.

Similarly, the threshold values for fatigue crack propagation are dependent on stress ratio as well. The higher the stress ratio, the higher the crack growth rates, and the lower the threshold. This is typically explained using the concept of crack closure where at the higher stress ratios, the crack spends the most of its time completely open

and not experiencing the beneficial effects of unloading on the plasticity in the crack wake.

The fatigue crack growth threshold data used in the DADTA for the F-111 has a very strong influence on the overall results for any evaluation. Recent work by Mills, Sharp and Loader (2000) in studying the effects of corrosion pitting on fatigue crack formation found that (at a given stress level) equivalent initial flaw size (EIFS) distributions for the pits could be shifted by a factor of two to an order of magnitude depending on which material model was used. Conversely, for a given EIFS distribution, fatigue life results could change radically depending on the material model selected. This early result certainly illustrates the necessity when developing this type of information of selecting the best model and sticking with it. If the model requires additional information for validation, then it should be included.

For the case of the F-111, Lockheed has historically used a Forman equation to describe the data in the Feddersen et al. (1972) report, which they use for assessing damage tolerance control points. It is interesting to note that Lockheed actually uses crack growth threshold values different from those reported in FZS-12-626. Lockheed uses a lower value of 2 ksi $\sqrt{in}$.

In the preliminary EIFS study by Mills, Sharp and Loader (2000), many of the equivalent crack sizes derived from the laboratory fatigue lives would not propagate in simulations using the original Forman data. But, obviously, these cracks grew in the laboratory. However, once the model was modified to a lower threshold, it was possible to generate EIFS values based on the experimental data. Clearly, something is amiss, either in the threshold data themselves, or in the way stress intensity is calculated at such small crack lengths, or a combination of both.

This anomaly commands more attention if robust modelling of corrosion fatigue interactions is to develop into the most useful tool possible. It is worth learning more about the techniques Lockheed used to generate the threshold data, as these details are not included in any of the literature perused to date. It could be that revisiting the threshold data with a small research program would be beneficial. However, some researchers [Taylor 1989] report that this type of data is difficult to measure consistently and is very sensitive to test and defect type, so it would be necessary to consider carefully the scenarios most beneficial to the F-111.

For instance, Piascik and Willard (1994) discuss the differences in the growth behaviour of short and long cracks, focusing on the belief that short cracks don't exhibit the same amount of crack tip shielding (closure). Since the relationship between threshold and stress ratio in long cracks is linked with closure, it is easy to extrapolate that a closure effect based on crack length could also manifest itself as a change in crack growth threshold.

In addition to closure, Piascik and Willard (1994) also mention that in dealing with short cracks, deviations from long crack data may be partially explained by the possible violation of elastic fracture mechanics assumptions at small crack lengths.

Additional complexity could be brought on by combining short cracks and associated closure/threshold interactions with chemical environment/threshold interactions. Again, Piascik and Willard (1994) make a good point in referencing two papers by Gangloff and Wei (1986) and Gangloff and Duquette (1987) that cover chemically short cracks (less than 5 mm or 0.20 inch) in high-strength steels. The findings of these researchers suggest that chemically short cracks can exhibit from 1.5 to 500 times faster growth rates than long cracks in the identical corrosion fatigue environment. In this case, the environment was salt water.

In summary, long crack data in these materials may not adequately cover crack propagation behaviour for D6ac steel. The reduction of plasticity induced closure and the added complexity of enhanced chemical synergisms could well mean that the threshold behaviour so crucial to successful life prediction may not be sufficiently accurate for D6ac steel. A more careful evaluation of Lockheed's techniques as compared to the state-of-the-art in short crack considerations should be accomplished.

3.7 Stress Corrosion Cracking Behaviour

High strength steels such as D6ac are susceptible to SCC, which usually manifests itself as intergranular attack. The stress corrosion cracks usually initiate from corrosion pits, but cracking was observed to start directly from a polished surface in 4340 and 3.5 Ni-Cr-Mo-V rotor steel tested in aqueous environment [Oehler and Atrens 1996]. The reason for the cracks starting from corrosion pits is two-fold: corrosion pits provide localised areas of stress concentration and also a favourable electrochemical environment.

The stress corrosion cracks in aqueous or hydrogen-containing environments propagate by diffusion of hydrogen into the highly stressed region ahead of the crack tip, where the hydrogen weakens the cohesiveness of the atomic lattice [Pollock 1974, Chu and Wei 1990]. The mechanism of hydrogen embrittlement of high strength steels, including D6ac, was studied extensively [Lynch and Ryan 1978].

Stress corrosion crack propagation rates for the F-111 D6ac steel were examined in the following environments [Nordquist 1971, Feddersen *et al.* 1972,]:

- Water saturated JP-4 fuel
- Distilled water
- 3.5% sodium chloride solution
- Trichloroethane + J-Oil
- Trichloroethane + J-Oil – 5% Gulf 51 + water – 2%Nital – 3% NH_4OH
- Trichloroethane + Distilled water

- Gulf 51 + Distilled water
- 90% trichloroethane + J-Oil+10%distilled water (cured sealant)
- 90% trichloroethane + 10% H_2O (FMS-1043)
- Gulf 51 (1:15) - trichloroethane in sealant (cured)
- Gulf 51(1:15) + 10 drops trichloroethane
- Distilled water for 24 hrs - replace water with $K_2Cr_2O_4$ solution
- $K_2Cr_2O_4$ solution
- $Zn_2Cr_2O_4$ solution
- Load with distilled water - dry - replace with $K_2Cr_2O_4$ solution
- $K_2Cr_2O_7$ solution
- Passivate with $K_2Cr_2O_4$ solution - dry - distilled water
- Mil-C-38736 cleaner (a mixture of Aromatic Naphta, Ethyl Acetate, Methyl Ethyl Ketone, Isopropanol and Toluene)
- Bo-Peep cleaner
- 8% volume NH_4OH

However, the results from most of these environments are not available.

The critical toughness values (K_{ISCC}) for initiation of SCC in various environments are listed in Table 8.

*Table 8. K_{ISCC} for D6ac Steel in Various Environments [*Feddersen et al. 1972, **Ryan 1976, ***Hagemeyer and Hillhouse 1970]*

Environment	K_{ISCC} (ksi$\sqrt{in}$)
Water saturated JP-4 fuel	52 - 53
Distilled water	*~21, **~16 MPa$\sqrt{m}$, ***9[1], ***18[2]
3.5% NaCl solution	~21, <18

[1]High toughness plate, K_{IC} = 101 ksi$\sqrt{in}$
[2]Low toughness forging, K_{IC} = 40 ksi$\sqrt{in}$

Feddersen et al. (1972) observed a slight decrease in K_{ISCC} in forgings compared to rolled plate. This result contradicts the results obtained by Hagemeyer and Hillhouse (1970), who observed higher K_{ISCC} in low toughness forgings than in high toughness plate.

As may be seen from Table 8, the distilled water environment reduces the K_{ISCC} value to the same extent as the 3.5% NaCl solution. This is in agreement with the observation made during corrosion fatigue, where distilled water was observed to be the most severe environment.

In aqueous environments, the mode of SCC is synonymous with the mechanism of hydrogen embrittlement. The hydrogen is generated at the crack tip by breakdown of water and oxidisation (rusting) of the iron. The excess hydrogen is available to be adsorbed onto the surface of the steel and to diffuse into the interior where it can

weaken the lattice coherency. Under these circumstances, the crack growth is usually intergranular.

Figures 17-21 describe SCC of D6ac in various environments ranging from JP-4 fuel, to distilled water, to 3.5% salt water. Rates in JP-4 are the slowest, whereas rates in 3.5% NaCl can get quite high, approaching 18 mm/hour in Feddersen's tests of high-toughness plate. No SCC data for D6ac in the F-111 heat treat has been found for the JP-8 fuel now used in the F-111.

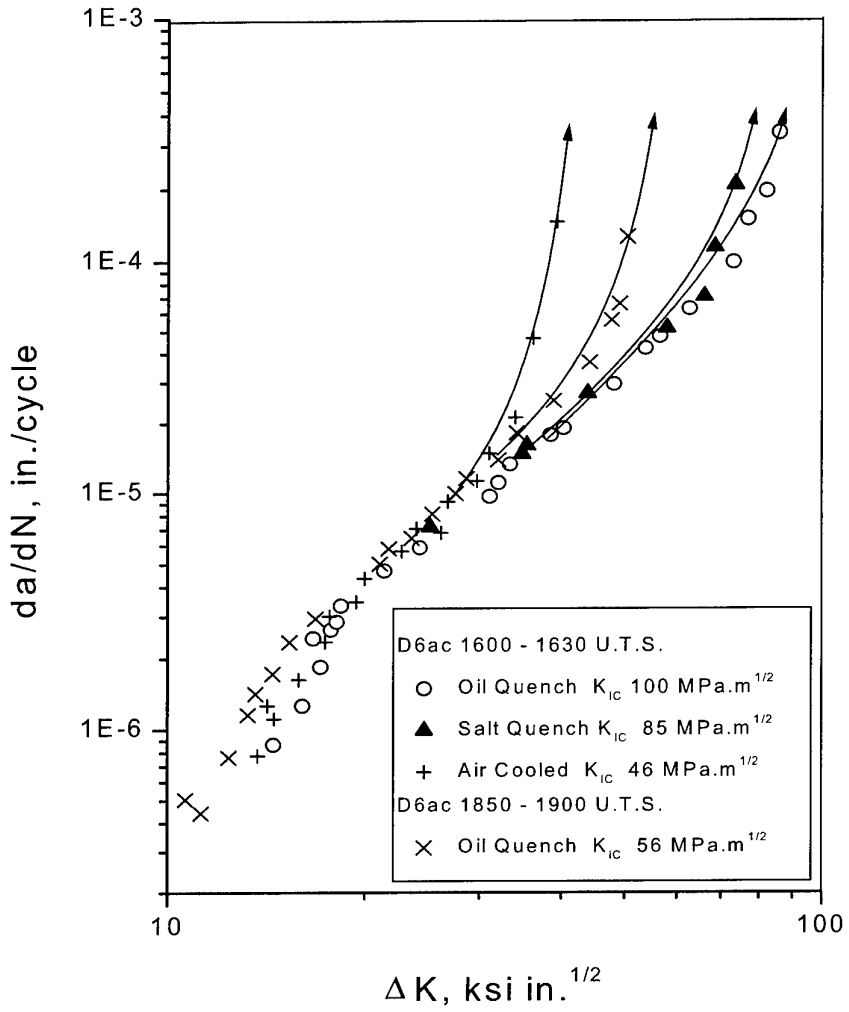

Figure 4. The effect of fracture toughness on crack growth rate for D6ac steel of two different strengths: 220-240 ksi (1600-1630 MPa) and 260-280 ksi (1850-1900 MPa) [Ryan 1976].

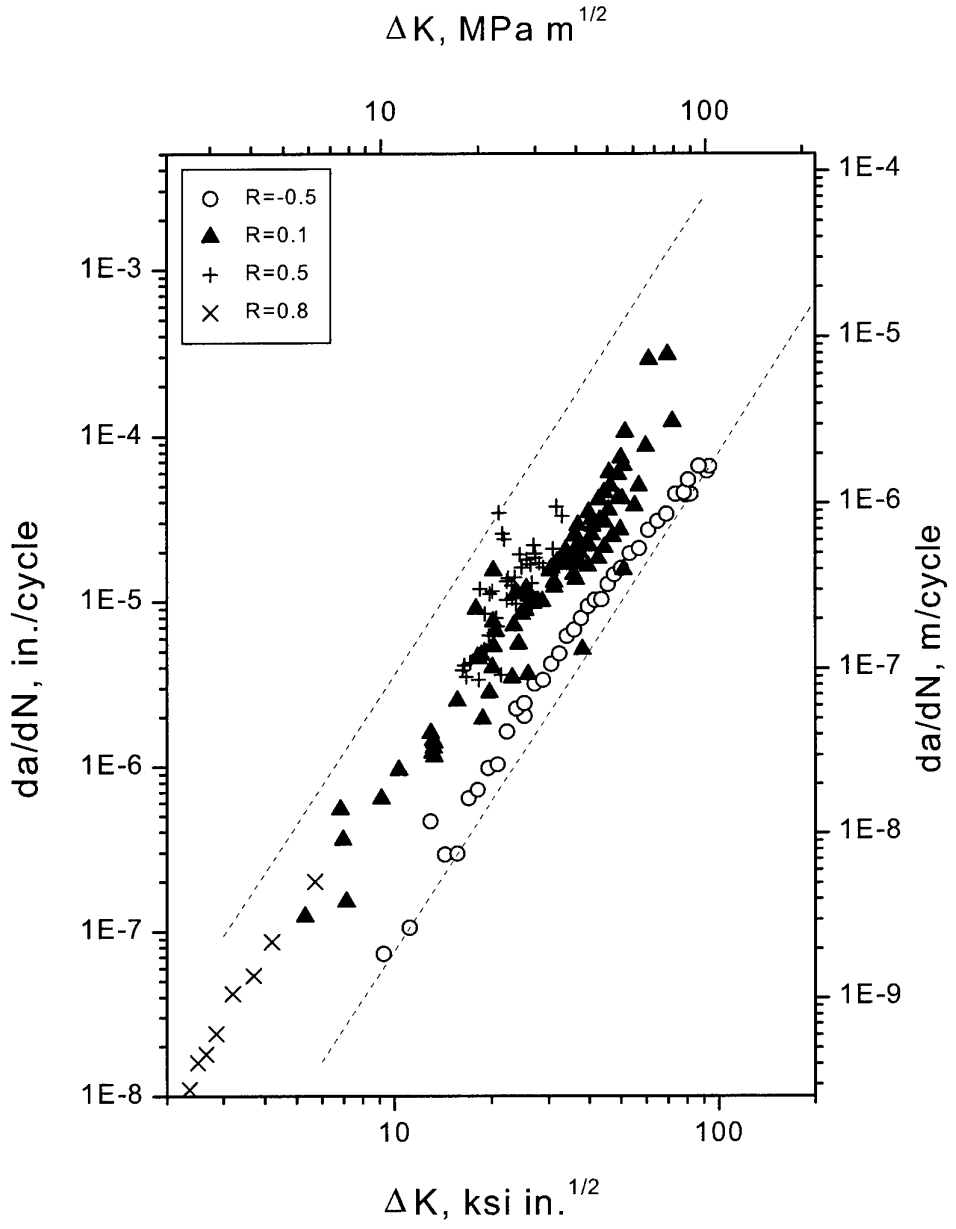

Figure 5. Crack growth rate in dry/lab air, D6ac steel, L-T orientation [Ball and Doerfler 1996]. The dashed lines represent the upper and lower bounds for all the D6ac data and are shown here for comparison.

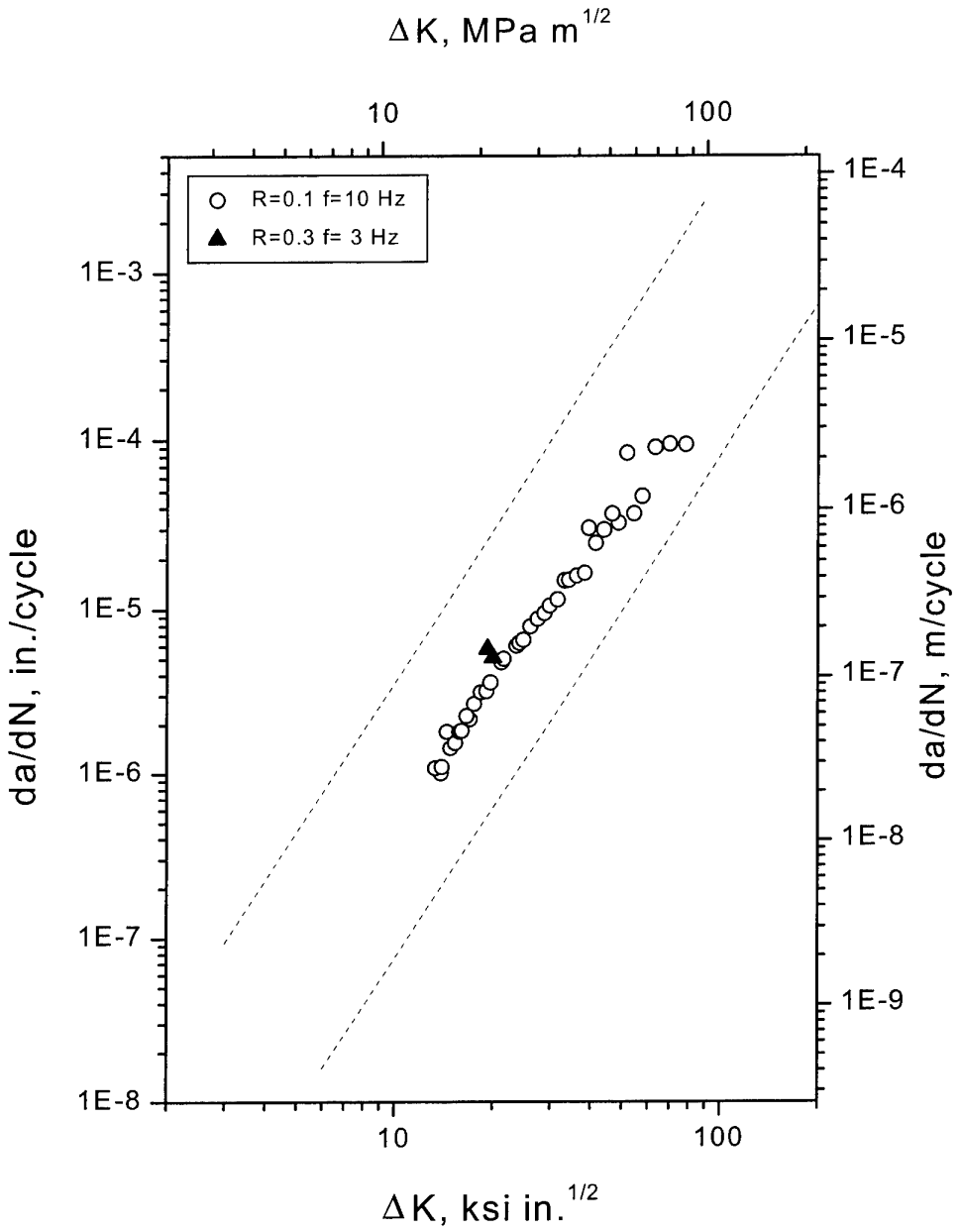

Figure 6. The effect of load frequency and stress ratio on crack growth rate in laboratory air, D6ac steel [Paris et al. 1972]. The dashed lines represent the upper and lower bounds for all the D6ac data and are shown here for comparison.

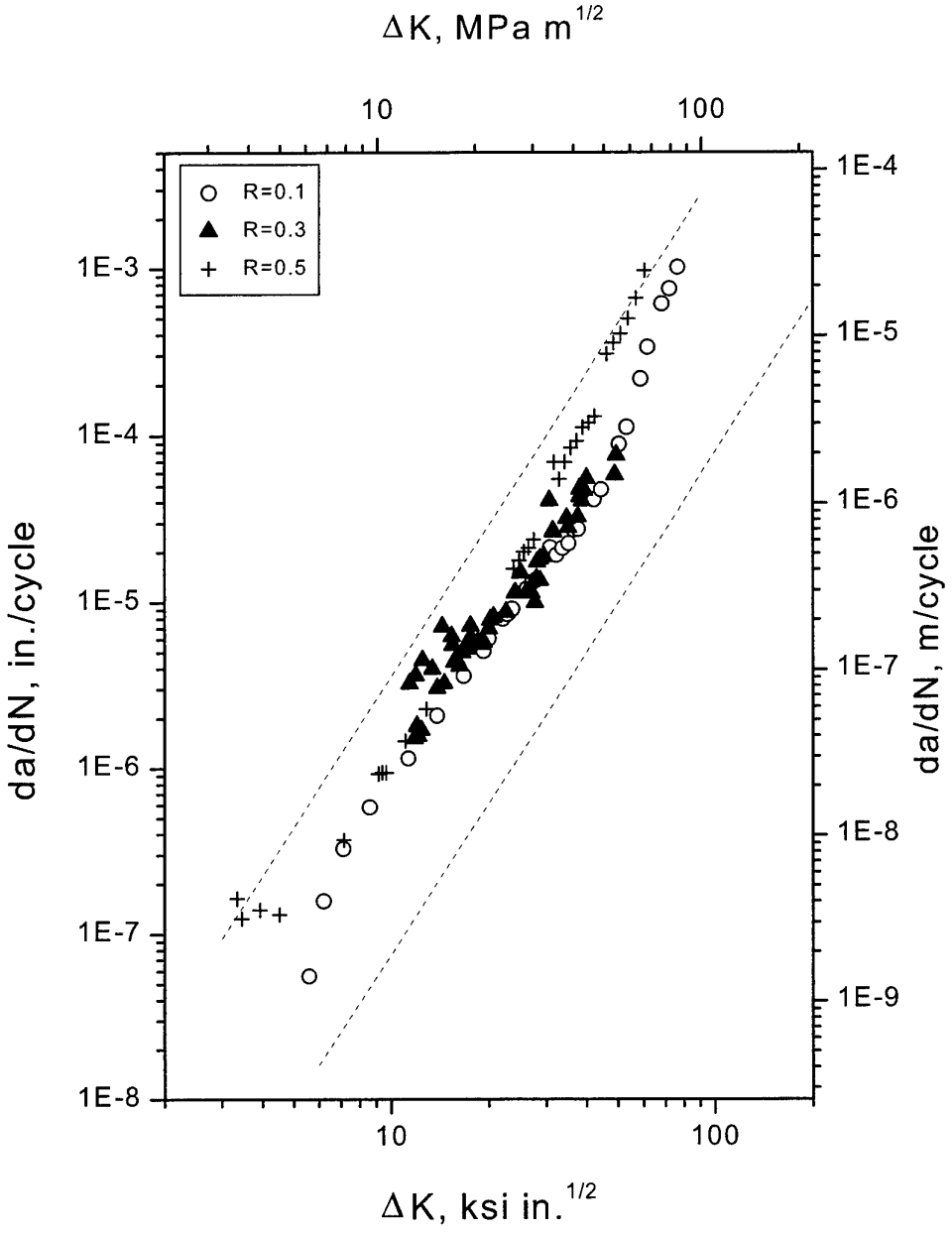

Figure 7. Crack growth rate in high-humidity air, D6ac steel, L-T orientation [Ball and Doerfler 1996]. The dashed lines represent the upper and lower bounds for all the D6ac data and are shown here for comparison.

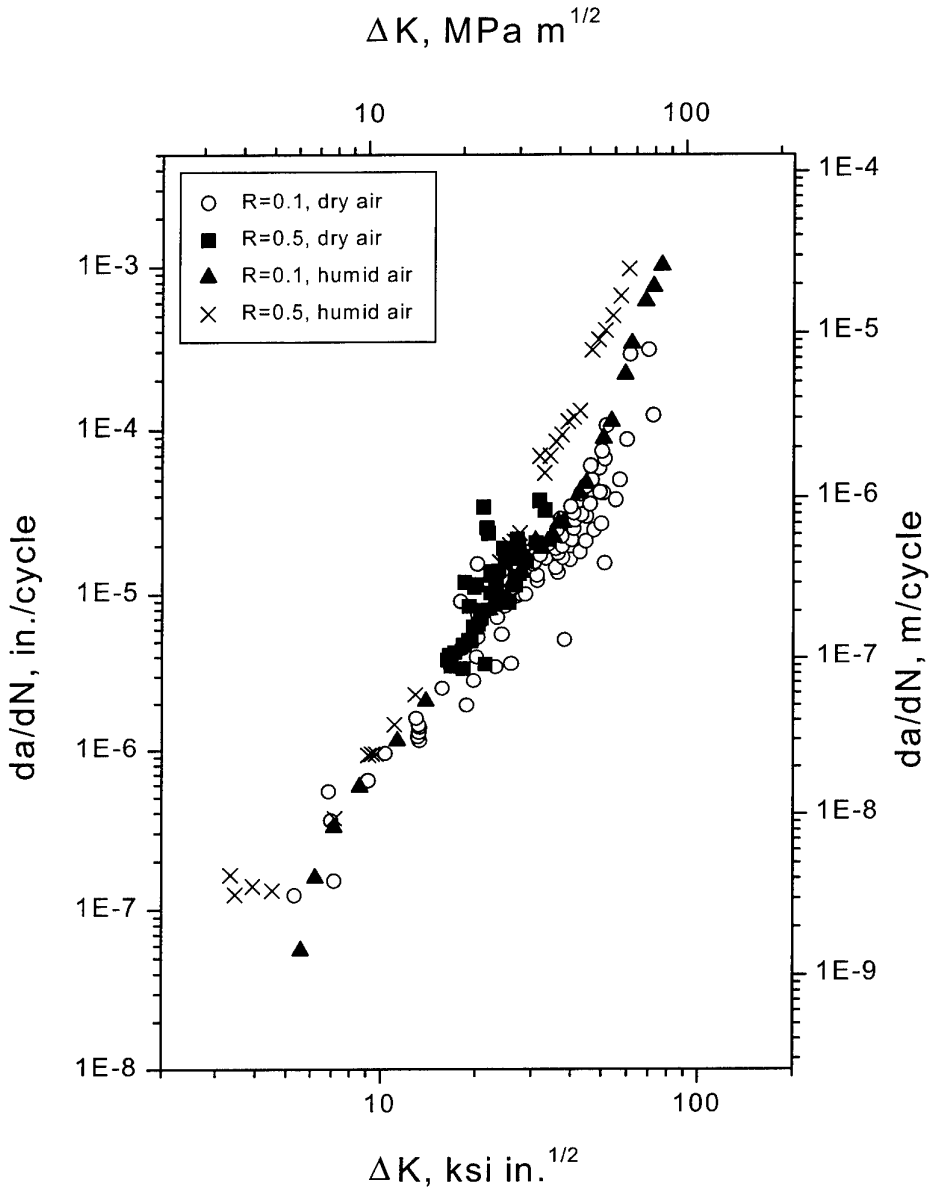

Figure 8. Compilation of Figures 6 and 7 comparing crack growth rate between dry air and high-humidity air.

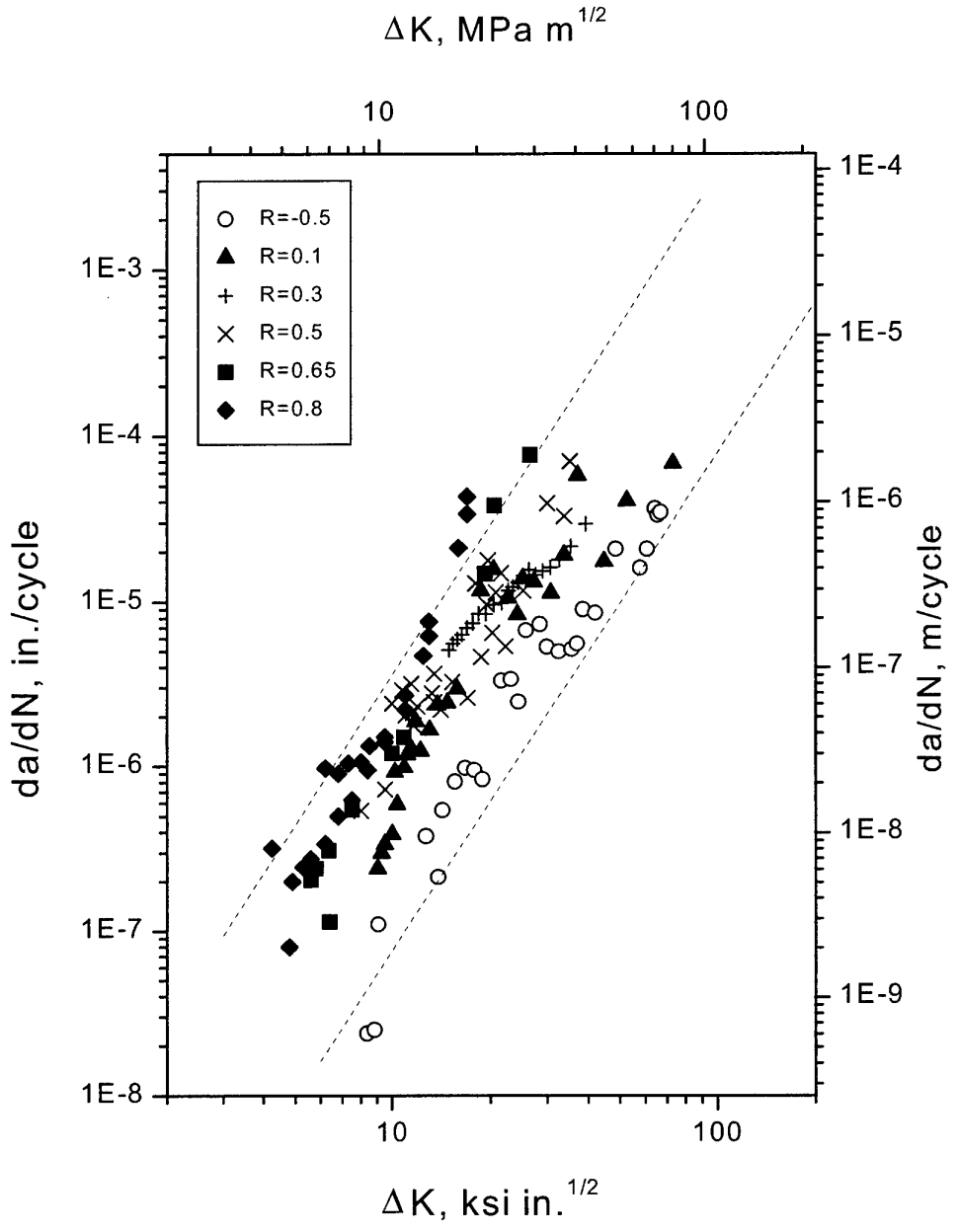

Figure 9. Crack growth rate in JP-4 fuel, D6ac steel, L-T orientation [Ball and Doerfler 1996]. The dashed lines represent the upper and lower bounds for all the D6ac data and are shown here for comparison.

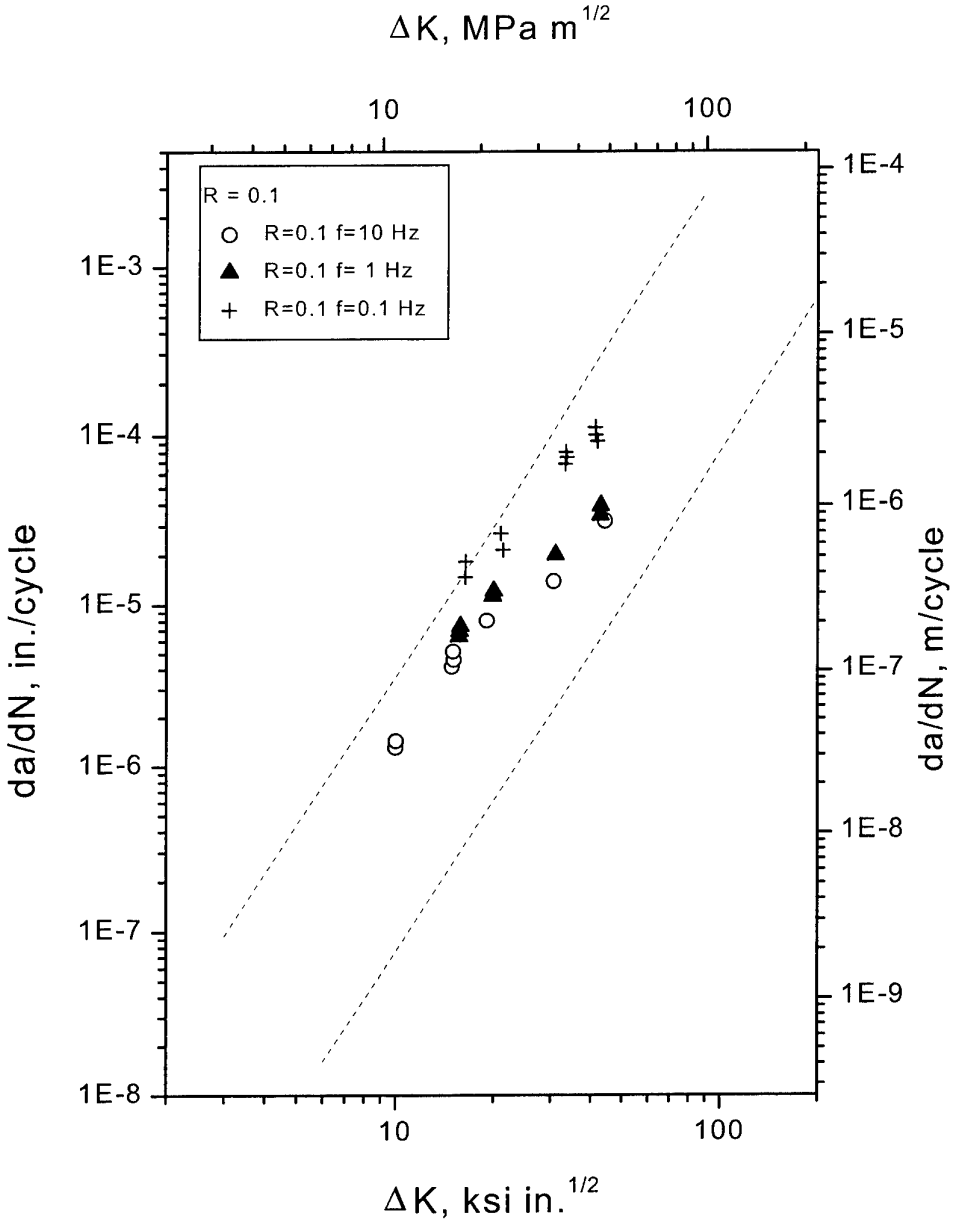

Figure 10. The effect of load frequency on crack growth in distilled water, D6ac steel, R=0.1 [Paris et al. 1972]. The dashed lines represent the upper and lower bounds for all the D6ac data and are shown here for comparison.

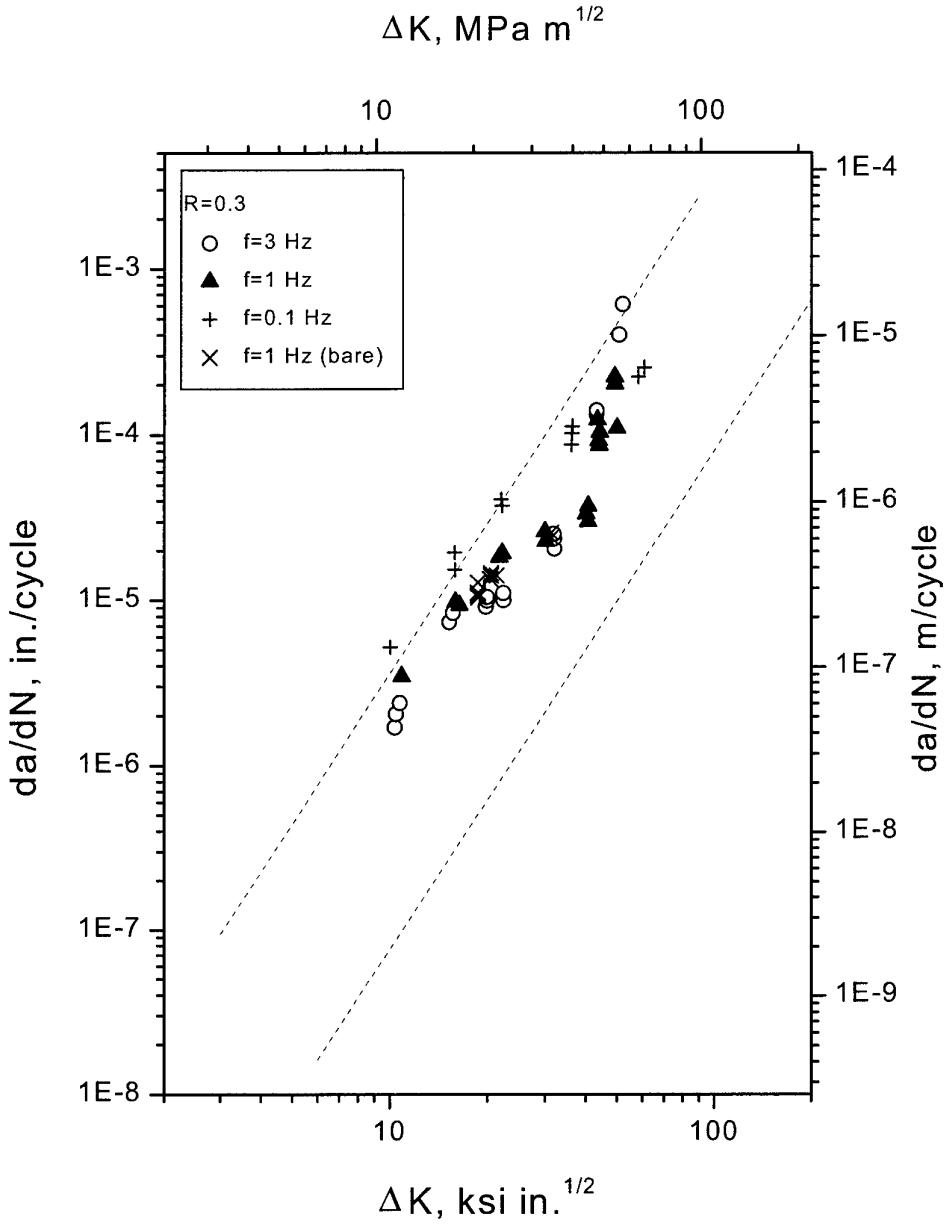

Figure 11. The effect of load frequency on crack growth in distilled water, D6ac steel, R=0.3 [Paris et al. 1972]. The dashed lines represent the upper and lower bounds for all the D6ac data and are shown here for comparison.

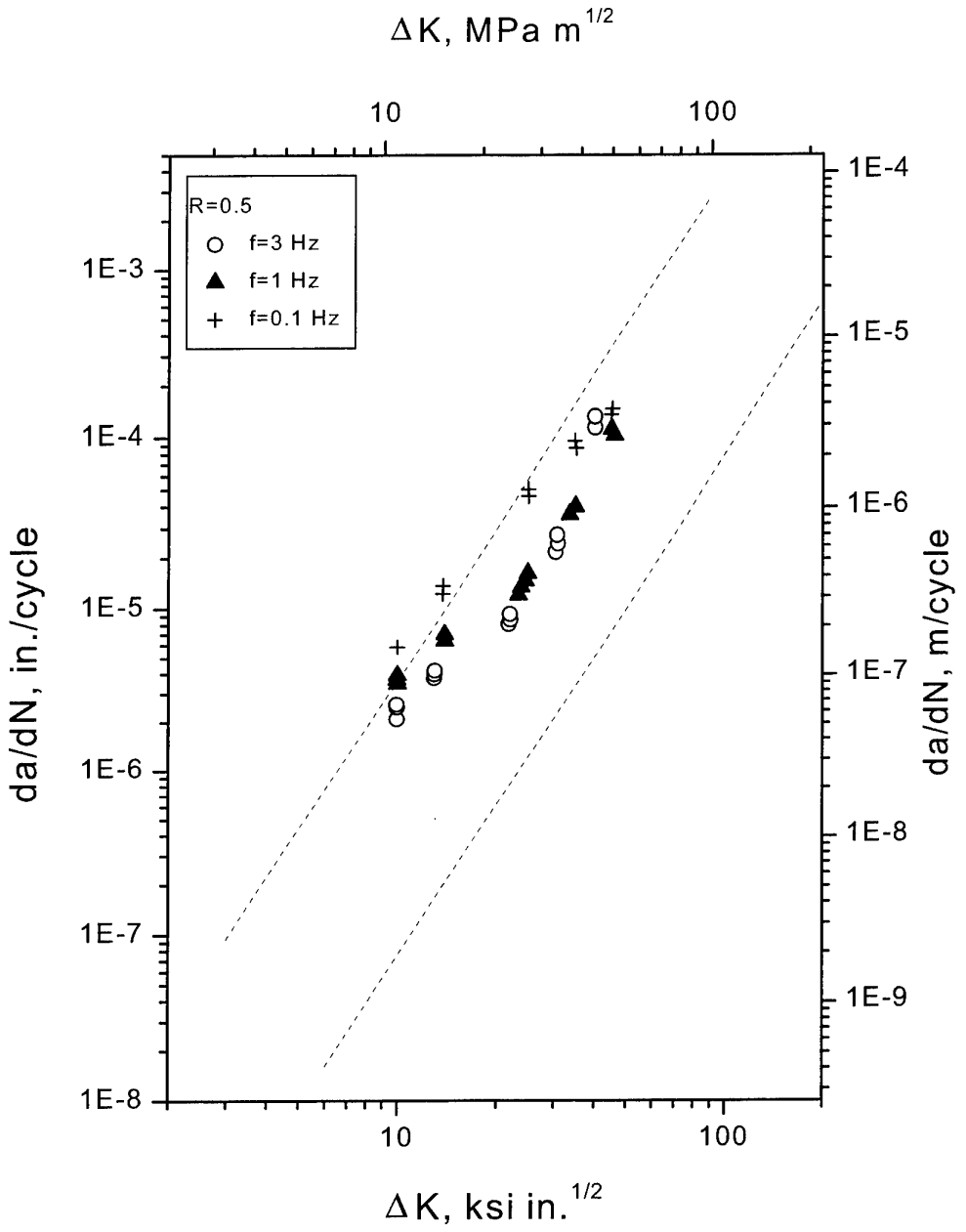

Figure 12. The effect of load frequency on crack growth in distilled water, D6ac steel, R=0.5 [Paris et al. 1972]. The dashed lines represent the upper and lower bounds for all the D6ac data and are shown here for comparison.

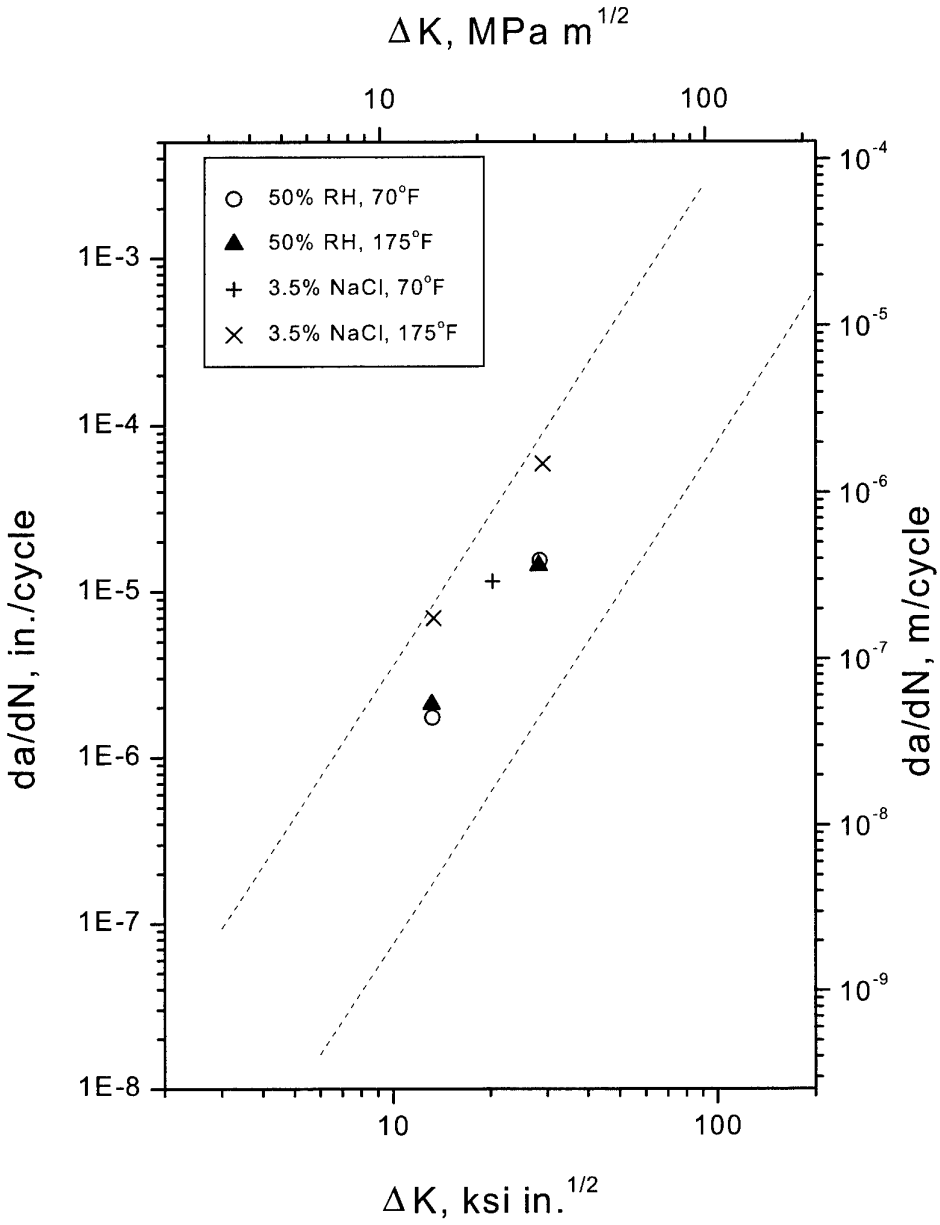

Figure 13. The effect of temperature on crack growth rate in 50% RH air and 3.5%NaCl solution, D6ac Steel [Feddersen et al. 1972]. The dashed lines represent the upper and lower bounds for all the D6ac data and are shown here for comparison.

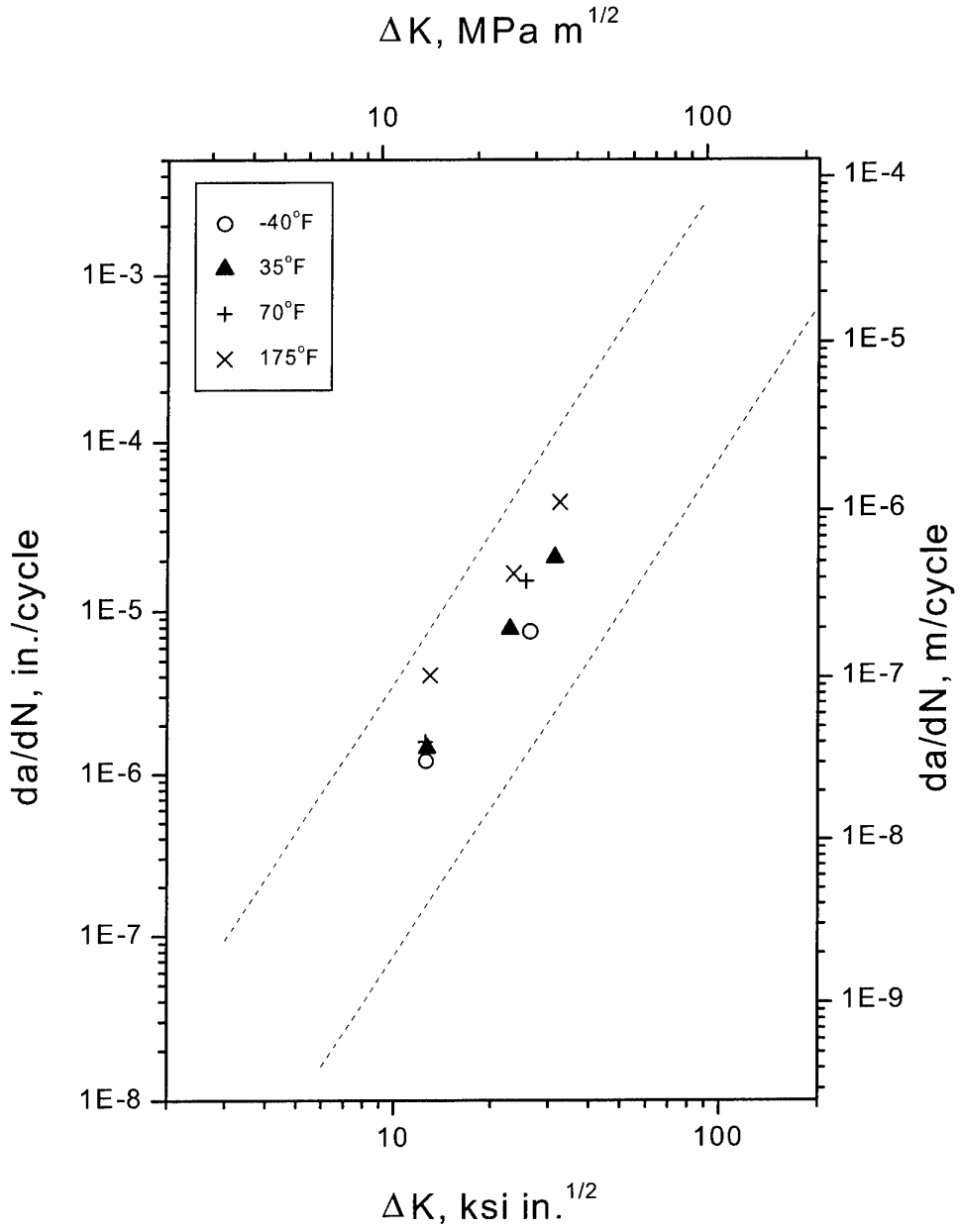

Figure 14. The effect of temperature on crack growth rate in water-saturated JP-4 fuel, D6ac steel [Feddersen et al. 1972]. The dashed lines represent the upper and lower bounds for all the D6ac data and are shown here for comparison.

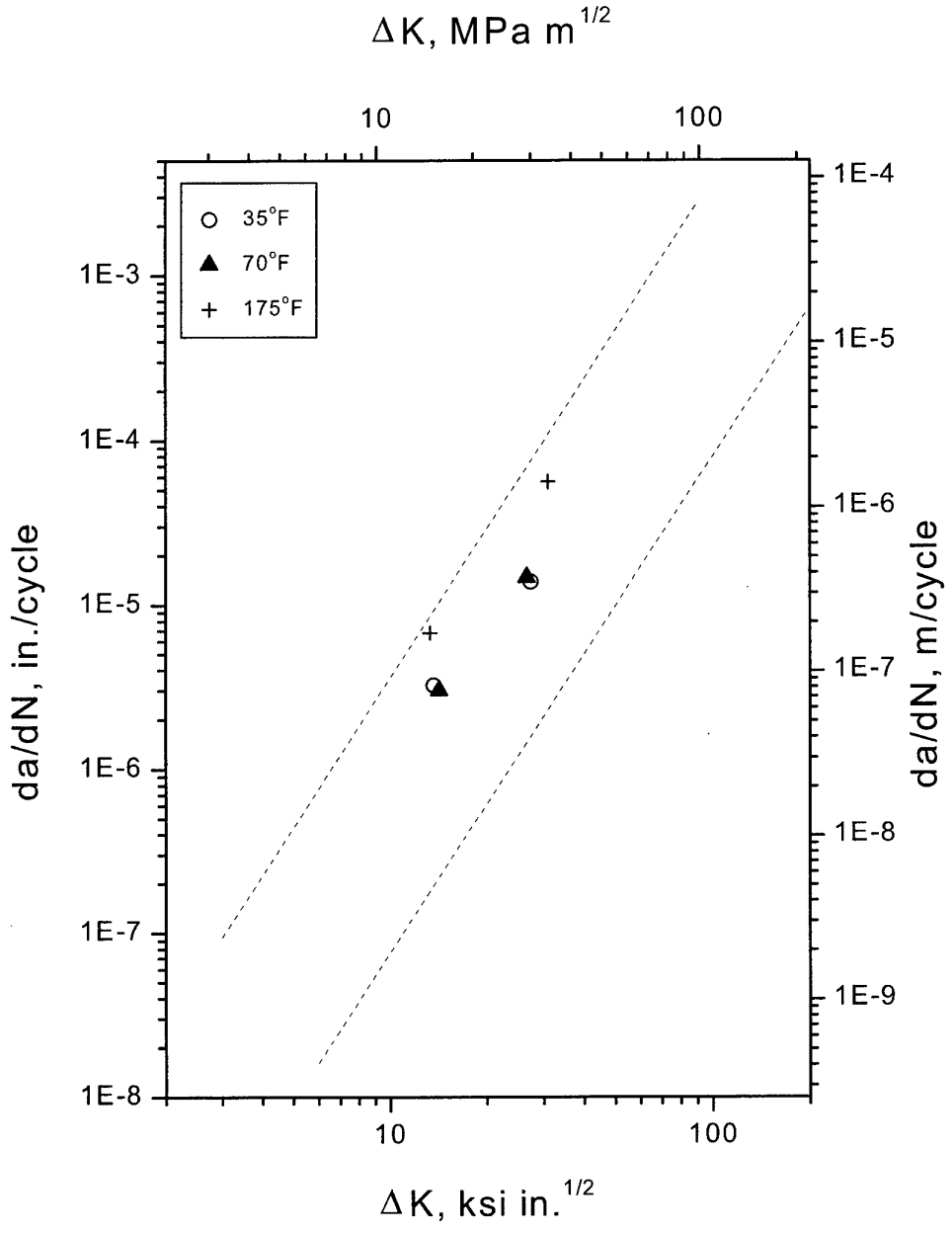

Figure 15. The effect of temperature on crack growth rate in distilled water for medium-toughness forgings, D6acsSteel, R=0.3 and 1 Hz [Feddersen et al. 1972]. The dashed lines represent the upper and lower bounds for all the D6ac data and are shown here for comparison.

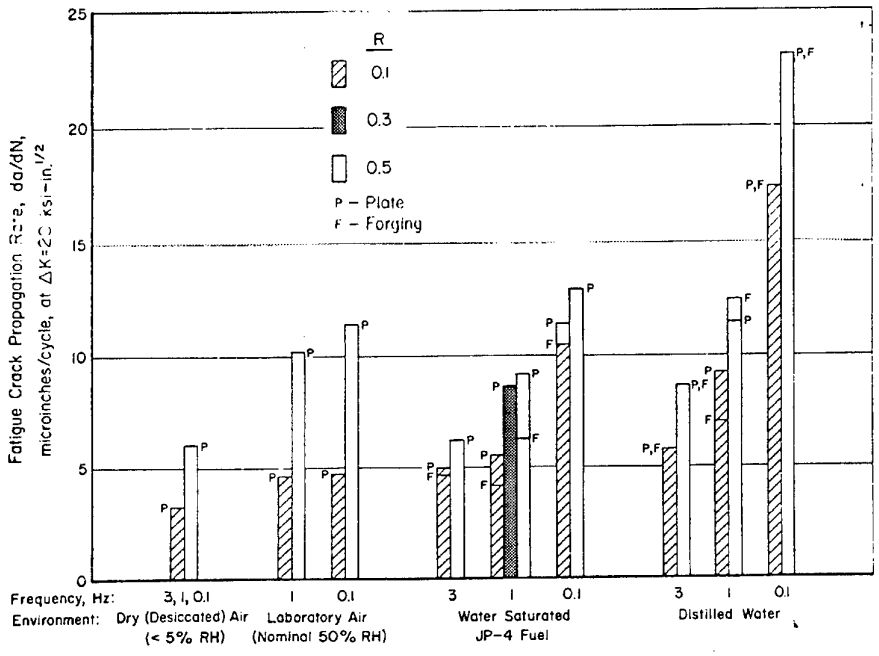

Figure 16. Summary of the effect of environment, stress ratio, and frequency on the fatigue crack growth rate in D6ac plate and forging at ΔK = 20 ksi √in. [Feddersen et al. 1972].

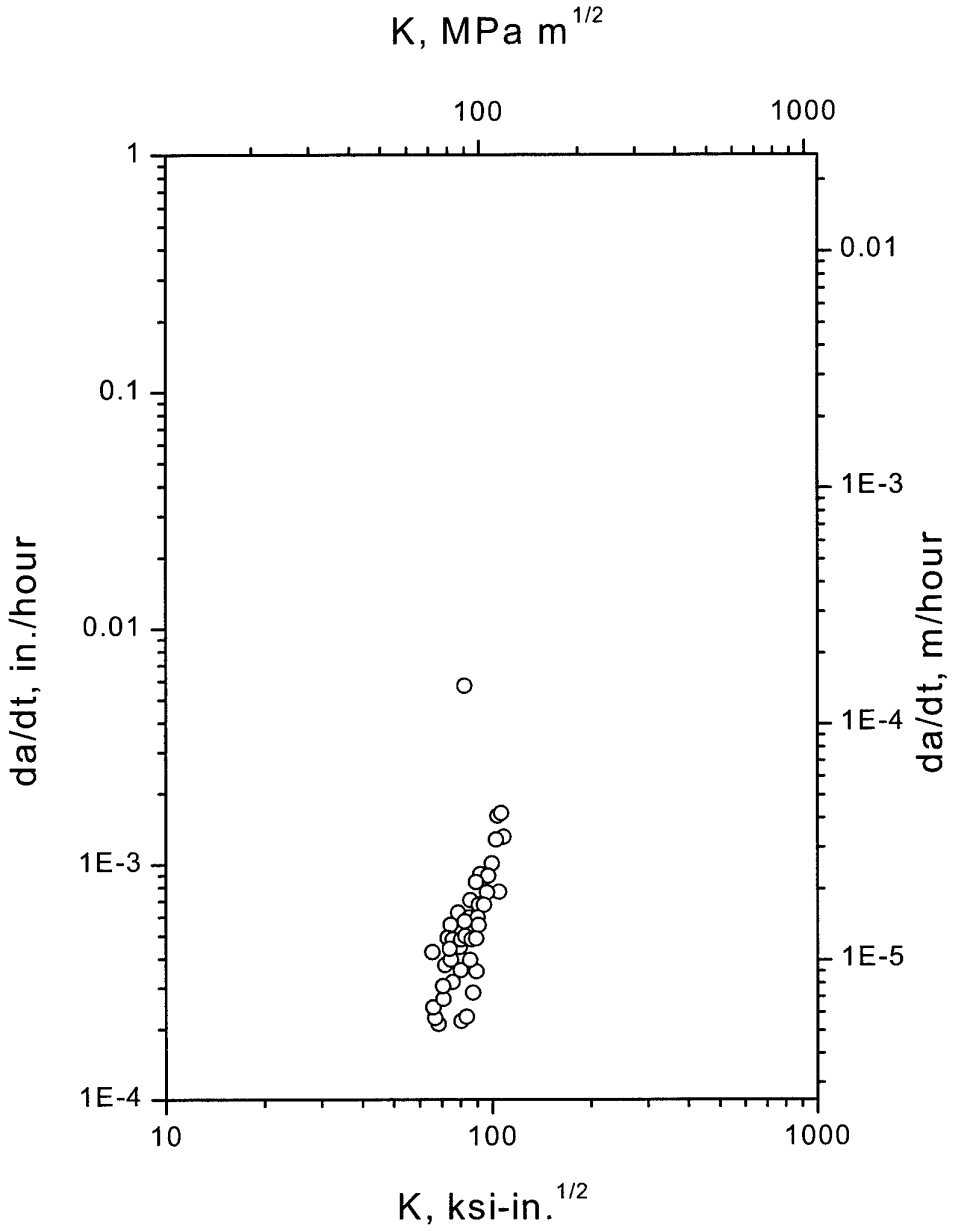

Figure 17. Stress corrosion crack propagation rate in water-saturated JP-4 fuel for high toughness plate compact tension specimens [Feddersen et al. 1972].

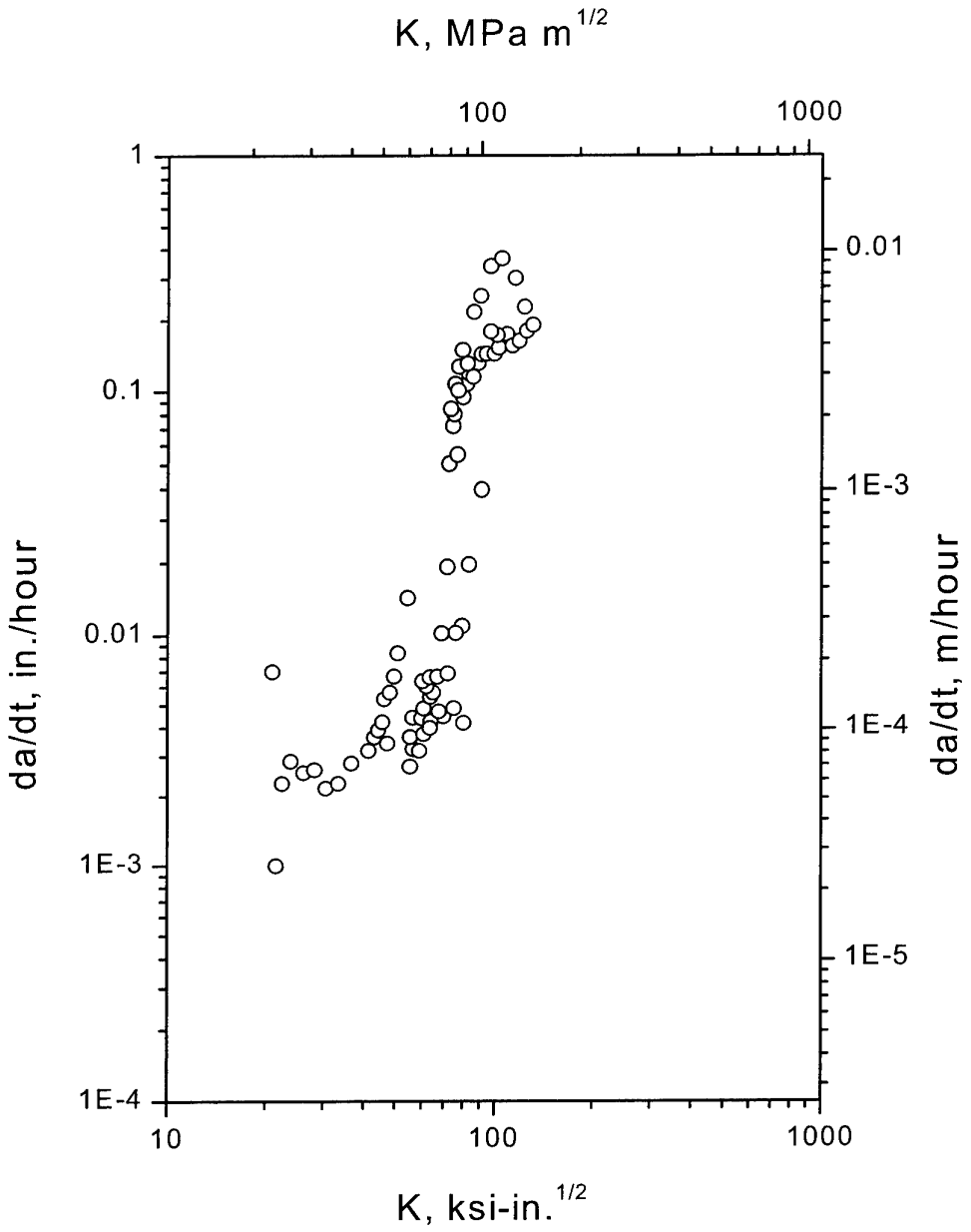

Figure 18. Stress corrosion crack propagation rate in distilled water for high toughness plate compact tension specimens [Feddersen et al. 1972].

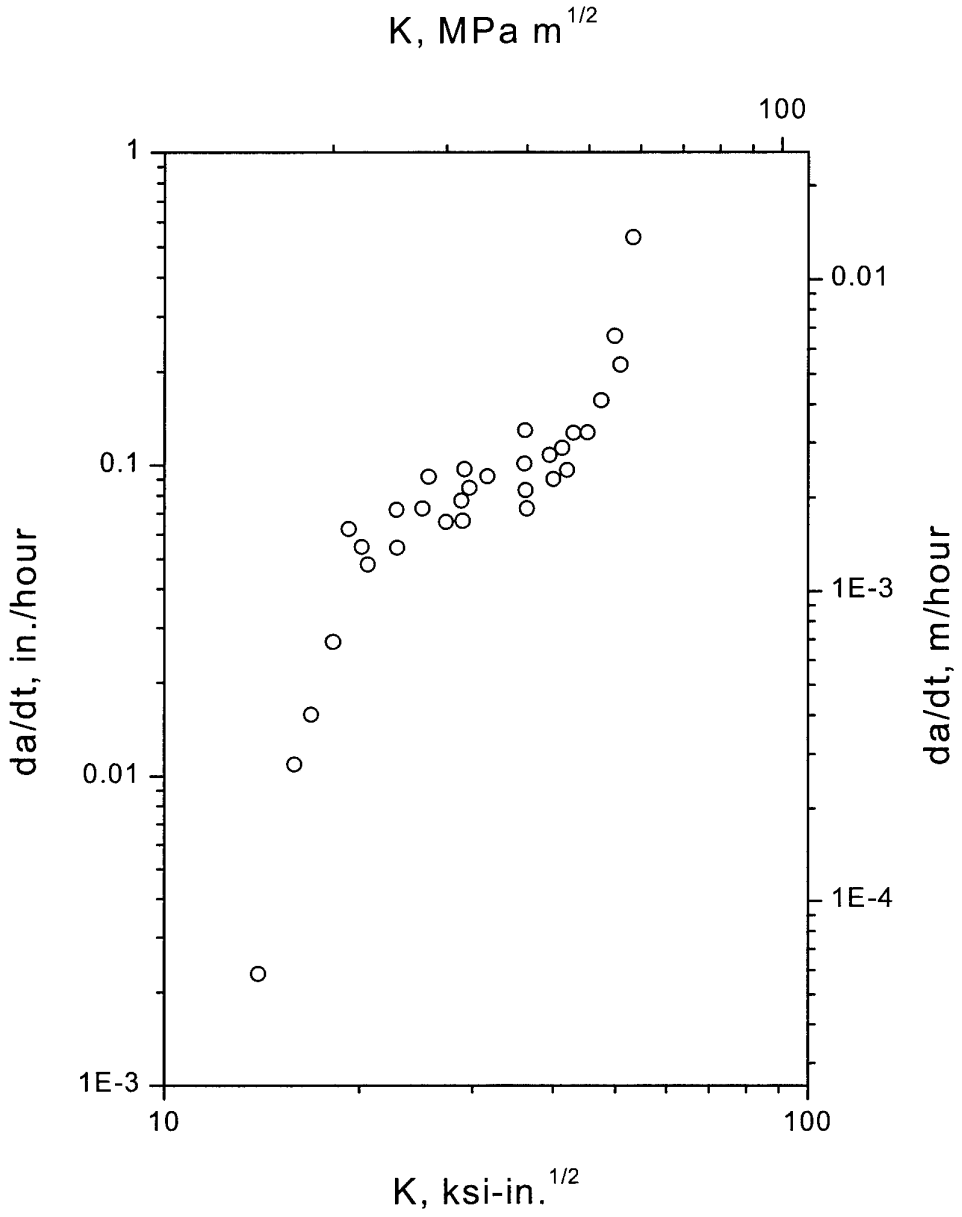

Figure 19. Stress corrosion crack growth rate in distilled water [Ryan 1976].

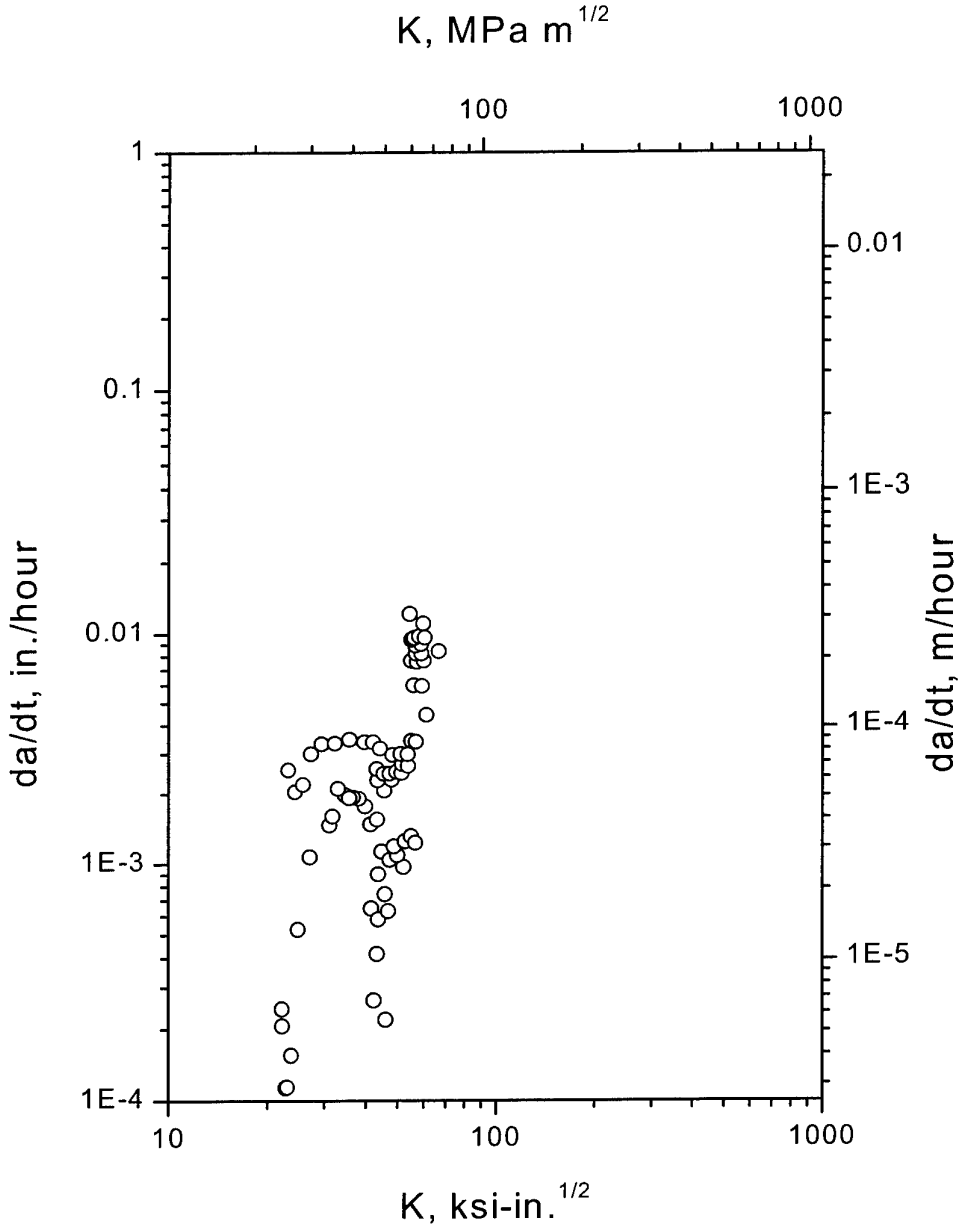

Figure 20. Stress corrosion crack propagation rate in distilled water for medium toughness compact tension specimens [Feddersen et al. 1972].

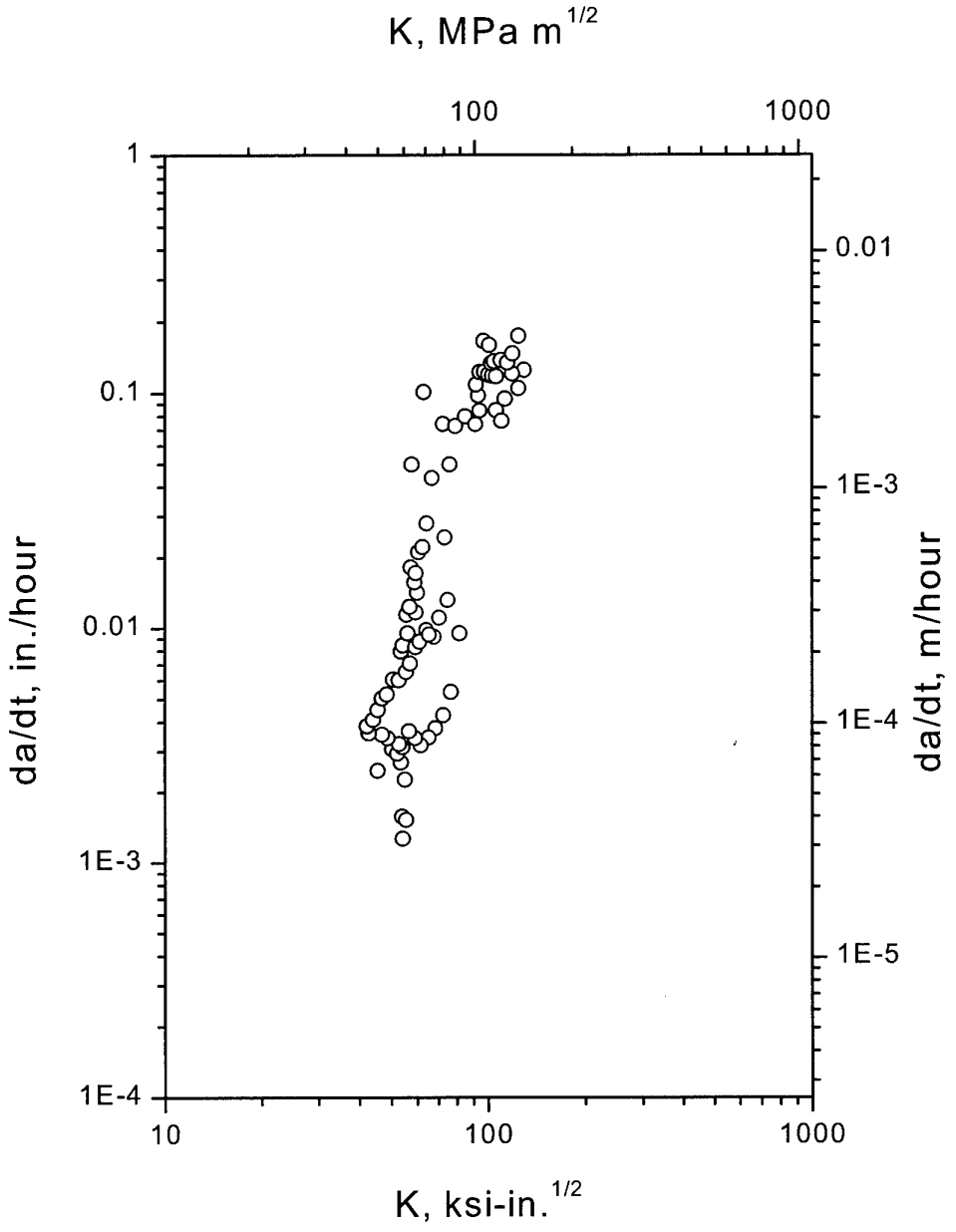

Figure 21. Stress corrosion crack propagation rate in 3.5% NaCl solution for high toughness plate compact tension specimens [Feddersen et al. 1972].

3.8 Summary and Conclusions on D6ac Steel

D6ac steel components are the heart of the F-111 structure and are also the most critical. The majority of structural problems that could or do threaten flight safety are linked to D6ac steel. In the early days of the F-111, these problems were largely manufacturing related, but these problems have been rectified, and the new challenges are linked to the passage of time and usage.

The fracture toughness of D6ac presents an interesting problem, because early processing was highly variable, and some time passed before a more rigorously controlled quenching process was introduced that ensured higher fracture toughness. However, poor record keeping means that it is not possible to track what D6ac components have the lower toughness, and hence, shorter critical crack length. Thus, it is necessary to treat all components as if they are of the lower toughness variety.

Corrosion will continue to be the biggest enemy of D6ac. Residual stress related cracking problems resulting mainly from the cold proof load test have been identified and solutions are progressing. However, the best ways to handle corrosion have not yet been solved. In the interest of moving away from the "find and fix" philosophy to "inspect and manage", which should be done to reduce unscheduled and unnecessary maintenance burden, ways to analyse the impacts of corrosion damage need to be developed.

Corrosion pitting is one of the most insidious and common forms of corrosion for D6ac steel. In its unprotected state, D6ac will normally undergo general corrosion. However, the very system put in place to prevent corrosion, cadmium plating, will exacerbate corrosion when the plating breaks down locally. In these cases, very deep, structurally threatening pits may develop.

Data on crack nucleation mechanisms in D6ac steel is by no means widespread in the literature. More work needs to be done to describe these processes and learn more of the possible effects they could have on the F-111 structure. Methods are currently under development within DSTO/AMRL to describe corrosion pitting as an engineering parameter that can be fed into the F-111 DADTA. This is important for a number of reasons:

- pitting causes fatigue cracks,
- pitting causes stress corrosion cracks,
- stress corrosion and fatigue may combine to render inspection intervals unconservative, and
- pitting damage could cause cracking damage to develop in areas not previously considered to be structurally sensitive based on pure fatigue.

The plan is to validate corrosion engineering parameters for use in the DADTA by using increasingly complex tests and loading conditions. Current efforts have been

limited to low-stress concentration specimens under constant amplitude loading. This will be expanded to use specimens with pitted holes that have been subjected to the F-111 DADTA 2B spectrum. Ultimately, more advanced structural component specimens and even a full-scale wing test will validate the process. The pits have already been placed in the wing, and testing is in progress. It remains to be seen what will actually cause failure.

One of the more prominent findings to come out of some of the modelling efforts for pitting/fatigue interactions is that the material fatigue crack growth model has a significant impact on predictive results. Questions remain as to the validity of threshold crack growth data and, for that matter, the validity of the stress intensity solutions for such small crack sizes. Specimen design and initial discontinuity size and type are all believed to influence fatigue crack growth threshold, so this should be revisited.

Stress corrosion cracking has occurred in many D6ac components in the F-111. As protection systems deteriorate, we can expect this trend to worsen. In the F-111, SCC has been known to occur in the same plane as that favouring fatigue loading, which creates an interesting scenario for life prediction. Propagation rates in SCC are often quite high, and even if they could be predicted for service conditions, we probably would not like the answer. The conservatism required by the high level of scatter in environmental effects would make the results unusable. To better understand SCC behaviour in D6ac, basic tests could be performed that use JP-8 fuel as the environment. The original data for the F-111 was based on water saturated JP-4, the common jet fuel at the time of the F-111s introduction to service. The new fuel environment could also be applied to fatigue crack growth experiments to generate updated da/dN data.

4. Aluminium Alloys

Aluminium alloy selection for the F-111 required elevated temperature strength, due to the effects of aerodynamic heating; hence a 2000 series alloy was selected. The structural framework and exterior surfaces consist largely of artificially aged (T6 and T8) 2024 alloy. Structural elements of the fuselage, and the landing gear, which are not exposed to higher temperatures, use 7079-T651 and 7075-T651.

4.1 Service History

As with the D6ac steel components, aluminium structure has suffered its share of corrosion and cracking problems. However, none have been as severe as the problems encountered in the high-strength steel. This is partially explained by the fact that most critical components in the F-111 involve the WCTB, WPF, or horizontal tail pivot shaft, which are all primarily D6ac structures.

For the aluminium alloys, though, 2024-T851 deserves unique attention as the wings are comprised mostly of this material, and they have had a few notable structural problems. In February 1994, a crack was discovered in the outer lower wing skin of a USAF F-111G. In the same month, a similar crack was discovered in a RAAF F-111C at 4750 flight hours. The crack was substantial in size, about 48 mm long, and was in a critical component. The crack originated from fatigue in an area of localised yielding, and a bonded composite repair was developed and applied to that location. Since then, similar damage has been detected in three other RAAF aircraft at 3850, 6720, and 7372 flight hours [Boykett and Walker 1996, Walker 1999]. Certainly, this problem was one of the most significant for aluminium in the F-111, as it involved crack patching over critical structure.

Other aluminium components deserve attention as well for other cracking and corrosion problems. From the information contained in two different reports [Bandara and Armitage 2000, Turk and Russo 2000], the majority of corrosion and cracking problems (for aluminium) belong to alloy 7079-T6.

Bandara and Armitage included a table that listed the top 20 part numbers based on total defect count from maintenance databases. A lot of these top 20 components were bonded panels, another area of concern for the F-111 but not the focus of this report. Still others were D6ac components. A few aluminium components made the top 20, however, and these are summarised in Table 9. From most of the records, the actual causes for the cracking were, unfortunately, undefined.

This result is very similar to problems uncovered by Hoeppner et al. (1995) when reviewing corrosion involvement in aircraft accidents in the United States. The most important conclusion was that the true magnitude of the problem and possible solutions would not be known until reporting becomes more accurate and detailed.

Although the causes of the cracking in the following components are largely undefined, Russo, Turk and Hinton (2000) say that conversations with personnel at RAAF Amberley led them to believe that the majority of these problems are stress corrosion cracking related. The FS 119.5 Radome Bulkhead deserves special mention (as denoted by the asterisk) because the original specifications called for 2024-T851 to be used on this component. This alloy is fairly immune to SCC, but the RAAF aircraft were produced differently and have a 7079-T651 substitute at that location.

Table 9. Aluminium structure leading in corrosion and cracking occurrences [Bandara and Armitage 2000, Russo, Turk and Hinton 2000].

Part Name	Part Number	Alloy	Occurrences	DADTA Item
Floor Trusses	12K2413	7075-T6	160	3
FS 119.5 Radome Bulkhead	12B2011	7079-T651*	104	
FS 364 Glove Bulkhead	12B2703	7079-T651	98	
Upper Routing Tunnel Floor	12B4710	7079-T651	78	
Mid Fixed Glove Longeron	12B1710	7079-T651	54	

*7079-T651 was used in the radome bulkhead on RAAF aircraft. USAF aircraft used 2024 in that location, and it has not been a problem in that fleet.

4.2 Chemical Compositions

The nominal compositions of the three major aluminium alloys found in the F-111, specifically, 2024, 7075 and 7079, are listed in Table 10.

Table 10. Chemical composition of 2024 [QQ-A-250-4e 1971], 7075 [ASM Handbook, Vol. 2 1979] and 7079 Aluminium Alloys [MIL-A-8877A 1965].

Element	Alloy Composition		
	2024 (wt.%)	7075 (wt.%)	7079 (wt.%)
Cu	3.8-4.9	1.2-2.0	0.4-0.8
Mg	1.2-1.8	2.1-2.9	2.9-3.7
Mn	0.3-0.9	<0.3	0.1-0.3
Si	<0.50	<0.4	<0.3
Zn	<0.25	5.1-6.1	3.8-4.8
Fe	<0.50	<0.5	<0.4
Cr	<0.10	0.18-0.28	0.1-0.25
Ti	-	<0.20	<0.10

4.3 Heat Treatments

Artificially aged tempers of aluminium are the most common in the F-111. Both of the 7xxx-series alloys covered in this report are of the T6 (peak-aged temper) variety, while 2024 is most common in the T8 form on this aircraft. The T6 temper in particular is used with the 7xxx-series alloys because they do not respond well to the T8 treatment. For that matter, only certain 2xxx-series alloys respond well to T8 processing, which involves cold working between quenching and ageing [ASTM Handbook Vol. 4 1981]. This treatment results in greater strength as the extra cold work increases dislocation density and promotes the precipitation of greater numbers of smaller, evenly distributed secondary particles. The usual trade-off in performance applies, though, in that the artificially-aged T8 temper has lower fracture toughness and fatigue resistance than the naturally-aged, lower-strength T3 and T4 tempers most commonly found in alloy 2024.

4.4 Fracture Toughness

Typical fracture toughness values for the three alloys in thicknesses representing plane stress (or near-plane stress) and plane strain are given in Table 11. The values were all found summarised in Lockheed document FZS-12-626, but in turn these were all extracted from the Damage Tolerance Design Handbook [MCIC-HB-01R 1983].

As would be expected, the materials show a doubling of fracture toughness in the thinner sections. The low values of toughness for the thicker sections are common for older materials. Little was understood about fracture mechanics in the days these alloys were created, and indeed aircraft were designed based largely on static strength at the time. Thus, the 7xxx-series alloys (7079 in particular), were most sought after for their strength-to-weight ratio. Everything has a trade-off, of course, and with hindsight, the emphasis on high-strength materials in the F-111 design led to unfortunate reductions in fatigue resistance, corrosion resistance, and fracture toughness. Newer materials try to achieve a better compromise in terms of strength and toughness.

Table 11. Fracture toughness of 7079-T651 in T-L orientation [Ball and Doerfler 1996].

Alloy	Fracture toughness, thickness	(ksi√in)
7079-T651	K_c @ t = 0.250 in.	40.5
7079-T651	K_{Ic} @ t > 1.370 in.	18.6
7075-T651	K_c @ t = 0.250 in.	43.9
7075-T651	K_{Ic} @ t > 0.500 in.	22.5
2024-T851	K_c @ 0.125 in.< t < 0.400 in.	45.0
2024-T851	K_{Ic} @ t > 0.400 in.	20.7

4.5 Corrosion/Fatigue Interactions and Mechanisms

This next section is a detailed discussion on corrosion fatigue mechanisms with particular focus on 2xxx-series and 7xxx-series alloys. Cole, Clark and Sharp (1997) produced an extensive report dedicated to this subject related to aircraft structural integrity.

Concepts covered in this section include environmentally assisted crack propagation, stress concentrations caused by different types of corrosion, and even the possibility that a crack could encounter a weakened or thinned area in a structure. Also included in the more detailed list below is the possibility that corrosion could cause significant structural changes affecting load transfer and, ultimately, the overall performance of the structure. The Aloha Airlines accident [NTSB 1989] is probably the most well known example of such a situation. This latter failure mode is very case specific, and while it has caused a major incident, it is only pointed out here as a possibility.

As many of the names for different mechanisms sound remarkably similar, the following definitions are offered to distinguish them. Only the first one is an actual ASTM standard definition.

- Corrosion fatigue--the process in which a metal fractures prematurely under conditions of *simultaneous* corrosion and repeated cyclic loading at lower stress levels or fewer cycles than would be required in the absence of the corrosive environment [ASTM Standard Definitions 1986].
- Corrosion nucleated fatigue--the process in which physical corrosion damage (e.g., exfoliation, pitting) and/or chemical damage (e.g., embrittlement) accelerates the *formation* of fatigue cracks in a component or structure.
- Prior-corrosion fatigue--occurs when a propagating fatigue crack encounters a prior corroded region. A propagating fatigue crack in a prior-corroded region may be propagating by *corrosion fatigue* if an aggressive chemical environment is present and assists in further altering crack propagation in a synergistic manner.
- Corrosion induced fatigue via load transfer--occurs when corrosion damage or environmental degradation in a structure causes load to be transferred to nearby structure. The increased stresses or strains associated with the transfer may promote fatigue cracking.

4.5.1 The Earliest Corrosion and Corrosion Fatigue Studies

With all the attention focused currently on aircraft sustainment, or ageing aircraft, these days, it would be easy to surmise that corrosion and its interaction with fatigue is a post-Aloha [NTSB 1989] phenomenon. On the contrary, corrosion fatigue in its many forms has been around as long as we have been using metals. Admittedly, the detrimental effects are most pronounced in high-strength alloys, but those materials

worked their way into the aircraft industry, as duralumin and super-duralumin, in the 1920s and 1930s. Many cracking failures occurred in sheet and plate components, and the cracking was often intergranular in nature.

Haigh (1917) first put forth by the concept of a synergism between corrosion and fatigue when looking at fatigue in brasses. Research into the effects of environmental exposure on aluminium alloys quickly followed with Moore and McAdam (1927) publishing two (sequential) papers in the same journal. These two researchers observed severely detrimental effects of corrosion on fatigue in aluminium; the corrosion damage took both the form of intergranular cracking and pitting.

4.5.2 Corrosion Influences on Crack Nucleation

As Haigh, Moore and McAdam discovered, the influence of corrosion on fatigue damage has many facets. Perhaps one of the most insidious contributions of corrosion to structural degradation is the acceleration of fatigue or stress corrosion crack formation. Many researchers have published papers that address the effects of corrosion, particularly pitting, on crack formation in high-strength aluminium alloys. Some of the more impressive works on this subject came from US Air Force's Wright Laboratory and the US Naval Research Lab in the 1960s.

In 1961, Harmsworth (1961) studied the influence of pitting corrosion on the fatigue performance of alloy 2024-T4. The effort focused on determining the stress concentration factors of pits.

In the mid-1960s, the US Navy encountered problems with 7075-T651 extrusions that formed the wing spars of air-sea rescue aircraft. The subsequent research program identified pitting and intergranular degradation (exfoliation) as the culprits in the reduced fatigue performance [Shaffer *et al.* 1968].

Another US Air Force study prompted by the US Navy's work dealt with corrosive environments and manoeuvre spectrum loading on fatigue in popular aluminium alloys such as 7075-T651 as well as the less-used aluminium-lithium alloy, 2020-T651 [Gruff and Hutcheson 1969]. This study was primarily concerned with fastener hole integrity, as Gruff hypothesised that fretting damage in the hole made the wing skin materials more susceptible to pitting and exfoliation damage by removing protective films in the holes. Once the corrosion damage was in place, fatigue performance suffered dramatically.

With the potential severity of these effects realised, the next burst of activity from the research community tried to bring pitting corrosion into the conceptual framework of corrosion fatigue and fracture mechanics, as the majority of the corrosion fatigue research to that point was focused on crack propagation phenomena. Hoeppner (1971) identified pitting corrosion as a mechanism to generate multiple-site damage (MSD) in that pitting may form numerous fatigue cracks in a component or structure.

As repeatedly mentioned in this report, the formation of fatigue damage is extremely sensitive to surface integrity (especially in high-strength materials), and corrosion pits violate surface integrity. The subsequent efforts [Hoeppner 1979, Hoeppner *et al.* 1981, Kondo 1989, Komai and Minoshima 1989, Kawai and Kasai 1985, Lindley *et al.* 1982, Ma and Hoeppner 1994, Chen *et al.* 1994] focused largely on the surface integrity issue by seeking answers, in part, to the following questions:

- Once corrosion pits form, how large do they have to grow before a propagating fatigue crack will nucleate from the pit?
- Furthermore, how long will it take for corrosion pits to reach a critical size?

A DSTO report to be published by Loader and Sharp (2001) nicely summarises several pitting models.

Unfortunately, no easy answers have presented themselves. On the contrary, the answers to those questions depend widely on the material type, the chemical environments causing the corrosion, the loading nature (unloaded, sustained, dynamic) [Grimes 1996], and the load distribution among other variables.

Pitting is not the only form of corrosion damage that can cause early failures under fatigue. Exfoliation corrosion, described earlier, has this same ability, although this type of damage is widely regarded as affecting net-section stress. Many studies have sought to address the surface integrity issue associated with exfoliation.

Most of the interest regarding exfoliation interactions with fatigue damage has formed in the last seven years. However, Shaffer et al. (1969) were conducting studies as early as 1968. Their investigation into cracks detected in the wing spar cap of a Navy air-sea rescue aircraft yielded important information. Fatigue life in the exfoliated material was reduced to 30% of the original, and metallographic examination of the post-test specimens showed that the corroded laminar paths were preferential sites for fatigue crack nucleation. The exfoliation problems originated deep inside rivet holes that suffered pitting attack under crevice corrosion conditions, and the resulting corrosion damage was undetectable by normal visual observation. In all cases, the intergranular corrosion cracks propagated from corrosion pits, and as many as 20 cracks were detected (via ultrasonic inspection) emanating from a given area.

Hubble and Chubb (1994) tested alloys 2024-T3 and 7075-T6 damaged with exfoliation. In this study, panels containing fastener holes were subjected to exfoliation corrosion and then fatigue tested. The results illustrated that the end grains exposed in the rivet holes were particularly susceptible to corrosion penetration; therefore, Hubble and Chubb concluded that corrosion in those locations could influence the formation of MSD.

The multiple-site damage generating nature of exfoliation corrosion was further affirmed by Mills (1995) in prior-corrosion/fatigue, stress-life tests in 1994. The

damage reduced the fatigue life of 7075-T651 dog-bone specimens by at least 88%. The undamaged specimens did not fail after 5 000 000 cycles and reached an end-of-test condition. The corroded specimens failed, on average, at 250 000 cycles. In some cases, the failed specimens exhibited more than one crack nucleation site.

Recent efforts at DSTO/AMRL are focusing on the modelling of this damage type by exploiting the similarity of exfoliation to pitting corrosion [Sharp *et al.* 2000].

Other studies in DSTO/AMRL [Athiniotis 1999] have sought to determine the influence of stress corrosion cracking on airframe structural integrity in general, including the nucleation of fatigue damage. Clark and Sharp (2000) wrote a summary of how laminar damage, such as SCC or exfoliation, can influence fatigue. Often SCC occurs along parting planes in forgings, directions that are aligned with the principal structural load. This is a more structurally benign scenario in both static strength and fatigue, as demonstrated by recent Macchi tailplane spar tests [Athiniotis 1999].

Perhaps the most dangerous scenario occurs when SCC and fatigue are propagating in the same geometric plane. Cracks over 100 mm (4 inches) long have been found in the upper fuselage lobe skin of the USAF C-5 Galaxy, the material being 7079-T6 aluminium. The concern here is that the cracks grew quite long independent of flight cycles before fatigue started to dominate. One hundred millimetres of crack growth represents a significant number of flight hours in terms of pure fatigue, and here the damage was most likely accumulating while the aircraft was idle.

Although in D6ac steel, this failure mode combination been found in the F-111 at a former splice to main landing gear bulkhead [Redmond 1993, Clark and Sharp 2000] In this case, corrosion pitting in the degraded cadmium plating worked with fit up stresses to nucleate an SCC crack. This crack continued to grow, most likely, until the fit up stresses were relieved and the crack tip stress intensity fell below K_{ISCC}. By now, though, the crack was long enough to continue propagating by fatigue. Like the case with the C-5 Galaxy, this scenario can be particular dangerous because SCC rates can be very high and can consume much of the safe crack growth well before an inspection based on fatigue would be accomplished.

4.5.3 Crack Growth Acceleration Mechanisms

The proposed mechanisms by which aggressive chemical environments accelerate fatigue crack growth range from dissolution of material at the crack tip to hydrogen embrittlement [ASM Handbook, Vol. 11 1986].

Hydrogen embrittlement has been attributed to severe increases in crack propagation rates in several aircraft structural alloys. Hydrogen enters the picture as one of the by-products of corrosion processes. Electrochemical reactions in electrolytic solutions often yield hydrogen, and many believe that atomic hydrogen enters the strained plastic zone at the crack tip. The presence of hydrogen in lattice spaces weakens the

atomic bonds and reduces the energy required for fracture [ASM Handbook, Vol. 11 1986, Parkins 1988]. In addition, hydrogen is continually produced in the crack growth process, as newly produced crack faces are exposed to aggressive environments [Wei 1979], and protective oxide films are disrupted by fatigue crack closure.

Other mechanisms have been proposed in the literature, a summary of which was written by Jones (1992) in support of stress corrosion cracking. It appears, however, that the mechanisms for stress corrosion cracking and corrosion fatigue are closely related. One such theory is the adsorbed ion theory. This mechanism, supported by Gangloff (1990), involves the transport of critical species to the crack tip and the reduction of surface tension at the crack tip. The energy required for fracture is thereby lowered. As mentioned by Jones (1992), many film-based mechanisms have surfaced in the literature. These range from film-induced cleavage, in which a crack growing through the low-toughness oxide layer at a crack tip may reach sufficient velocity at the film-substrate interface as to penetrate into the base metal, to film rupture. In film rupture theories, galvanic couples between the passive film and the newly exposed metal promote dissolution of the metal.

Whatever the mechanism, environmental effects typically diminish at higher stress intensities. This occurs when the mechanical tearing or cleaving of the material occurs at such a high rate as to preclude effects of chemical dissolution or localised embrittlement [Krupp *et al.* 1972, Bowles and Schijve 1983]. Therefore, as with any environmentally-assisted fatigue mechanism, unless a failure process alters the critical toughness of a material, crack growth rates will converge with those of 'pure' fatigue near the region of critical instability.

4.5.4 Modelling Corrosion Fatigue

No discussion on corrosion fatigue crack propagation would be complete without at least mentioning the difficulties associated with modelling environmentally assisted crack growth. One of the most common methods for modelling corrosion fatigue is the superposition approach. The simplest models combined growth rates of da/dN (crack extension per cycle) for 'pure' fatigue with da/dt (crack extension per unit time) for stress corrosion cracking. These models have not been widely successful since the simple superposition does not completely account for the synergism observed [Holroyd and Hardie 1983].

Modifications of the superposition principle, such as the 'three component model' for gaseous environments [Wei and Simmons 1981, Wei and Shim 1983], have been investigated as well, and they involve the two previously mentioned parameters as well as a 'da/dN cf' (the 'cf' being an abbreviation for 'corrosion fatigue') scale factor. The scale factor, unfortunately, changes for different material/environment combinations, so as an engineering community, we essentially still rely on empirical data.

Scale factors have been used in practice for lack of something better. For instance, Miller and Meyer (1988) developed a computer model for predicting environmentally-assisted crack growth rates and setting subsequent inspection intervals for the C-5 Galaxy transport aircraft. Crack monitoring was already in use on the C-5 by calculating inspection intervals based on 100% relative humidity conditions. This new program accounted for the fact that many environments are more severe than 100% relative humidity, and crack growth scale factors were applied to aircraft according to the specific US Air Force bases from which they operated.

4.5.5 Corrosion Fatigue Environments

Popular and practical environments for corrosion fatigue research in high-strength aluminium alloys are humid air, 3.5% salt water, and salt sprays. Humid air (relative humidity > 50%), of course, is common, and salt water/salt spray environments are of concern for naval aircraft and other aircraft that see service in seacoast atmospheres or operate maritime patrol or strike missions.

Chlorides (the most suspected culprits in corrosion fatigue of aluminium) are present not only in salt water but in other chemical environments as well. Chlorides have formed the bases of studies focusing on chemical environments inside aircraft. One such study by Pettit et al. (1974) conducted for the USAF characterised crack growth in artificial sump tank water.

Swartz et al. (1995) reports that sump tank water was originally developed by Cooper and that this type of solution has been used for the majority of so-called "realistic chemical environment" studies. Swartz et al., with the cooperation of several U.S. airline maintenance facilities, sampled environments from the galleys, bilges, and lavatories of several commercial aircraft and developed new chemical solutions for use in corrosion fatigue investigations.

Many engineering materials suffer increased corrosive attack in relative humidity above 50% [ASM Handbook, Vol. 13 1985], and this behaviour can worsen in the presence of industrial pollutants such as sulfur dioxide (SO_2). Thus, artificial acid rain has started to appear as a corrosion testing solution. The acid rain produced by Shaw (1994) at Alcoa was used to generate prior-corrosion damage in KC-135 fuselage panels for the USAF. The acid rain was not used as a corrosion fatigue environment.

4.6 Fatigue Crack Growth Behaviour

This section covers several variables affecting long crack propagation behaviour in the three aluminium alloys covered in this report; 2024-T8xx, 7075-T6xx, and 7079-T6xx. Effects of stress ratio, frequency, and environment are all presented. The mechanisms behind the environmental effects were discussed in the previous section on corrosion fatigue. To a large extent, frequency effects can be tied to environmental influences,

because at lower frequencies, chemical environments have more time to act at the crack tip.

4.6.1 Fatigue Crack Growth in 2024-T851

A good summary of crack growth behaviour in 2024-T851 was provided by Pettit *et al.* (1974), and that report formed the basis of the information used for the F-111 DADTA materials data in FZS-12-626 [Ball and Doerfler 1996].

Pettit *et al.* (1974) found that increased stress ratio produced the standard layered effect in crack growth data, where higher R had the greatest crack growth rates. For the range in K covered by the experiments, the R = 0.5 data tended to lie above the R = 0.1 curve by a factor of one to five. Figure 22 shows the typical R shift for this alloy.

The results of the environmental fatigue and frequency effect studies conducted by these same researchers paints a picture which differs from conventional wisdom. Corrosion fatigue interactions in aircraft aluminium alloys are well known, and are quite obvious in the data presented for the 7xxx-series alloys in the next sections. Even 2024 in the naturally aged T3 and T4 tempers will show environmental effects. However, the behaviour of the T851 material seems to be stable in the presence of corrosive environments, a fact which is substantiated by the alloy's stress corrosion performance (discussed shortly).

In the work by Pettit et al. (1974), 2024-T851 in various thicknesses was tested in humid air and salt water at frequencies varying from 20 Hz down to 0.1 Hz. No effect of frequency or environment was noted except in cases where the specimens were tested with very high gross stresses. In these cases, the plate tended to delaminate along grain boundaries in the short transverse grain direction. This splitting seemed to impede fatigue crack propagation rates. Athiniotis (1999) observed similar evidence in stress corrosion / fatigue interactions in service components; such an influence is expected and occurs even without environmental attack. Clark (1976) reported reductions in fatigue crack growth rates associated with path deviation in a steel with strong laminar structure oriented normal to the fatigue crack growth direction.

Figures 23, and 25-26 all show the tight families of data for a variety of environments studied by several aerospace companies, including Lockheed, McDonnell Douglas, and Rockwell. Figure 24 gives an idea of where the Lockheed Forman curves fall compared to the data from which they were derived.

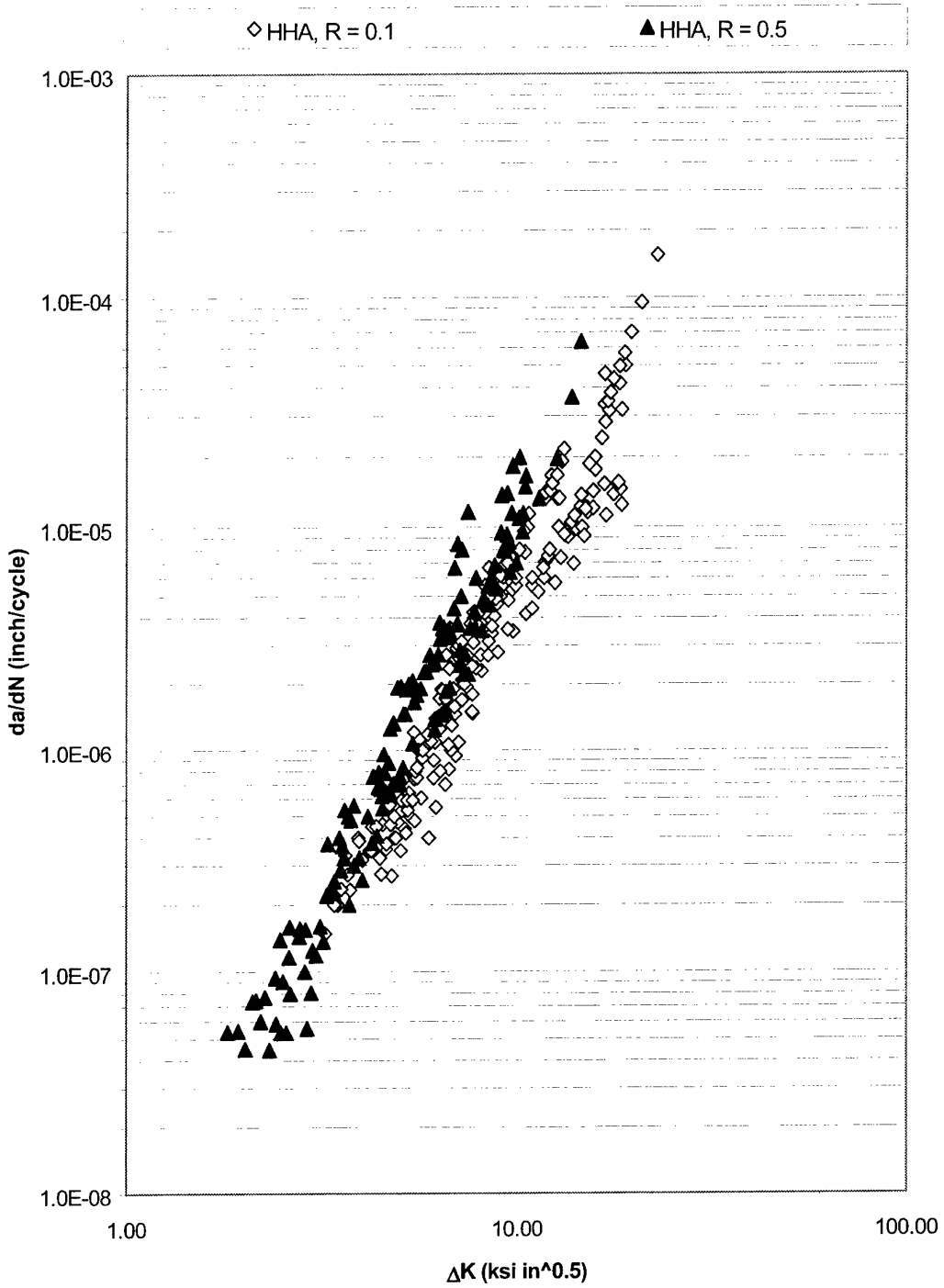

Figure 22. FCG growth rates for 2024-T851 in humid air [Krupp et al. 1974].

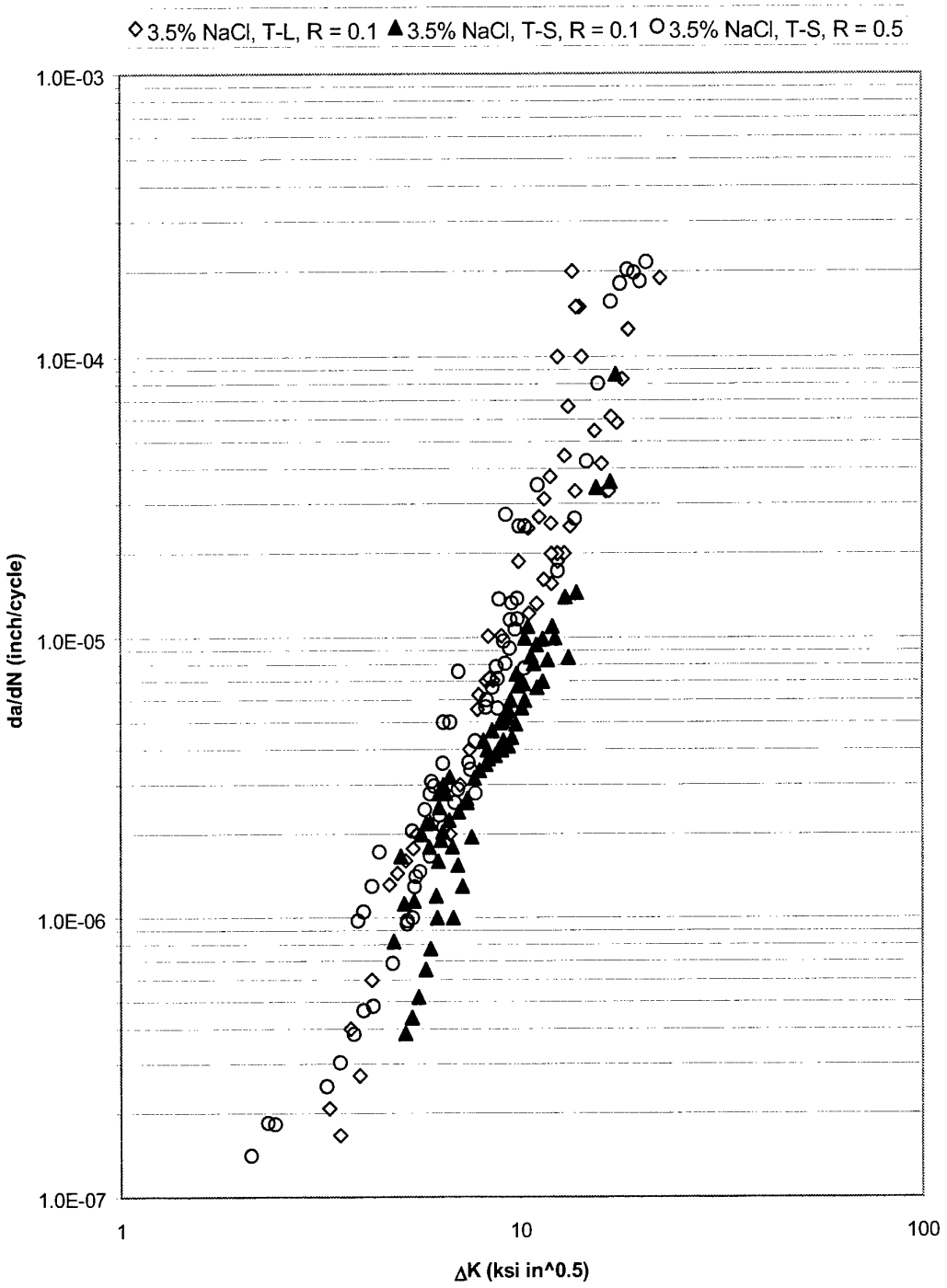

Figure 23. FCG data for 2024-T851 tested in 3.5% salt water [Krupp et al. 1974].

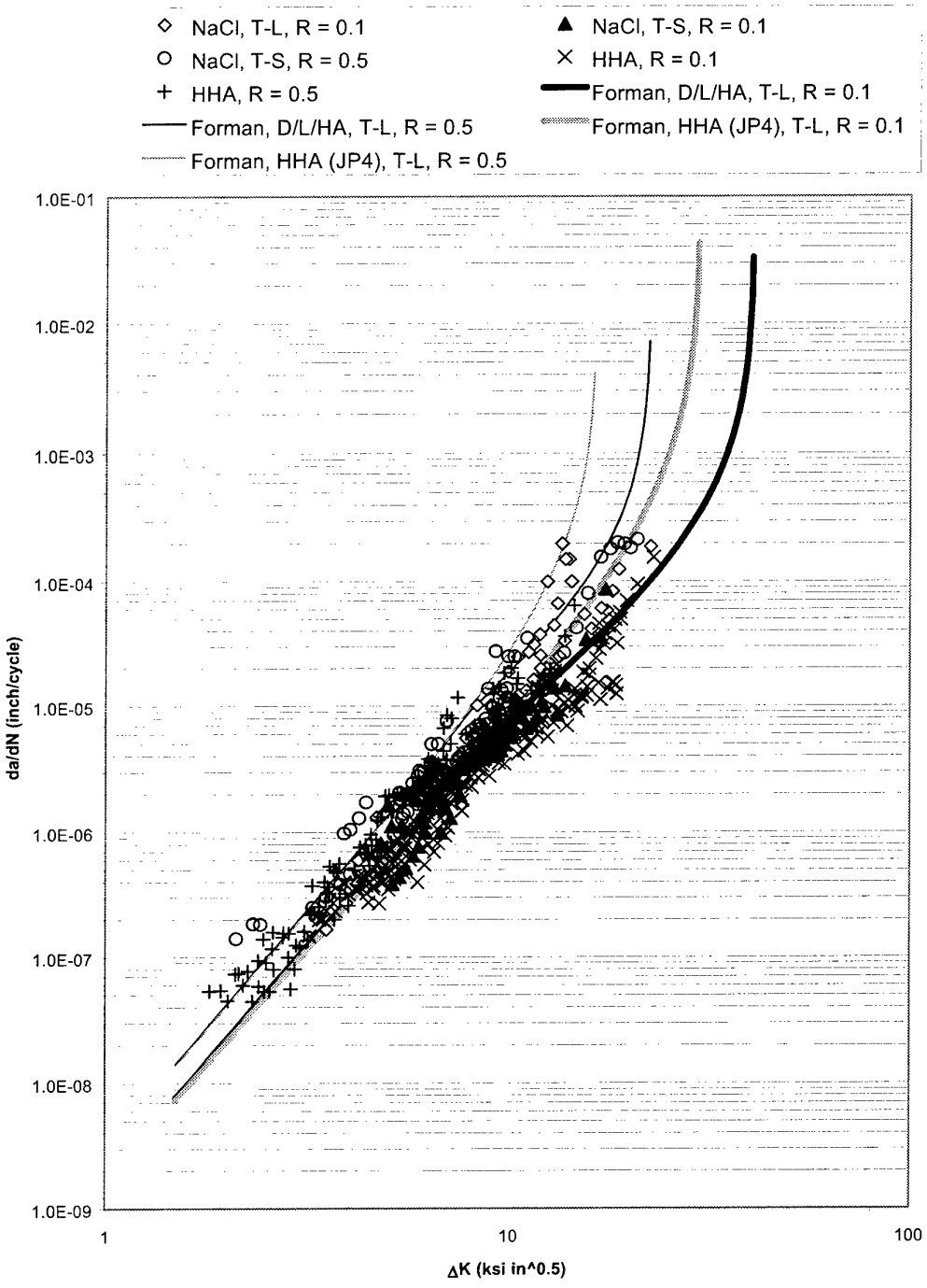

Figure 24. FCG data for 2024-T851 in humid air and NaCl [Krupp et al. 1974] shown with Forman curve fits [Ball and Doerfler 1996].

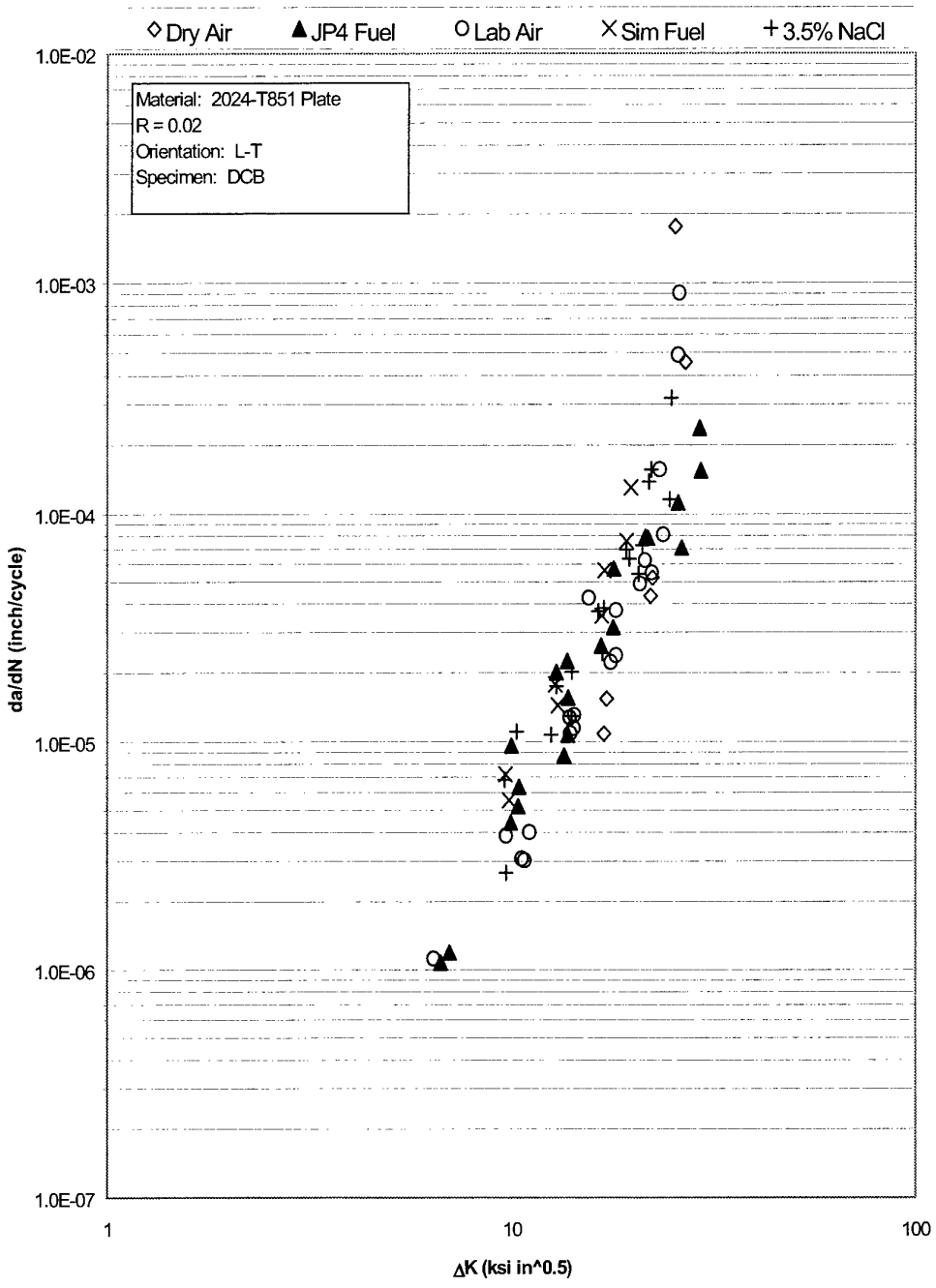

Figure 25. FCG data for 2024-T851 as generated by McDonnell Douglas for several chemical environments [MDC-A0913 1971].

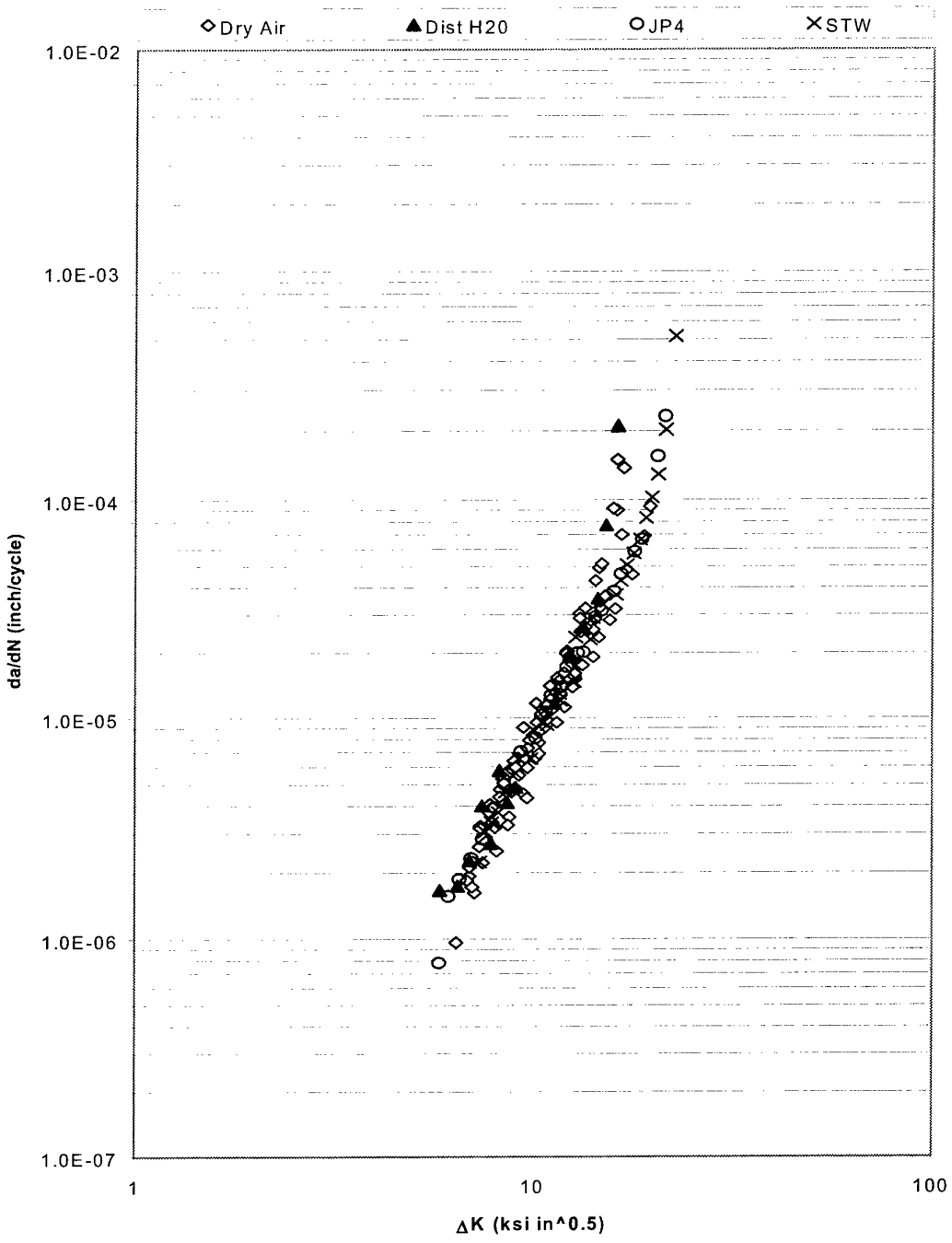

Figure 26. FCG data for 2024-T851 for various chemical environments [Cawthorne 1974].

4.6.2 Fatigue Crack Growth in 7075-T6xx

7075-T6 is probably one of the most widely researched aluminium alloys in the aerospace industry, so only a handful of data are presented here to illustrate the key points. The first plot (Fig. 27) shows the basic Damage Tolerance Design Handbook data used by Lockheed to generate the Forman curves for two different stress ratios at R = 0.1 and R = 0.5. The solid lines represent the Forman curves from Ball and Doerfler (1996).

The next two plots (Figures 28-29) are from two different sources and cover additional stress ratios. The Lockheed Forman curve fits are overlayed for reference. In Figure 28, data by Hudson and Newman (1973) show that the R = 0.02 data they obtained matches reasonably well the lower Forman curve by Lockheed. However, the data for R = 0.5 as found by Hudson and Newman is up to three times faster than the Lockheed Forman curve. It is difficult to draw any conclusions from only two data sets; perhaps scatter is responsible. Also, both sets of experiments were done in 'laboratory air,' so it is possible that differences in humidity levels (known to cause significant variation in fatigue crack growth rates) between the testing centres could cause a substantial difference in alloy behaviour.

Figure 29 shows a comprehensive set of data spanning multiple stress ratios as compiled by Abelkis (1982) from McDonnell Douglas. The data includes a fair amount generated at negative stress ratio, and these data follow the lower Forman curve for R = 0.1 fairly well. The data for the higher stress ratios falls well above the Lockheed Forman curve for most of the data range. In particular, the data at low stress intensity ranges shows much faster crack growth than the Lockheed model.

In Figure 30, the effect of product form can be seen for 7075-T6xxx. The graph compares sheet, plate, extrusion, and extruded bar all tested in lab air at R = 0.33. All grain orientations were L-T except the sheet, which was tested in the T-L orientation. Product form does have an effect for this alloy, with the extrusions having a faster crack growth rate than the plate and sheet.

The final graph (Figure 31) is merely an example of the environmental influence of humid air and cyclic wet/dry, artificial acid rain on the fatigue crack growth rate in this alloy. At the lower stress intensities, the more corrosive environments definitely accelerate crack growth over the baseline dry air case. At higher stress intensities, where mechanical tearing forces start to dominate as the crack approaches critical K, the environmental effects dissipate. This is normal behaviour for alloys susceptible to corrosion fatigue. It is also important to note that 7075 in the T6xx temper is very susceptible to corrosion attack including pitting, exfoliation, and SCC. As such, the mechanisms for accelerated crack nucleation discussed earlier apply strongly in this alloy, and there is a wealth of data in the literature on this subject.

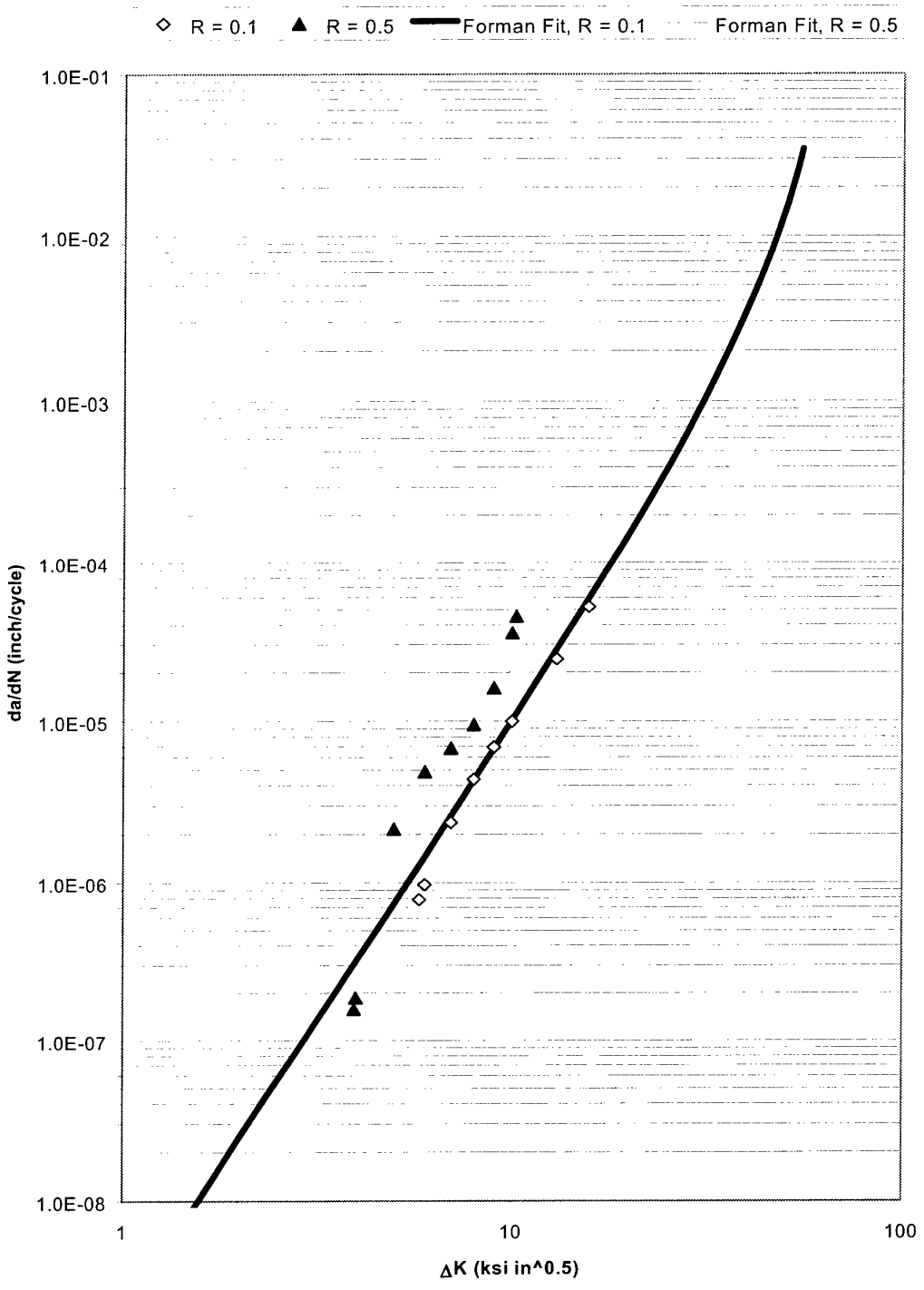

Figure 27. Original data fit used for Lockheed DADTA on F-111 [Ball and Doerfler 1996].

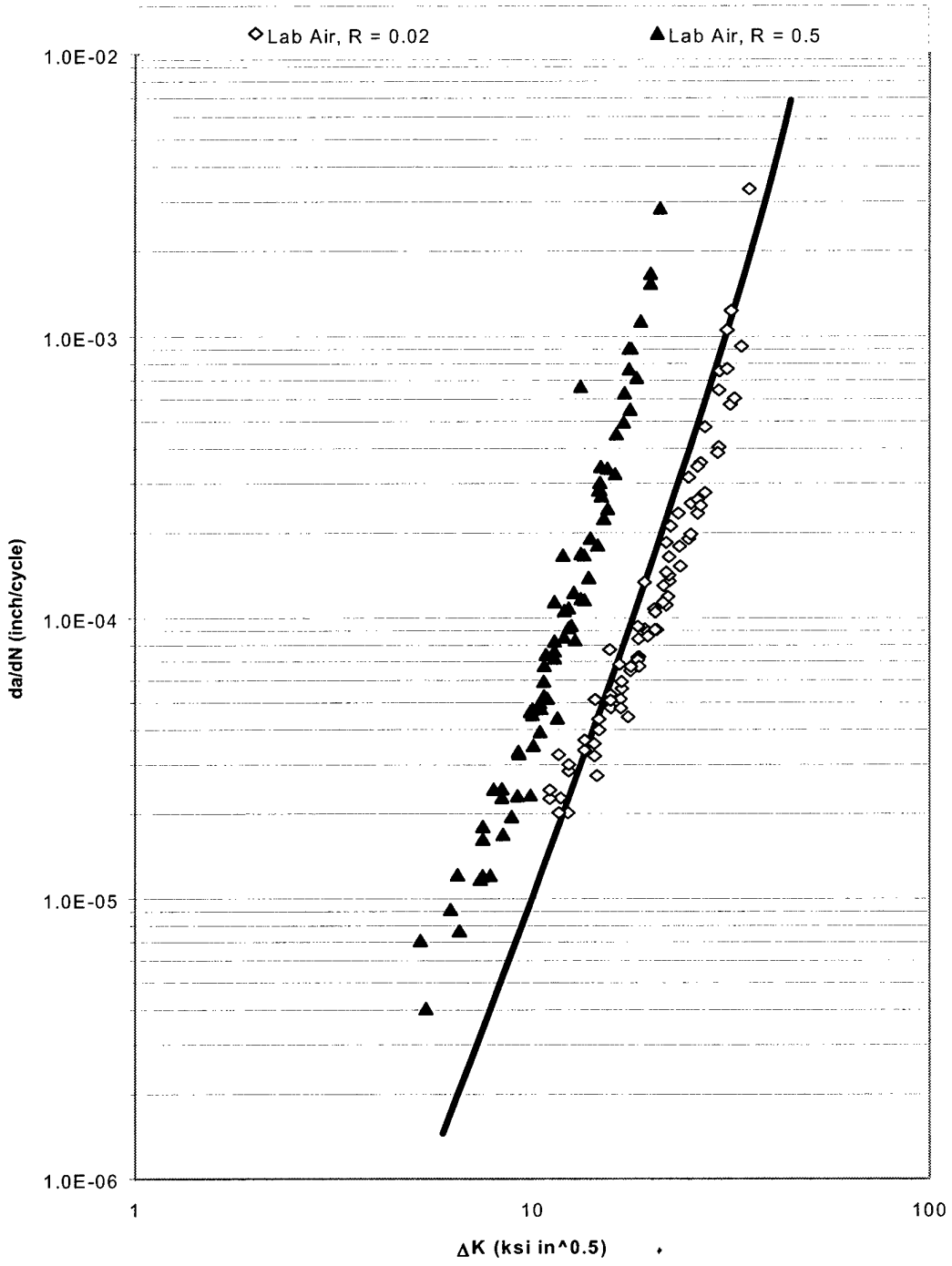

Figure 28. Effect of stress ratio in 7075-T651 fatigued in lab air [Hudson and Newman 1973]. Heavy and light lines are the Lockheed Forman fits for R = 0.1 and R = 0.5, respectively, as shown in Fig. 27.

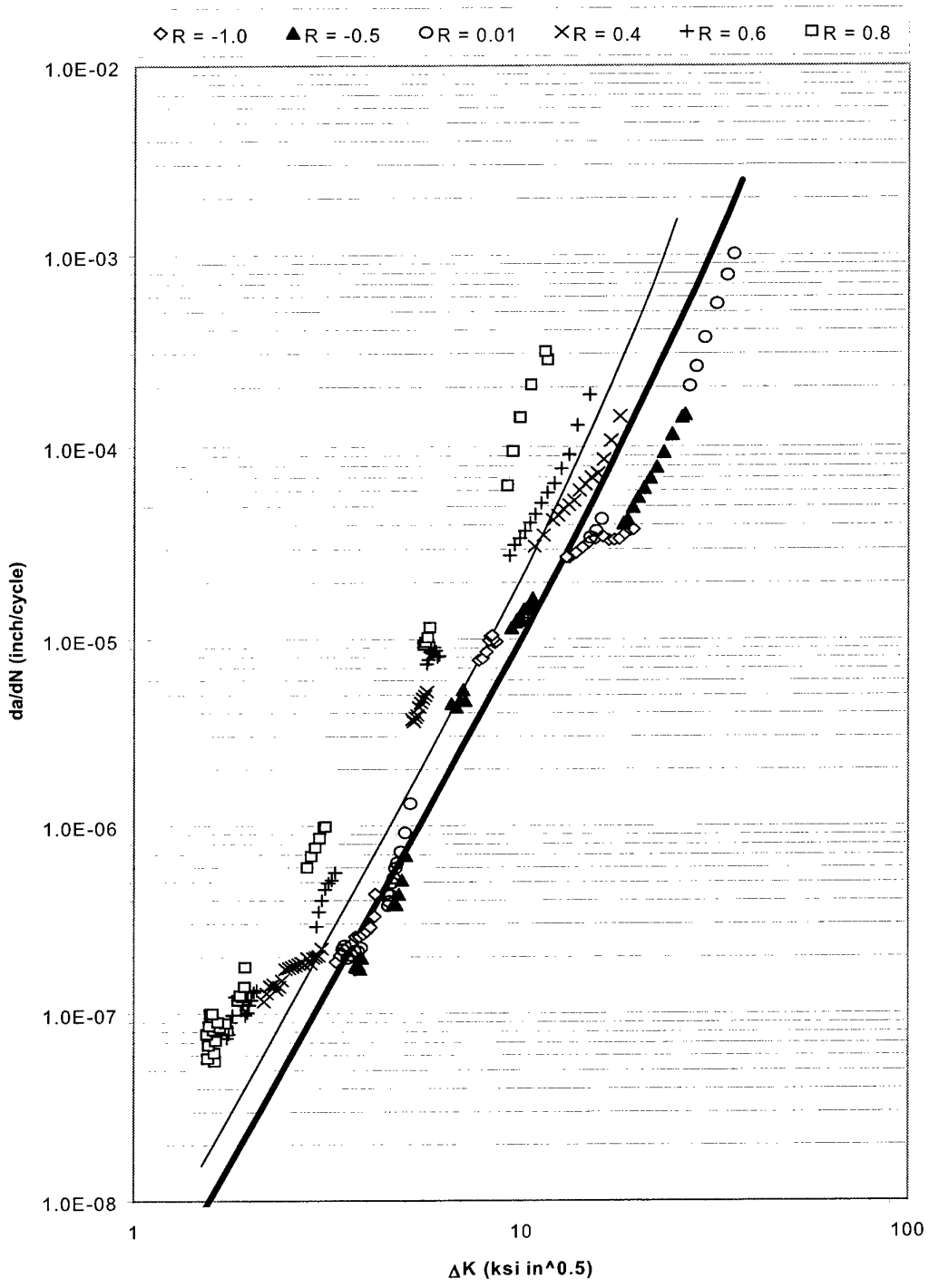

Figure 29. Wide range of stress ratio FCG data in 7075-T6511 [Abelkis 1982]. Heavy and light lines are the Lockheed Forman fits for R = 0.1 and R = 0.5, respectively, as shown in Fig. 27.

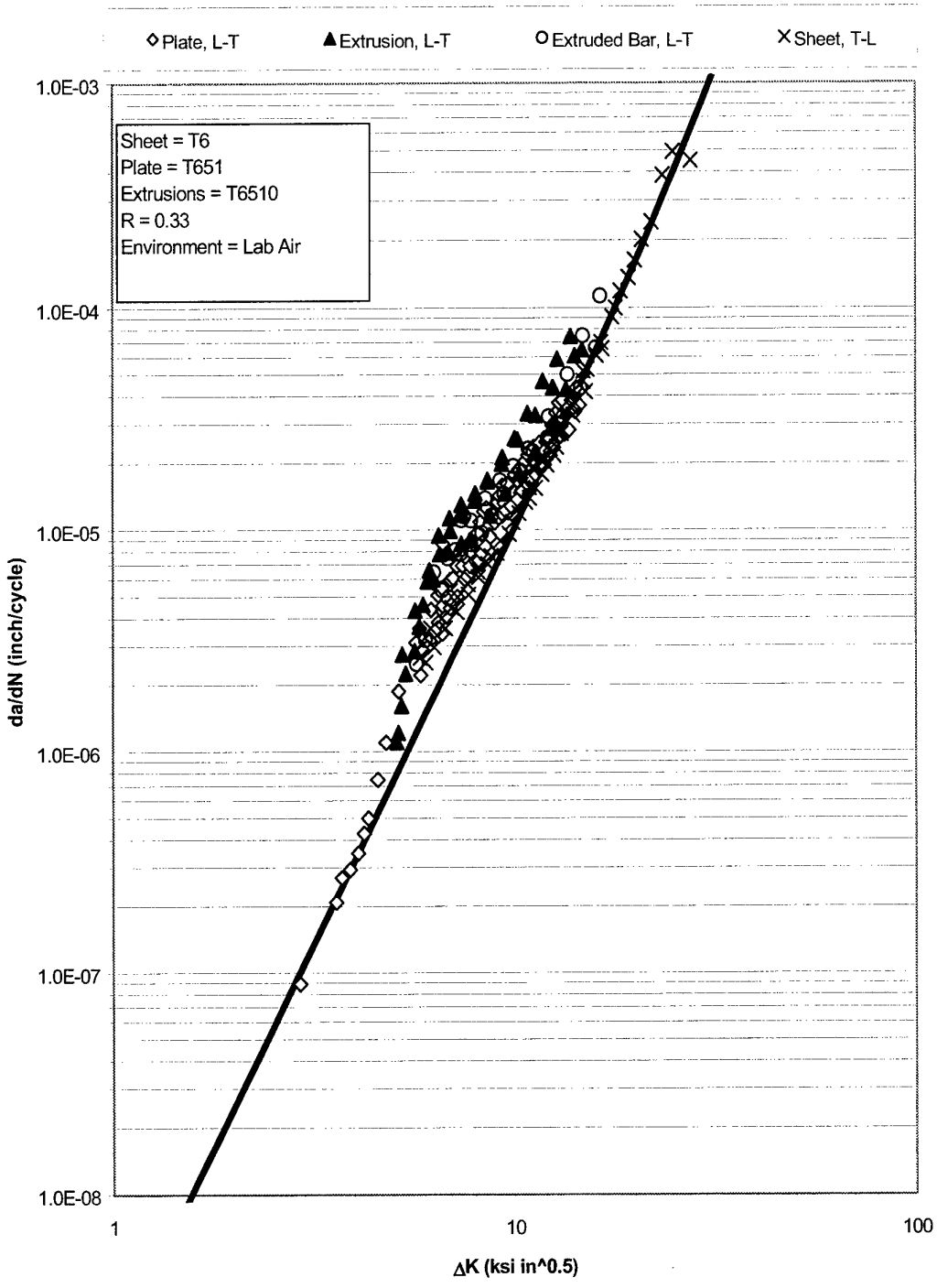

Figure 30. Effect of product form on FCG behaviour in 7075-T6xxx [Bucci 1982]. Heavy and light lines are the Lockheed Forman fits for R = 0.1 and R = 0.5, respectively, as shown in Fig. 27.

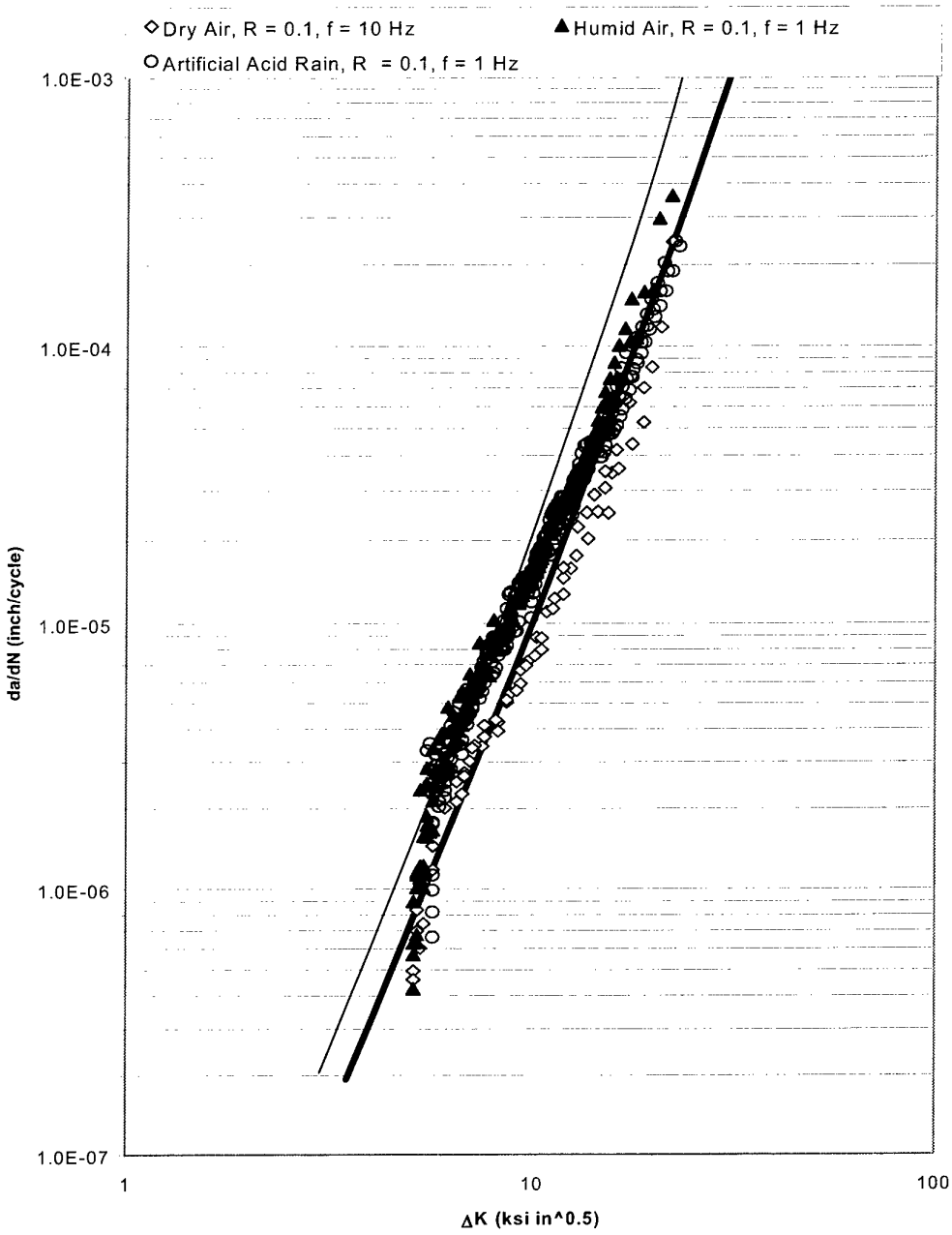

Figure 31. Effect of aggressive chemical environments on FCG in 7075-T651 [Mills 1997]. Heavy and light lines are the Lockheed Forman fits for R = 0.1 and R = 0.5, respectively, as shown in Fig. 27.

4.6.3 Fatigue Crack Growth in 7079-T6xx

The baseline material behaviour for this alloy is shown in Figure 32. This is the data that forms the basis of the F-111 DADTA by Lockheed. The data represents crack propagation in the T-L direction at low stress ratio, and what is probably a relatively benign environment. The problem with using 'laboratory air' as an environment is that it has not been characterised, and small changes in absolute humidity can have profound effects on cracking behaviour in copper-containing, 7xxx-series alloys.

Figure 33 shows environmental influence from a different perspective. Note first that this 7079-T6 behaves very differently from the more environmentally benign 2024-T851. In this study by Speidel (1979), 7079 was tested in saturated salt water at a number of frequencies, some so slow (0.001 Hz) that the mechanisms of corrosion fatigue and SCC probably started to become difficult to differentiate. At each successively lower frequency, the crack growth rates continued to get higher. The specimen orientation was one of the most severe, though, in that the loading direction was in the short transverse grain direction.

Figure 34 compares the crack growth for laboratory air with the more well defined vacuum baseline used by Speidel (1979). The laboratory air growth rates are higher, which shows an environmental effect and further reinforcing the need to quantify all laboratory fatigue environments carefully and control them whenever possible.

Figure 35 shows a good comparison of the effect of different chemical environments. Controlled low humidity air behaves better than 'laboratory air', and as expected, humid air caused a much more rapid crack growth rate on par with salt fog.

Figure 36 summarises traditional stress ratio dependence on crack propagation rates. Although the product forms are slightly different (T6 sheet, T651 plate, and T652 forging), the stress ratios of 0.05, 0.33 and 0.5 are all represented and show the expected behaviour. Brownhill et al. (1970) tested some at Alcoa, and the rest were tested by Smith (1966) at Boeing.

Figures 37 and 38 (Brownhill et al. 1970) show the effects of specimen orientation on crack propagation rates. In both graphs, the data for crack propagation in the short transverse direction (T-S or L-S) has the slowest rates. The highly flattened grain direction in this orientation makes a natural barrier to fatigue crack propagation.

The data in Figure 33 by Speidel (1979) illustrates how much more sensitive and rapid crack propagation becomes when the loading is in the short transverse direction. Residual and fit-up stresses are the most common cause for loads in this direction, and the less-tortuous crack paths offered by S-L or S-T loading make this the preferred orientation for SCC in particular, which is really the biggest problem for the F-111 in this alloy. Unfortunately, there does not seem to be any information available obtained from testing actual F-111 components. Spectrum loading data is also missing.

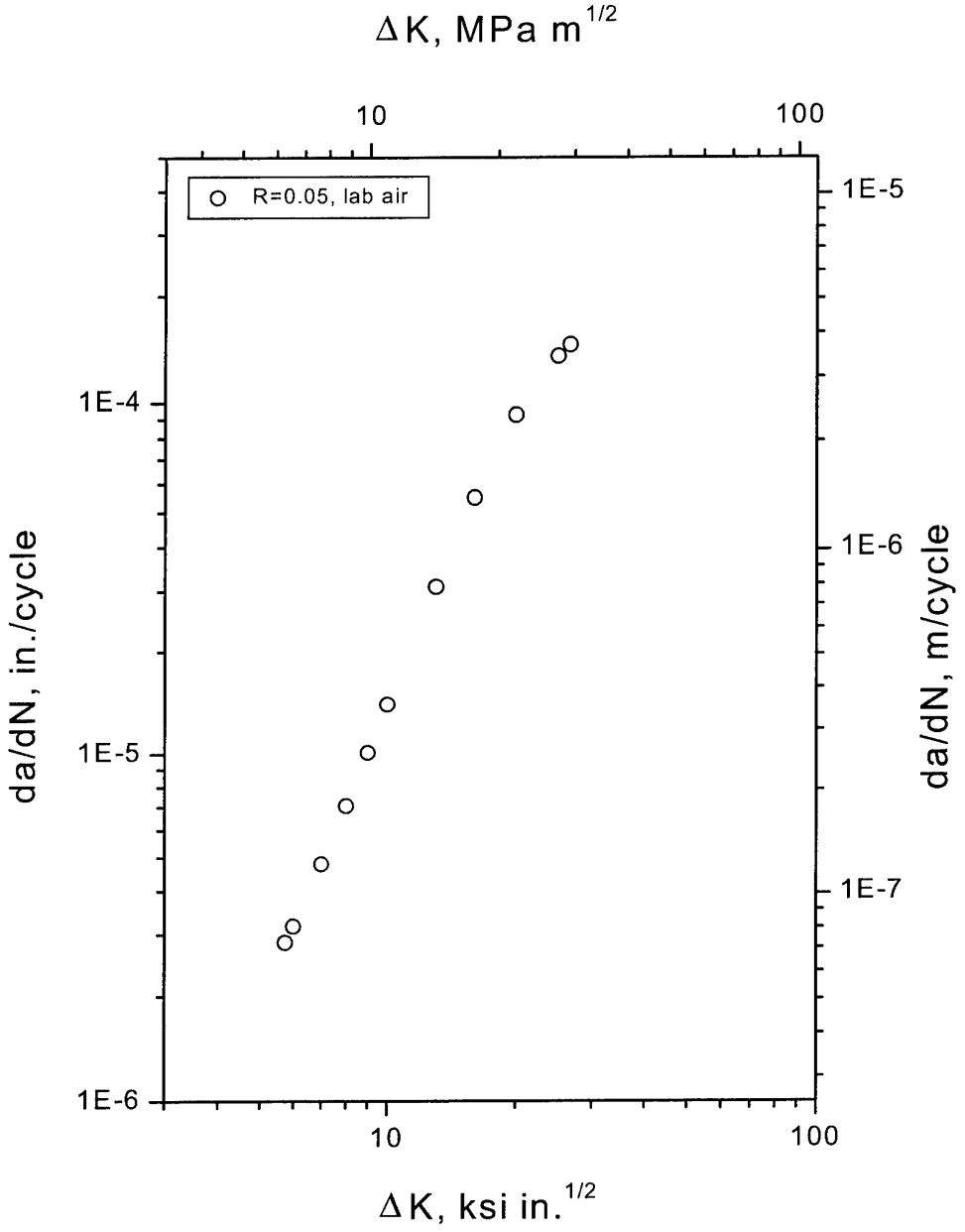

Figure 32. Fatigue crack growth in laboratory air, Al Alloy 7079-T6, R=0.05, T-L orientation [Ball and Doerfler 1996].

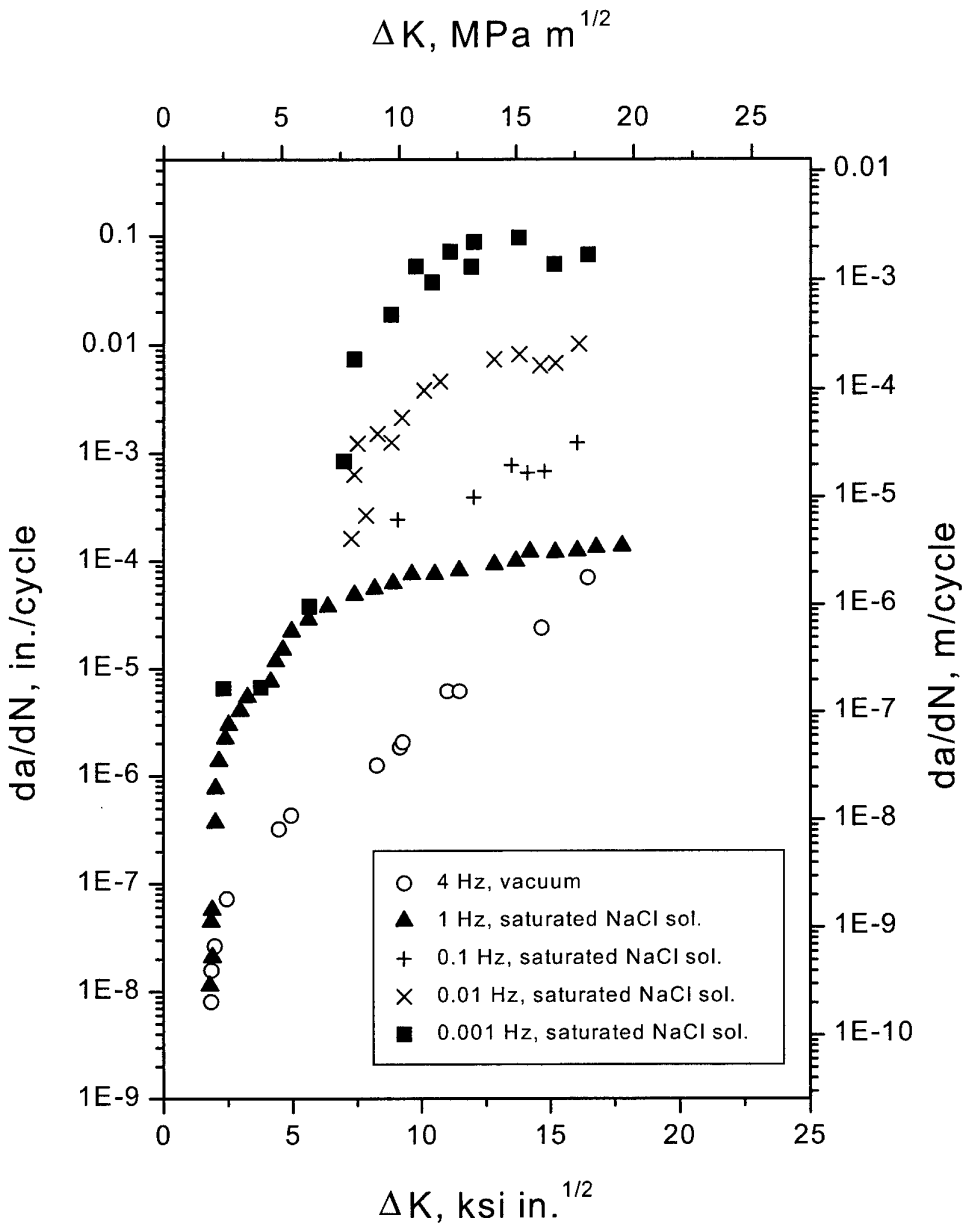

Figure 33. Crack growth in 7079-T651 in vacuum and saturated salt solution under different frequencies. R=0, S-L orientation, K_{IC}=21 MPa$\sqrt{m}$, 23°C [Speidel 1979].

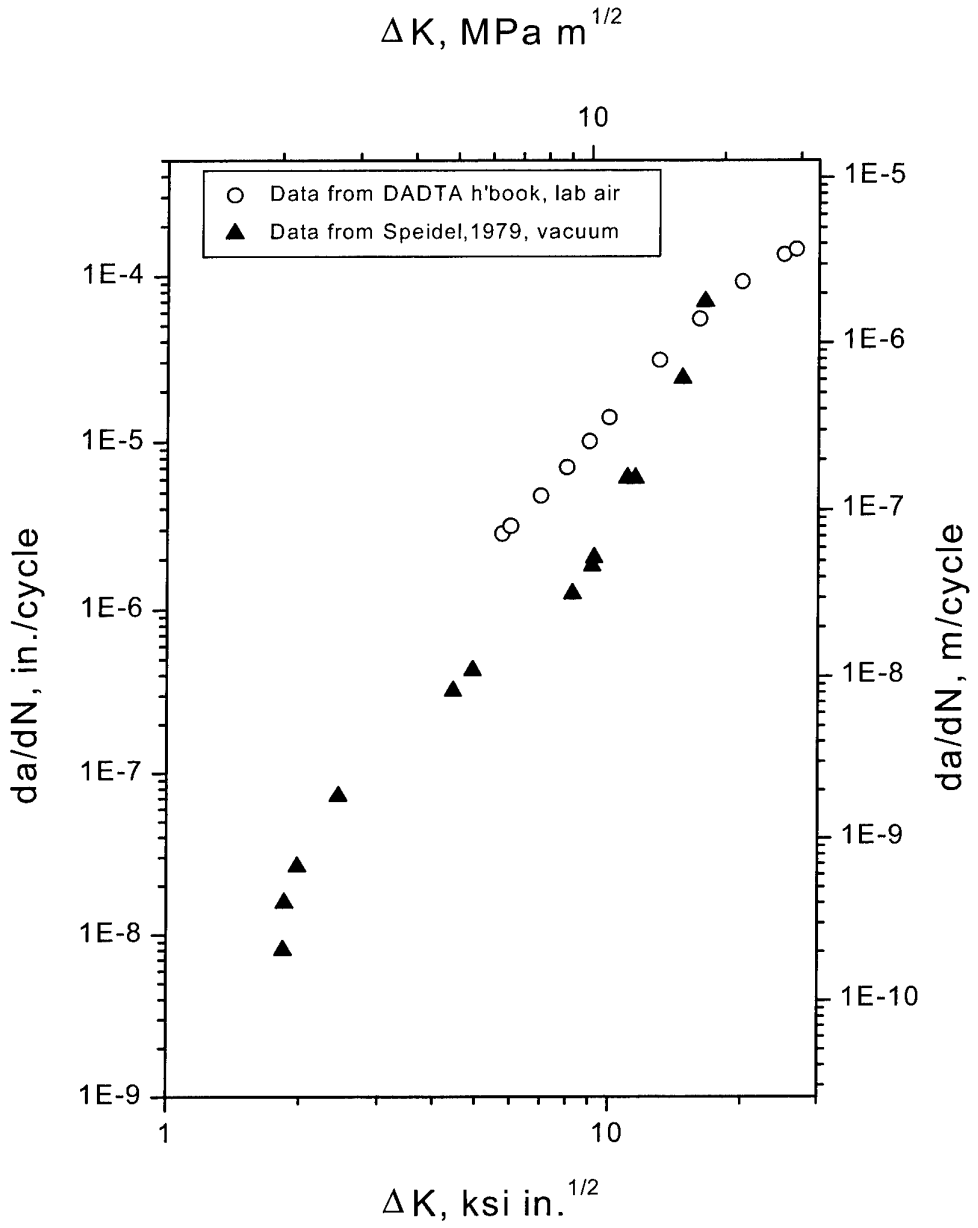

Figure 34. Comparison between crack growth in vacuum and laboratory air. Note that the laboratory air increases the crack growth rate.

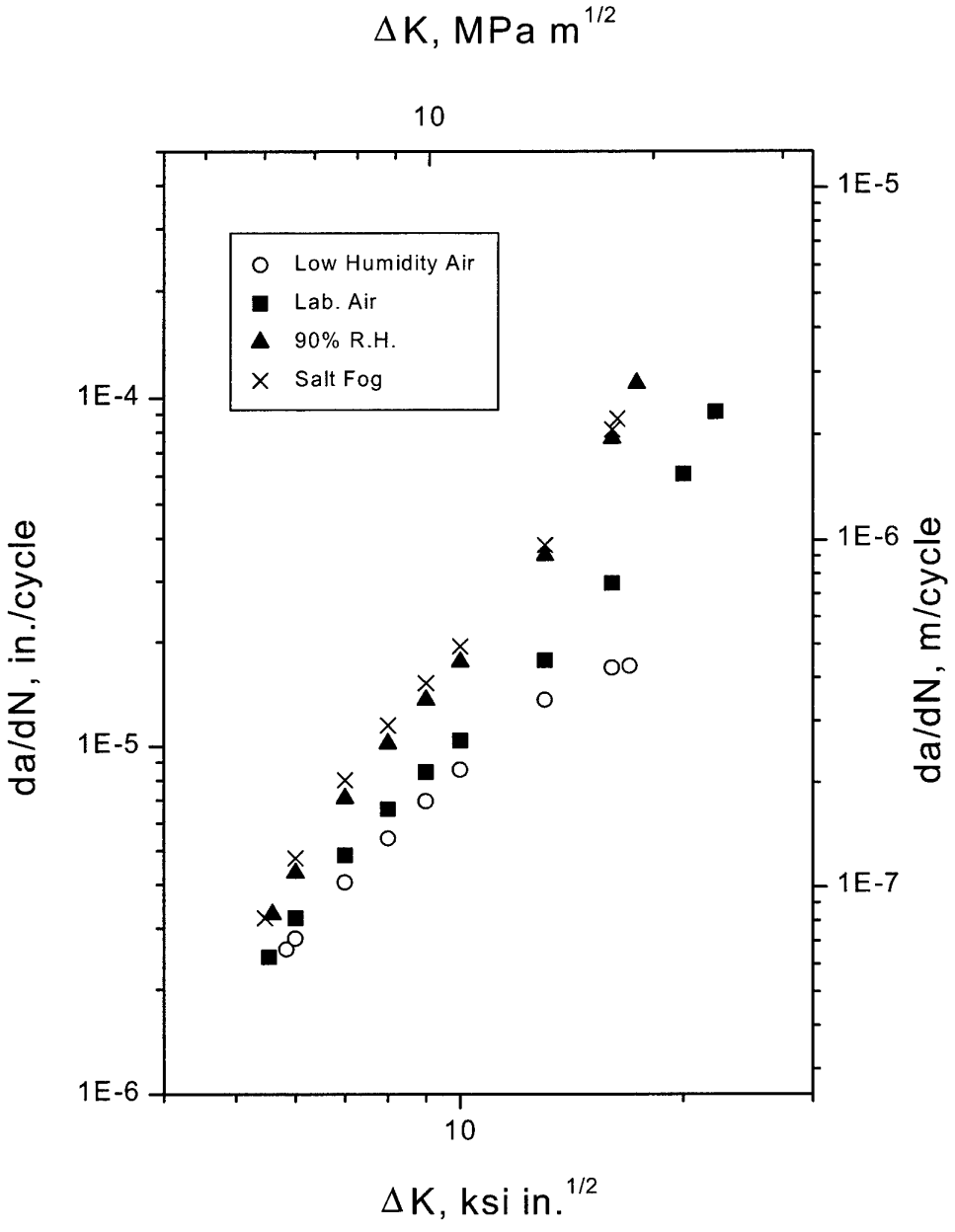

Figure 35. Effect of various environments on fatigue crack growth rates. Note that the high-humidity air is severe as salt fog [MCIC-HB-01R 1983].

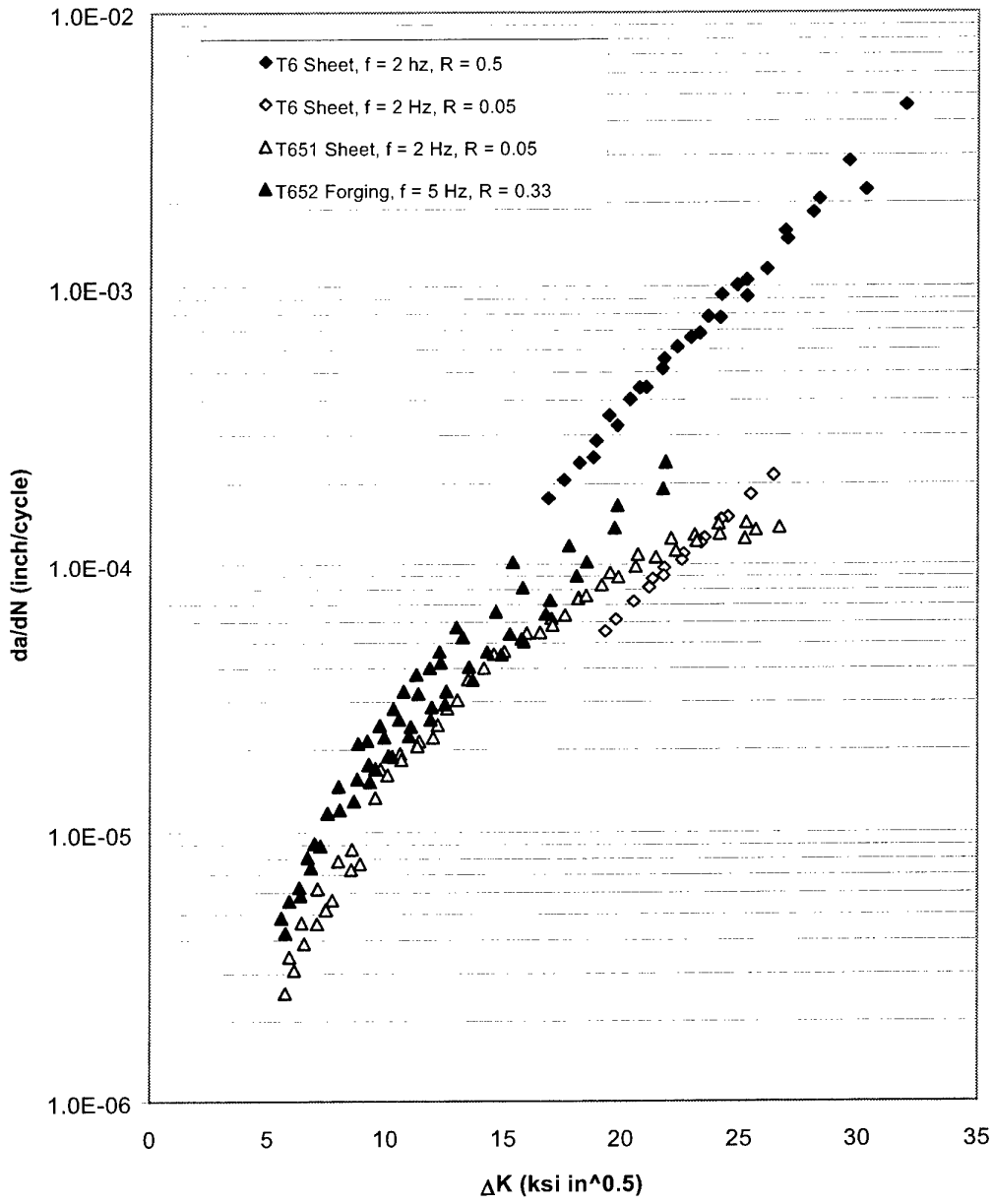

Figure 36. Effect of stress ratio on crack propagation in 7079-T6xx, L-T direction [Smith 1966, Brownhill et al. 1970].

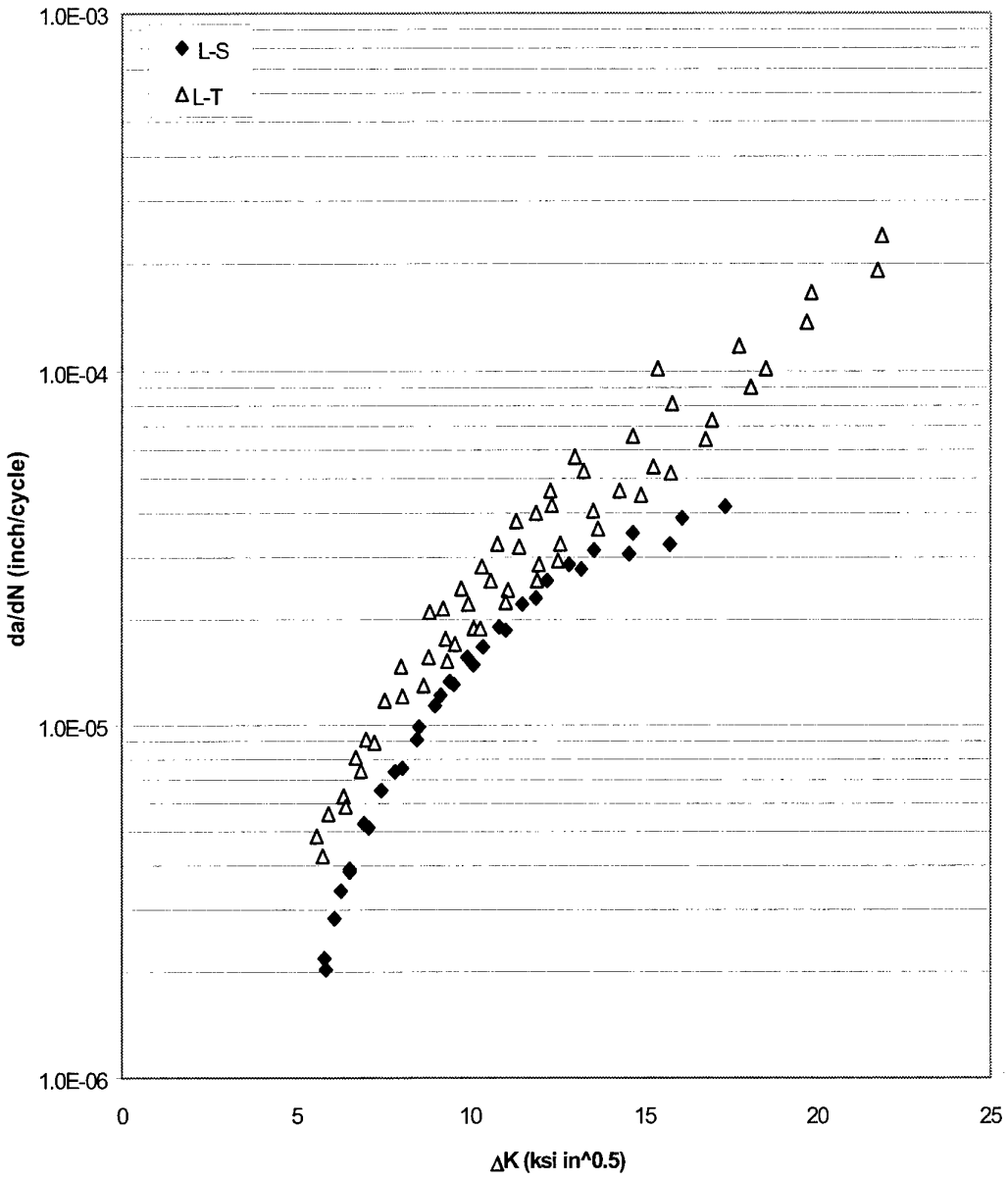

Figure 37. Comparison of fatigue crack propagation rates in 7079-T652 forging in the L-S and L-T orientations, lab air, R = 0.33, 5 Hz [Brownhill et al. 1970].

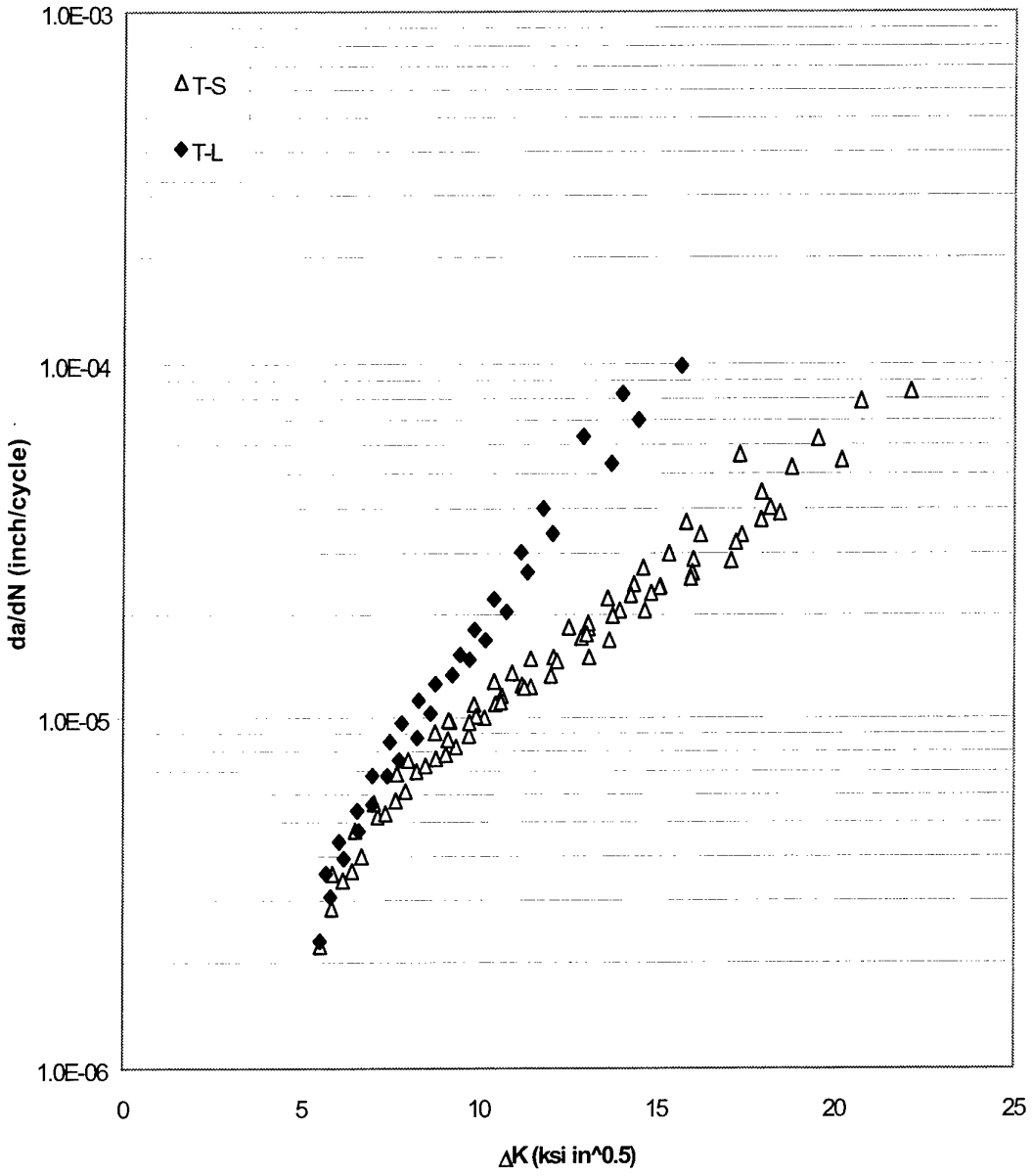

Figure 38. Comparison of fatigue crack propagation rates in 7079-T652 forging in the T-S and T-L orientations, lab air, R = 0.33, 5 Hz [Brownhill et al. 1970].

4.7 Fatigue Crack Growth Threshold

The threshold stress intensity range, ΔK_{TH}, for all three aluminium alloys in this report was measured to be 1.5 ksi$\sqrt{in}$ at R=0 [Ball and Doerfler 1996]. This value agrees well with the value reported in [Speidel 1979], where it is ~ 1.8 ksi$\sqrt{in}$ for R=0. A wide variety of research has been conducted on fatigue crack growth threshold in 7075-T6 and 2024, but in the naturally-aged T3 condition. Wanhill (1988) conducted one of the more comprehensive efforts for 2024-T3. Wanhill's tests were all conducted in laboratory air, whereas another effort by Stanzl, Mayer and Tschegg (1991) looked at the effects of humidity on threshold in the same alloy. These latter tests were unusual, though, in that they used ultrasonic resonance fatigue at 20 000 Hz and therefore are of questionable relevance. An earlier effort by Mackay (1979) looked at threshold crack growth in 2024-T3 and 7075-T6. The results of these three researchers are summarised in Table 12 for different stress ratios and environments.

Table 12. Fatigue crack growth threshold values for two common aluminium alloys.

Reference	Alloy	Thickness inch (mm)	R	Environment	ΔK_{th} ksi $\sqrt{in}$	ΔK_{th} MPa $\sqrt{m}$
Wanhill (1988)	2024-T351	1.18 (30)	0.1	Lab Air	2.59	2.85
Wanhill	2024-T3	0.157 (4)	0.1	Lab Air	2.91	3.20
			0.5		1.97	2.17
Wanhill	2024-T3 clad	0.149 (3.8)	-1	Lab Air	5.16	5.67
			0		2.72	2.99
			0.625		1.68	1.85
Wanhill	2024-T3	0.090(2.3)	-2	Lab Air	7.54	8.29
			-1		5.37	5.90
			0		3.05	3.35
			0.5		1.80	1.98
Stanzl et al. (1991)	2024-T3	0.157 (4)	-1	40-60% RH	1.91	2.1
			-1	Dry Air	3.00	3.3
			-1	Vacuum	2.09	2.3
Mackay (1979)	2024-T3	0.090 (2.3)	.05	45% RH	3.20	3.52
			0.2		2.50	2.75
			0.4		2.10	2.31
			0.6		1.70	1.87
Mackay	7075-T6 clad	0.090 (2.3)	0.05	45% RH	2.50	2.75
			0.2		2.20	2.42
			0.4		1.75	1.92
			0.6		1.35	1.48

From Mackay's results (1979), it is apparent that 7075-T6 has a lower threshold for crack growth than its lower strength counterpart, 2024-T3. This is not surprising, since in general, the fatigue resistance of the 7xxx-series alloy is inferior to 2024-T3. Also from Table 12, it is interesting to note that the data from Wanhill shows a much higher threshold than data from the other researchers. However, Wanhill's paper handles the adjustment of the reported values of ΔK_{th} for closure to derive $\Delta K_{eff,th}$ separately. Table 13 shows how the values in Table 12 are affected by adjustment for crack closure. These values are more in agreement with the other researchers, although the others do not discuss closure in their estimates of threshold.

Greatly diminished by adjusting for closure is the R dependence for threshold. This should be expected to a degree, since Newman's (1981) plane strain model was used to correct the data. This model has the effect of collapsing all the data for the entire stress intensity range at different R-values down to 'one' curve.

Table 13. Wanhill's (1970) data adjusted for crack closure effects.

Alloy	Thickness inch (mm)	R	ΔK_{th} ksi √in (MPa √m)	$\Delta K_{eff,th}$ ksi √in (MPa √m)
2024-T351	1.18 (30)	0.1	2.59 (2.85)	2.13 (2.34)
2024-T3	0.157 (4)	0.1	2.91 (3.20)	2.38 (2.62)
		0.5	1.97 (2.17)	1.94 (2.13)
2024-T3 clad	0.149 (3.8)	-1	5.16 (5.67)	2.11 (2.32)
		0	2.72 (2.99)	2.04 (2.24)
		0.625	1.68 (1.85)	1.68 (1.85)
2024-T3	0.090(2.3)	-2	7.54 (8.29)	2.28 (2.50)
		-1	5.37 (5.90)	2.20 (2.42)
		0	3.05 (3.35)	2.28 (2.51)
		0.5	1.80 (1.98)	1.77 (1.94)

All the values for threshold at or near R = 0 as measured by these three researchers are greater than the value used in the F-111 DADTA. The data used by Lockheed is likely to be slightly conservative.

4.8 Stress Corrosion Cracking Behaviour

The following pages summarise stress corrosion cracking performance for the three aluminium alloys covered in this report. Most of the information is provided as threshold stress intensity values, K_{IEAC} (formerly known and often referred to as K_{ISCC}). Some stress corrosion crack growth rate data was obtained for 7079-T651 and for 7075-T651, and the graphs are included from other sources.

4.8.1 SCC in 2024-T851

Only a few records of stress corrosion cracking data have been found for 2024-T851. Part of the data has come from the same McDonnell Douglas report (1971) as the FCG data referenced earlier in this report. Actual growth rate curves were not found in the database. Instead, only threshold stress intensity values for SCC were provided, as shown in Table 14. These values are essentially the same as the critical toughness of the material for the L-T orientation. Note that the threshold values are somewhat lower for the less-favourable S-L grain orientation. Product thickness was one inch.

Table 14. K_{IEAC} values for 2024-T851 [MDC-A0913 1971, Sprowls et al. 1973**].*

Environment	K_{IEAC} (ksi $\sqrt{in}$)	Grain Orientation
Air 78% Relative Humidity*	22	L-T
Distilled Water*	22	L-T
JP4 Fuel*	21	L-T
3.5% NaCl*	21	L-T
Industrial Atmosphere**	16	S-L
Salt Dichromate Acetate**	15	S-L
Seacoast Atmosphere**	16	S-L

The results of these experiments seem to agree well with Pettit et al. (1974) who concluded that 2024-T851 is not susceptible to stress corrosion cracking. Note that the K_{IEAC} values arrived at for the L-T grain orientations are very close to the plane-strain fracture toughness values, K_{Ic}, measured for this material. In their study, they held specimens under loads so high they approached 0.98 of the critical stress intensity with negligible crack propagation in 3.5% salt water.

4.8.2 SCC in 7075-T6xx

Table 15 gives examples of stress corrosion cracking threshold data for 7075-T651. In most cases, the values are for plate material, with one added for extrusions (noted). These data come from four different references. As with 2024-T851, the threshold values are substantially lower for the less-favourable S-L grain orientation. The S-L threshold values get quite low for 7075-T651 as compared to 2024-T851 showing the greater tendency for intergranular attack and SCC in the peak-aged T6 temper.

4.8.3 SCC in 7079-T6xx

Alloy 7079, especially in the T6 or T651 tempers, is very susceptible to SCC. Nordmark et al. (1970) observed stress corrosion cracking occur in a laboratory air environment. Hyatt (1969) measured the stress corrosion crack growth rate during repeated immersions of double-cantilever beam (DCB) specimens in 3.5% NaCl solution, which proved to be exceptionally high and approached 12.7 mm (½ inch) per hour. The stress corrosion crack growth rates for 7079-T651, 7075-T651 and 2024-T351

are compared in Figure 39. The reduced susceptibility to SCC with change in heat treatment in 7075 from T651 (peak aged condition followed by 1%-3% stretching of the alloy) to T73 (over-aged condition) may be seen in Figure 40.

Table 15. K_{IEAC} values for 7075-T651 [MDC-A0913 1971, NRL** 1968, Sprowls et al.** 1973, Proctor and Paxton*** 1969].*

Environment	K_{IEAC} (ksi $\sqrt{in}$)	Grain Orientation
Air 74% Relative Humidity*	25	L-T
Distilled Water*	24	L-T
3.5% NaCl*	28	L-T
3.5% NaCl**	19	S-L
3.5% NaCl**	17	S-L
Industrial Atmosphere**	10	S-L
Salt Dichromate Acetate**	5	S-L
Seacoast Atmosphere**	10	S-L
Ethanol***	9	T-L (extrusion)

Lauchner (1971), who compared SCC susceptibility of 7079-T6, 7075-T6 and -T73, 7175-T736, 7049-T73, 7001-T75 and -T73 forgings, also observed that 7079-T6 alloy was most sensitive to SCC. If SSC proves to be a problem in the desired application, Lauchner recommended replacing the alloy with 7075-T73. However, 7075 in the -T73 condition has approximately 15% lower strength than in the -T6 peak aged condition.

Alloy heat treatment, more than alloy composition, has more pronounced effect on the susceptibility to SCC. Overaging treatments of the -T7, -T736 and -T73 variety were developed specifically to avoid SCC problems [Speidel 1979]. However, neither the composition nor the heat treatment can render the alloys completely immune to SCC.

Chu and Wacker (1969) measured the K_{ISCC} of 7079-T6 alloy to be 5.5 ksi$\sqrt{in}$ in L-T and S-T directions. This value compares well to 7075-T6 where the $K_{ISCC} \approx 6$ ksi$\sqrt{in}$ when measured under similar conditions. Hyatt (1969) estimated K_{ISCC} to be about 3 ksi$\sqrt{in}$ during repeated immersions of DCB specimen in 3.5% NaCl solution.

In many high-strength aluminium alloys (and D6ac steel, too) SCC corrosion cracks are normally intergranular, whereas corrosion fatigue cracks are transgranular [Speidel 1979]. However, in lower frequency conditions, corrosion fatigue cracks were observed to propagate along favourably oriented grain boundaries, leading to either completely intergranular or mixed intergranular-transgranular fracture mode.

As alluded to in the previous section on fatigue crack growth in 7079-T6, when frequencies get low enough, it may be difficult to differentiate between corrosion fatigue and SCC. From this, Speidel (1979) proposed a third mode of crack growth where the loading frequency is low enough to approximate essentially sustained load during each cycle.

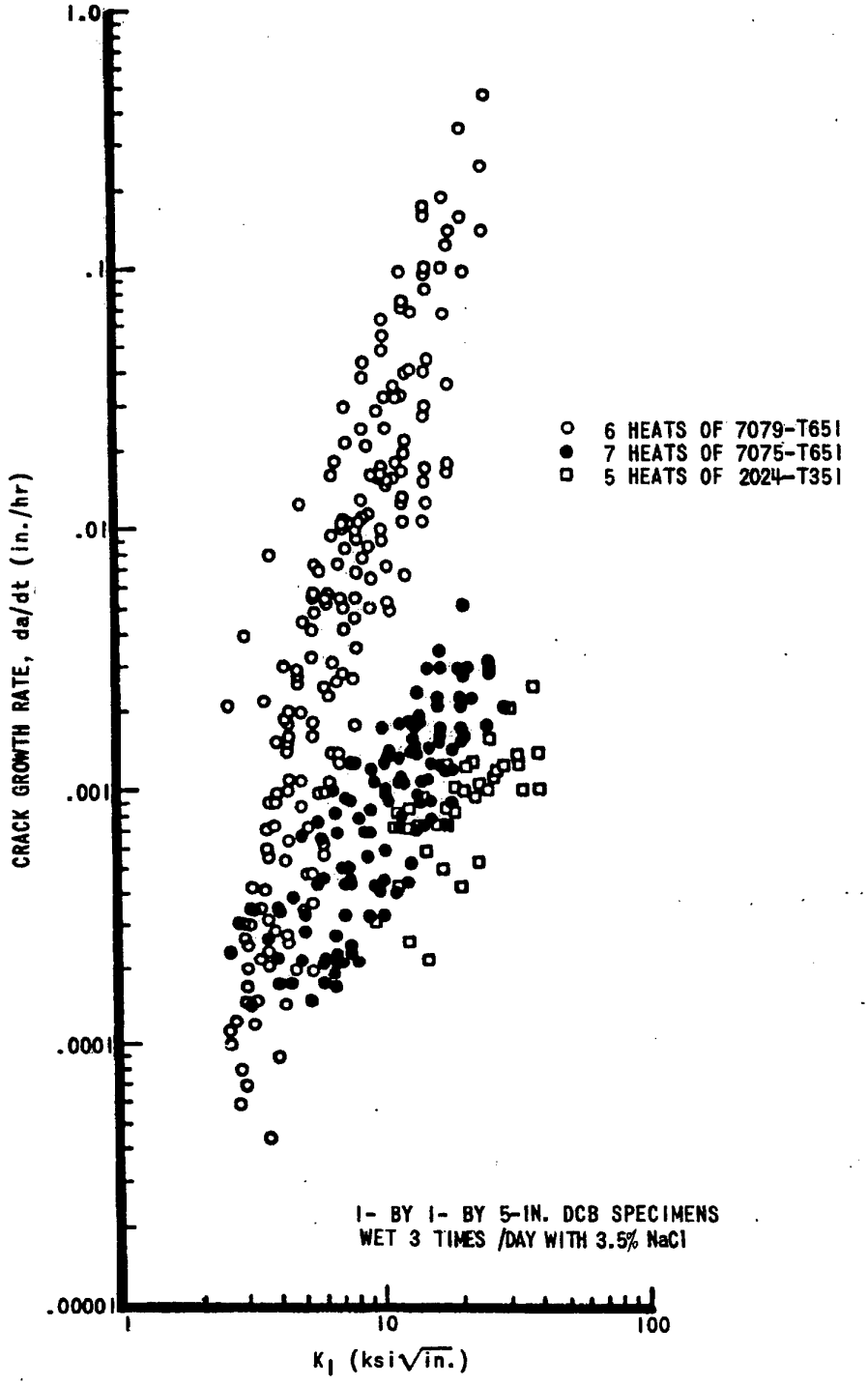

Figure 39. Stress corrosion crack growth rate data for 7079-T651, 7075-T651 and 2024-T351 plate [after Hyatt 1969].

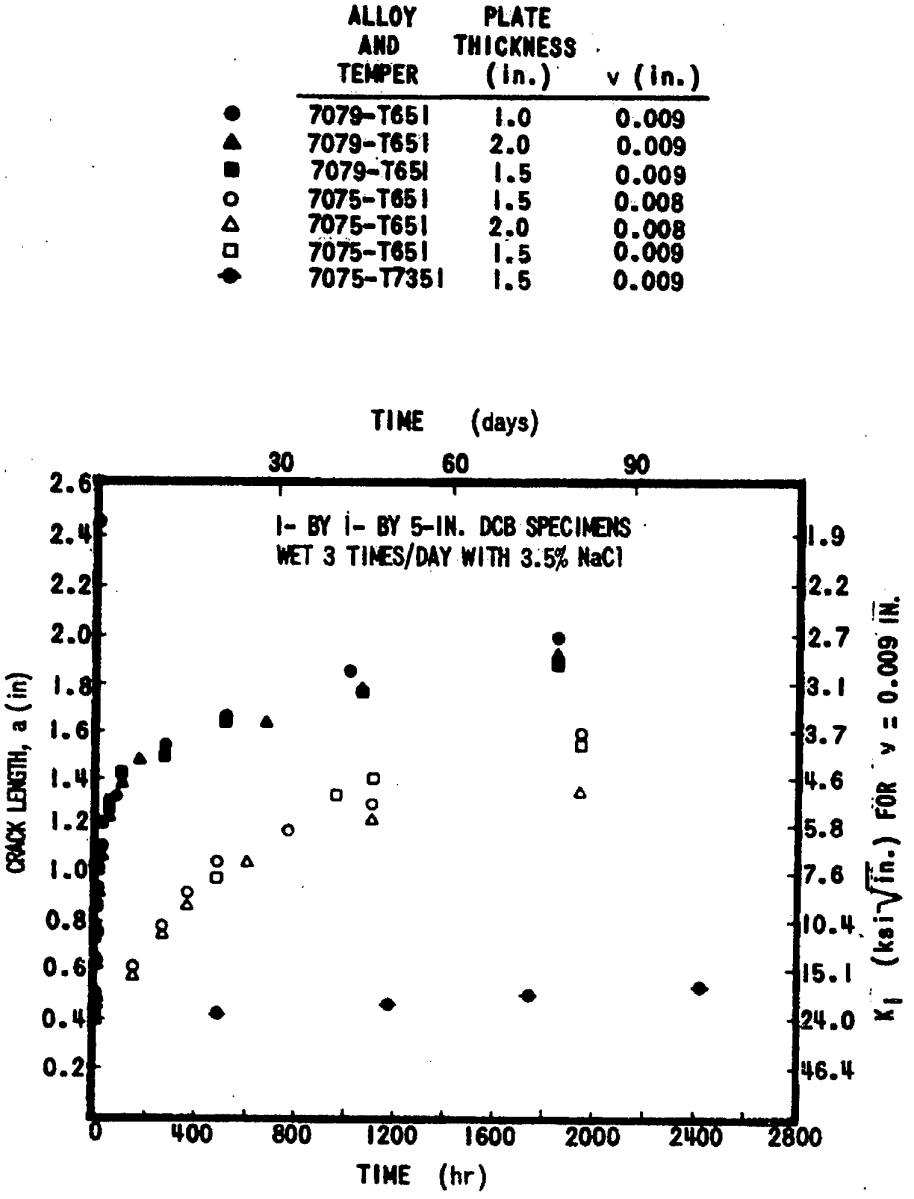

Figure 40. Crack length and stress intensity versus time curves for specimens of 7075-T651, 7079-T651 and 7075-T7351 [after Hyatt 1969].

4.9 Conclusions for Aluminium Alloys

Compared to D6ac steel, information on most aluminium alloys is much more plentiful. The exception to this is 7079-T651, which has not been used in aircraft applications for many years now. The material is so poor, it has been excluded from more recent editions of the Damage Tolerance Design Handbook. Alloy 7079-T651 has the unfortunate distinction of being developed, coming into common use, and then falling from grace during a period when corrosion fatigue research was a lower priority. The advent of damage tolerance in the early 1970s in particular led to reduced corrosion fatigue research in most laboratories except for a few universities. The Aloha airlines accident in 1988 was the rebirth of aging aircraft research, and a heavy focus on corrosion fatigue interactions followed.

The push to defer maintenance to save money and increase aircraft availability has meant that ways to account for corrosion in life and residual strength analyses have been needed. There seems to be no shortage of information on corrosion impacts on crack nucleation in the more common alloys. The information on the uncommon heat treatment, 2024-T851, seems to be harder to come by. This alloy is most common on military aircraft such as the F-111, the USAF B-1B Lancer, and even the Space Shuttle, so it has not populated the literature as much as alloys in wider commercial use.

Fatigue cracking of aluminium components does not appear to be prominent on the F-111 just yet. Some problems have arisen and are being dealt with. Although 2024-T851 is very resistant to environmentally assisted cracking (K_{IEAC} is nearly the same as plane strain fracture toughness in thicker sections, and it shows benign behaviour in corrosion fatigue situations), it is not resistant to other forms of corrosion. In fact, the material rates poorly against corrosion attack. It is important to be on guard for this type of degradation as the F-111 ages. Numerous research efforts into crack nucleation (such as pitting influences on fatigue) are ongoing worldwide including several in-depth studies at DSTO/AMRL.

Most of the cracking damage detected on the F-111 is classified as undefined, as the cause simply was not recorded. It is believed that most of this damage is related to SCC, particularly in the 7079-T651 and 7075-T6xx components. Fortunately for the aircraft, most SCC is in directions less threatening from a structural integrity aspect. DSTO/AMRL efforts suggest that laminar damage in these orientations does not readily generate fatigue cracking. However in some situations SCC and fatigue could act in nearly the same plane, and care must be taken because such a combination could render inspection intervals grossly inadequate.

The material data used by Lockheed for the DADTA on the F-111 seems to agree closely with that found elsewhere in the literature for 2024 and 7075. Most of the literature data for 7079 is limited to older versions of the Damage Tolerance Design Handbook, and this is the same data used by Lockheed.

The fatigue crack growth threshold data found in numerous literature sources for 2024 (although in the T3 condition) and 7075 agrees well with the values used by Lockheed. In fact, the Lockheed DADTA data use a threshold that is conservative compared to what others have found.

The long crack propagation data used by Lockheed for 2024-T851 is actually for high humidity air, even though it is listed as being for JP-4 fuel. It may be desirable to generate data for JP-8 fuel to update the DADTA data set for future management of the F-111. Caution needs to be exercised, however, as such a program would best be carried out using material from the era of F-111 manufacture. It is widely accepted that the 2024 of today is not the same as that of the 1960s. Fracture and fatigue properties of the newer alloys are greatly improved, because they are cleaner.

5. Concluding Remarks

This report gave an overview of the more prominent structural materials in the RAAF F-111 aircraft. Although a wide variety of materials were used in the construction of this machine, the most important are limited to D6ac steel and 2024-T851 aluminium, in that all the Class I critical parts (those whose failure would probably result in the loss of the aircraft) are made from one of these two materials—mostly D6ac. Alloy 7079-T651 has also been included as it is widely used in bulkheads and is very susceptible to stress corrosion cracking.

One of the main objectives was to look at available literature data and compare it with the data used by Lockheed for the DADTA on the F-111. In some cases, literature data was so sparse that it was essentially limited to the same data sources used by Lockheed.

5.1 D6ac Steel

With D6ac steel, especially in the heat treatment used for the F-111, only few sources of data seem to exist. Most of these studies have been limited to fatigue crack growth and stress corrosion cracking studies. The long crack propagation data in the literature seems to agree well with that used by Lockheed. However, crack nucleation studies are woefully deficient, but programs underway in DSTO/AMRL and Aerostructures are covering some important issues.

Fatigue crack growth from corrosion pits is the area of primary concern because pitting is the most threatening form of corrosion to D6ac. Cracking in service as well as in the laboratory has originated from corrosion pits. An interesting fact to note is that the material model used by Lockheed does not predict crack growth (in laboratory specimens) from crack sizes as small as some corrosion pits, whereas the cracks grow in reality. This behaviour of the model indicates possible problems with the near-threshold crack growth data or in the validity of the stress intensity solution for such small crack sizes ($\approx$20 microns). Many researchers point out the sensitivity of threshold data to specimen type, and initial discontinuity size and type, so it may be necessary to revisit the material models and threshold crack growth data for D6ac if corrosion is to be accurately incorporated into life predictions.

Particularly damaging to D6ac is the possibility of pitting leading to SCC rather than or in combination with fatigue or corrosion fatigue. Service examples of this scenario have been uncovered, and the unpredictable nature of SCC makes the situation potentially dangerous. Most of the difficulty associated with predicting SCC rates is in knowing the stress state responsible. Substantial portions of SCC problems are caused by driving forces from residual or fit-up stresses. Every situation, even between similar components, could be unique, especially where fit-up stresses are responsible.

Work at DSTO/AMRL indicates that most laminar cracks (typical of SCC) are not a high fatigue threat since the laminar cracks are typically aligned with the primary loading direction. It is possible, though, for a stress corrosion crack to be perpendicular to the primary load axis (as a fatigue crack would be) and could actually cause fatigue to extend the crack even further. Locations where this could occur should be treated very carefully as inspection intervals in such areas could be rendered unconservative.

Fatigue data for D6ac steel covers a variety of chemical environments including poorly-defined laboratory air, humid air, and JP-4 fuel. The F-111 now uses JP-8 fuel, which has different composition and additives. Many of the critical areas in the aircraft made from D6ac also serve as fuel cells, so it may be worth looking at crack propagation, SCC and threshold behaviour in this new chemical environment. The same could be said for aluminium alloy 2024-T851, the wing skin material.

5.2 Aluminium Alloys

Aluminium alloys are much more widespread in the aircraft industry than D6ac steel, but not necessarily the alloys used in the F-111. Alloy 7079-T651 is avoided in new aircraft. The alloy is no longer made, and as such is no longer included in most references for material property and selection. That alloy, like D6ac, came from the days when static strength really governed aircraft design, so strength-to-weight ratio was the most important.

Alloy 2024 is one of the most common aircraft alloys ever, but the T851 heat treatment used on the F-111 is much less common. Not much literature data was uncovered on this material, but what was found seems to be sufficient for managing the F-111. The main benefit of the T8 temper is better 'high' temperature performance than the 7xxx-series alloys, and it has greatly increased stress corrosion and corrosion fatigue performance. However, the artificially aged variant (which starts life as T3) is still very susceptible to corrosion damage. Because of this, it is also vulnerable to fatigue originating from this type of damage. Fortunately, a large number of programs are underway worldwide to find ways to model corrosion damage as an engineering parameter for life prediction. DSTO/AMRL has several programs looking at different types of corrosion damage in various aluminium alloys, to include 2024-T3, 7075-T6, and 7050-T7451. This should provide enough information without starting anything new specifically for the F-111.

The same concerns for SCC in D6ac apply to the aluminium alloys, particularly the 7xxx-T6xx materials. As far as crack growth threshold data are concerned, comparisons with literature data show that the Lockheed values are conservative.

6. Acknowledgments

The authors wish to acknowledge Mr. Harold Chin Quan for use of Appendix I.

7. References

Abelkis, P. (1982) Fatigue Crack Growth Rate Data Sheets on Al Alloys 2024, 7010, 7050, 7075, and 7475, McDonnell Douglas.

ASTM Standard E 647-95a (1995) Standard Test Method for Measurement of Fatigue Crack Growth Rates, American Society for Testing and Materials, Philadelphia.

ASTM Standard G34-90 (1990) Standard Test Method for Exfoliation Susceptibility in 2xxx and 7xxx Series Copper Containing Alloys, American Society for Testing and Materials, Philadelphia.

Athiniotis, N. (1999) Survey of Stress Corrosion Cracking in RAAF Aircraft Components, DSTO-TN-0198.

Ball, D.L. and Doerfler, M.T. (1996) Metallic Material Data for F-111 Durability and Damage Tolerance Analysis, LMTAS Report FZS-12-626.

Bandara, S. and Armitage, R. (2000) F-111 Structural Condition Audit, ER-F111-51-177, Aerostructures.

Bell, R. (1999) Personal conversation, Technical interchange meeting, Wright-Patterson Air Force Base, Ohio, USA.

Bowles, C.Q. and Schijve, J. (1983) Experimental Observations of Environmental Contributions to Fatigue Crack Growth, Corrosion Fatigue: Mechanics, Metallurgy, Electrochemistry, and Engineering, ASTM STP 801, Crooker, T.W. and Leis, B.N., (eds.), American Society for Testing and Materials, 96-114.

Boykett, R. and Walker, K. (1996) F-111C Lower Wing Skin Bonded Composite Repair Substantiation Testing, AMRL Technical Report, DSTO-TR-0480.

Brownhill, D.J. et al. (1970) Mechanical Properties, including Fracture Toughness and Fatigue, Corrosion Characteristics, and Fatigue Crack Propagation Rates of Stress-Relieved Aluminium, AFML-TR-70-10.

Bucci, R. (1982) Fatigue Crack Growth Rate Data Sheets on Aluminium Alloy 7075—Conditions T651, T6510, T7351, T73510, Plates, Bars, and Extrusions.

Buntin, W.D. (1971) Concept and Conduct of Proof Test of F-111 Production Aircraft, Presented to Royal Aeronautical Society, London, England.

Cawthorne, E.W. (1974) B-1 Program da/dN Data for Aluminium Alloys, Rockwell International Corporation.

Chen, G.S., Gao, M., Harlow, D.G., and Wei, R.P. (1994) Corrosion and Corrosion Fatigue of Airframe Aluminium Alloys, NASA Conference Publications 3274 Part I, Harris, C.E. (ed.), FAA/NASA International Symposium on Advanced Structural Integrity Methods for Airframe Durability and Damage Tolerance, 157-173.

Chin Quan, H. (1992) Aircraft Materials and Corrosion Protection Handbook, Defence Instruction (Air Force) AAP 7021.014-2.

Chu, H.C. and Wei, R.P. (1990) Stress Corrosion Cracking of High-Strength Steels in Aqueous Environments, Corrosion 46, (6), 468-476.

Chu, H.P. and Wacker, G.A. (1969) Stress Corrosion Testing of 7079-T6 alloy in Seawater Using Smooth and Precracked Specimens, Transactions of ASME, Series D, Journal of Basic Engineering, Vol. 91, no. 4, 565 – 569.

Clark, G. (1976) Fatigue Crack Growth from Notches, Ph.D Thesis, University of Cambridge, 1976.

Clark, G. and Sharp, P.K. (2000) The Significance of Laminar Corrosion Defects in Aircraft, ICAS 2000 Congress, 446.1-446.7.

Cole, G.K., Clark, G. and Sharp, P.K. (1997) The Implications of Corrosion with respect to Aircraft Structural Integrity, DSTO-RR-0102.

Compilation of ASTM Standard Definitions (1986) , 6th ed., American Society for Testing and Materials, Philadelphia.

Cox, A.. (1985) Fatigue Cracking in the Upper Plate of Wing Pivot Fittings in RAAF F-111 Aircraft, Defect Assessment & Failure Analysis Report (ARL Letter Report No. M34/85).

Cox, A.F., Goldsmith, N.T., Bland, L.M., Glanvill D.W. and Patching, C.A. (1983) Preliminary Investigation into Failure of F-111C A8-129 Wing Pivot Fitting in Cold Proof Load Test, ARL-MAT-TECH-MEMO-383, ARL-STRUC-TECH-MEMO-360.

Feddersen, C.E., Moon, D.P. and Hyler, W.S. (1972) Crack Behaviour in D6ac Steel; An Evaluation of Fracture Mechanics Data for the F-111 Aircraft, MCIC Report number 72-04, ARL Ref. 70908, Damage Tolerance Design Handbook Reference 82543.

Findley M.C. and Sutherland, B.J. (1982) F-111 Structural Integrity Assessment Addressing Royal Australian Air Force (RAAF) Concerns, Engineering Report SM-ALC (MMKR) 82-1.

Gangloff, R.P. and Wei R.P. (1986) Small Crack-Environment Interactions: the Hydrogen Embrittlement Prospective. In: Small Fatigue Cracks, eds. Ricthie, R.O. and Lankford, J., TMS-AIME, 239-264.

Gangloff, R.P. and Duquette, D.J. (1987) Corrosion Fatigue of Metals: a Survey of Recent Advance and Issues, In: Chemistry and Physics of Fracture, eds. Latanision, R.M. and Jones, R.H., Martinus Nijhoff Publishers B.V., 612-645.

Gangloff, R.P. (1990) Corrosion Fatigue Crack Propagation in Metals, NASA Contractor Report N. 4301.

General Dynamics (1968) Wing Carry Through Box Status Report as at 25 Nov. 1968, 68FW290.

General Dynamics (1970) Recovery Program Status Report to SPO, FZM-12-10962.

Grimes, L.R. (1996) A Comparative Study of Corrosion Pit Morphology in 7075-T651 Aluminium, thesis University of Utah.

Gruff, J.J. and Hutcheson, J.G. (1969) Effects of Corrosive Environments on Fatigue Life of Aluminium Alloys under Manoeuvre Spectrum Loading, AFFDL Technical Report 70-144, 521-537.

Gunderson, A.W. (1970) Preliminary Mechanical Property Evaluation of D6ac Steel in Support of the F-111 Recovery Program, Technical Memorandum MAA 70-6, Project No. 7381, Air Force Materials Laboratory, Air Force Systems Command, Wright-Patterson Air Force Base, Ohio.

Gunston, B. (1987) The Great Book of Modern Warplanes, Salamander Books Ltd., 266-238.

Hagemeyer, J.W. and Hillhouse, L. (1970) Environmentally Enhanced Cracking of D6ac Steel, General Dynamics Research & Engineering Dept. Report ERR-FW-1114.

Haigh B. (1917) Experiments on the Fatigue of Brasses, Journal of the Institute of Metals 18, 55-86.

Harmsworth, C.L. (1961) Effect of Corrosion on the Fatigue Behaviour of 2024-T4 Aluminium Alloy, ASD Technical Report 61-121.

Hinders, U.A. (1970) F-111 Design Experience—Use of High-strength Steel, AIAA Paper No. 70-884.

Hoeppner, D.W. (1971) Corrosion Fatigue Considerations in Materials Selections and Engineering Design, Corrosion Fatigue, NACE-2, 3-11.

Hoeppner D.W. (1979) Model for Prediction of Fatigue Lives Based Upon a Pitting Corrosion Fatigue Process, Fatigue Mechanisms, Proceedings of an ASTM-NBS-NSF symposium, Kansas City, Mo., May 1978, Fong, J.T. (ed.), ASTM STP 675, American Society for Testing and Materials, 841-870.

Hoeppner, D.W., Mann, D., and Weekes, J. (1989) Fracture Mechanics Based Modelling of the Corrosion Fatigue Process, AGARD Report No. 316: Corrosion Fatigue.

Hoeppner, D.W., Grimes, L., Hoeppner, A., Ledesma, J., Mills, T. and Shah, A. (1995) Corrosion and Fretting as Critical Aviation Safety Issues: Case Studies, Facts, and Figures from U.S. Aircraft Accidents and Incidents, Presented at the International Committee on Aeronautical Fatigue, Melbourne, Australia.

Holroyd, N.J.H. and Hardie, D. (1983) Factors Controlling Crack Velocity in 7000 Series Aluminium Alloys During Fatigue in an Aggressive Environment, Corrosion Science 23 (6), 527-546.

Hubble, M.J. and Chubb, J.P. (1994) The Effect of Corrosion on Fatigue Crack Initiation in 2024-T3 and 7075-T6 Aluminium Alloys, Cranfield University.

Hudson, C.M. and Newman, J.C. (1973) Effect of Specimen Thickness on FCG Behaviour and Fracture Toughness of 7075-T6 and 7178-T6, NASA TN D-7173.

Hyatt, M.V. (1969) Use of Pre-Cracked Specimens in Stress-Corrosion Testing of High Strength Aluminium Alloys, Boeing Commercial Airplane Group D6-2466.

Jones, D.A. (1992) Principles and Prevention of Corrosion, Macmillan Publishing Company.

Kawai, S. and Kasai, K. (1985) Considerations of Allowable Stress of Corrosion Fatigue, (Focused on the Influence of Pitting), Fatigue of Engineering Materials 8 (2), 115-127.

Kendall, G. (1971) Aerospace Stress Corrosion Program, General Dynamics Report FZM-12-13383.

Komai, K. and Minoshima, K. (1989) Current Status and Future Trends on Environmental Strength of Materials, JSME International Journal 32 (1) (1989) 1-13.

Kondo, Y. (1989) Prediction of Fatigue Crack Initiation Life Based on Pit Growth, Corrosion Science 45, 7-11.

Krupp, W.E., Hoeppner, D.W., and Walker, E.K. (1972) Crack Propagation of Aluminium Alloys is Corrosive Environments, Corrosion Fatigue, NACE-2 468-483.

Krupp, W.E., Wimmer, F.T., Pettit, D.E., and Hoeppner, D.W. (1974) Data Sheets for Final Report on "Investigation of the Effects of Stress and Chemical Environments on the Prediction of Fracture in Aircraft Structural Components, Lockheed.

Laffe and Sutherland, B.J. (1994) F-111 Cold Temperature Proof Testing, Interest Item, Lockheed Memorandum.

Lauchner, E.A. (1971) Preventing Stress Corrosion Cracking in High-Strength Aluminium Forgings, Metals Engineering Quarterly, Vol. 11.

Lindley, T.C., McIntyre, P., and Trant, P.J. (1982) Fatigue Crack Initiation at Corrosion Pits, Metals Technology 9, 135-142.

Little, C.E. (1971) Heat Treatment, Forging and Process requirements, Type D6ac Steel, General Dynamics, FPS -1092D.

Loader, C. (2000) Personal Communication, AMRL.

Loader, C. and Sharp, P.K. (2001) Review of Pitting Corrosion and Pitting Effects on Structural Integrity, DSTO Technical Report, publication pending.

Lynch, S.P. and Ryan, N.E. (1978) Mechanisms of Hydrogen Embrittlement - Crack Growth in a Low Alloy Ultra-High-Strength Steel Under Cyclic and Sustained Stresses in Gaseous Hydrogen, L'Hydrogene Dans Les Metaux, Second International Congress on Hydrogen in Metals, Paris, France.

Ma, L. and Hoeppner, D. W. (1994) The Effects of Pitting on Fatigue Crack Nucleation in 7075-T6 Aluminium Alloy, NASA Conference Publications 3274 Part I, Harris, C.E. (ed.), FAA/NASA International Symposium on Advanced Structural Integrity Methods for Airframe Durability and Damage Tolerance, 425-440.

Mackay, T.L. (1979) Fatigue Crack Propagation Rate at Low DK of Two Aluminium Sheet Alloys, 2024-T3 and 7075-T6, Engineering Fracture Mechanics 11, 753-761.

McAdam, D.J. (1927) Corrosion-Fatigue of Non-Ferrous Metals, Proceedings of the ASTM 27 (2), 102-125.

McHenry, H.I. and Key, R.E. (March 1968) The F-111 Logic: Familiar Materials; Proven Processes, Metal Progress, 62-68.

MCIC-HB-01R (1983) Damage Tolerant Design Handbook, Vol. 4.

MDC-A0913 (1971) Phase B Test Program Report, McDonnell Douglas.

Metals Handbook, 9th ed., Vol. 2 (1979) Properties and Selection: Nonferrous Alloys and Pure Metals, American Society for Metals, Metals Park, Ohio.

Metals Handbook, 9th ed., Vol. 4 (1981) Heat Treating, American Society for Metals, Metals Park, Ohio.

Metals Handbook, 9th ed., Vol. 13 (1985) Corrosion, American Society for Metals, Metals Park, Ohio, 584-609.

Metals Handbook, 9th ed., Vol. 11 (1986) Failure Analysis and Prevention, American Society for Metals, Metals Park, Ohio.

MIL-A-8877A (1965) Military Specification Aluminium Alloy Sheet and Plate, 7079.

Miller, R.N. and Meyer F.H. (1988) Computerised Corrosion Forecasting Model for C-5 Aircraft, Proceedings of the 1987 Aircraft/Engine Structural Integrity Program Conference, 543-564.

Mills, T.B. (1995) The Effects of Exfoliation Corrosion on the Fatigue Response of 7075-T651 Aluminium Plate, thesis University of Utah.

Mills, T.B. (1997) The Combined Effects of Exfoliation Corrosion and Aggressive Chemical Environments on the Fatigue Crack Growth Behaviour in Aluminium Alloy 7075-T651, dissertation University of Utah.

Mills, T.B., Sharp, P.K., Loader, C. (2000) Progress Report to RAAF: Equivalent Initial Flaw Size Distributions for Corrosion Pitting in D6ac Steel, AMRL File Number F111/COR/01.

MIL-PRF-5624S Military Standard JP-4 Fuel.

MIL-T-83133D Military Standard JP-8 Fuel.

Moore, R.R. (1927) Effect of Corrosion Upon the Fatigue Resistance of Thin Duralumin, Proceedings of the ASTM 27 (2), 128-152.

Morrow, J.W. and Hales, G.J. (1973) Fracture Mechanics Volume II, Analysis for Operational Aircraft Operations, FZM-12-13467.

Nankivell, J.F. (1972) An Investigation of Environmental Factors Built into the Humphries Number Four Fatigue Specimen, Metallurgy Report 90.

National Transportation Safety Board, Aloha Airlines (1989), Flight 243, Boeing 737-200, N73711, Near Maui, Hawaii, April 28, 1988, Aircraft Accident Report, NTSB AAR-89/03, Washington D.C.

Newman, J.C.. Jr. (1981) A Crack-Closure Model for Predicting Fatigue Crack Growth under Aircraft Spectrum Loading, Methods and Models for Predicting Fatigue Crack Growth under Random Loading, ASTM STP 748, 53-84.

Nguyen, H.C. (1991) Failure Analysis of F-111E P/N 68-043 Wing Carry-Thru-Box and Upper Plate, General Dynamics Report FZM-12-14705.

Nordmark, G.E., Lifka, B.W., Hunter, M.S. and Kaufman, J.G. (1970) Stress-Corrosion and Corrosion Fatigue Susceptibility of High-Strength Aluminium Alloys, Technical Report AFML-TR-70-259.

Nordquist, F.C. (1971) Convair Stress Corrosion Program, General Dynamics Report FZM-12-13383.

NRL (1968) NRL Progress Report, Washington D.C.

Oehler, A. and Atrens, A. (1996) The Initiation and Propagation of Stress Corrosion Cracking in AISI 4340 and 3.5 Ni-Cr-Mo-V Rotor Steel in Constant Load Tests, Corrosion Science, 38, (7), 1159-1169.

Paris, P.C., Bucci, R.J. and Little, C.E. (1972) Fatigue Crack Propagation of D6ac Steel in Air and Distilled Water, Stress Analysis of Cracks, ASTM STP 513, 196-217.

Parkins R.N. (1988) Localised Corrosion and Crack Initiation, Material Science and Engineering, 143-156.

Pettit, D.E., Ryder J.T., Krupp, W.E., and Hoeppner, D.W. (1974) Investigation of the Effects of Stress and Chemical Environments on the Prediction of Fracture in Aircraft Structural Materials, AFML-TR-74-183.

Piascik, R.S. and Willard, S.A. (1994) The Growth of Small corrosion Fatigue Cracks in Alloy 2024, Fatigue and Fracture of Engineering Materials and Structures, 17 (11), 1247-1259.

Pollock W.J. (1974) The role of Atomic Hydrogen in the Stress-Corrosion Cracking of Two Ultra-High Strength Steels in Gaseous Environments, Note ARL/Met. 102.

Proctor, R.P.M, Paxton, H.W. (1969) Stress Corrosion of Aluminium Alloy 7075-T6512 in Organic Liquids, Journal of Materials, 4 (3), 729-760.

QQ-A-250/4E (1971) Federal Specification Aluminium Alloy 2024, Plate and Sheet.

RAAF (1975) RAAF Engineering Bulletin No. 4.

Redmond, G. (1993) Report on Metallurgical Investigation F-111 Splice PN 12B7928, 501WG/270/A08/MET/I/1 Pt 1.

Romans, H.B. (1969) An Accelerated Laboratory Test to Determine the Exfoliation Corrosion Resistance of Aluminium Alloys, Materials Research and Standards 9 (11), 31.

Russo, S. and Turk, S. and Hinton, B. (2000) Corrosion Rates in the F-111 Aircraft, DSTO-TR-XXXX, publication pending.

Ryan, N.E. (1974) Relationship between Microstructure and Fracture Toughness in D6ac Steel, ARL Metallurgy note 103.

Ryan N.E. (1976) Fatigue-Crack Growth and Fracture in D6ac Steel, Tech. Memo. ARL/MAT. 368.

Shaffer, I.S., Sebastian, J.C., Rosenfeld, M.S., and Ketcham, S.J. (1968) Corrosion and Fatigue Studies of Extruded 7075-T6 Spar Caps, Journal of Materials 3 (2), 400-424.

Sharp, P.K., Mills, T.B., Russo, S.G., Clark, G., Liu, Q. (2000) Effects of Exfoliation Corrosion on the Fatigue Life of Two High-Strength Aluminium Alloys, Proceedings of DoD/FAA/NASA 2000 Ageing Aircraft Conference, St. Louis, Missouri, USA.

Shaw, B.J. (1994) An Artificial Corrosion Protocol for Lap-Splices in Aircraft Skin, FAA/NASA International Symposium on Advanced Structural Integrity Methods for Airframe Durability and Damage Tolerance, NASA Conference Publications 3274, Part 2, 725-739.

Smith, S.H. (1966) Fracture Mechanics Applications to Material Evaluation and Selection for Aircraft Structure and Fracture Analysis, D6-17756, Boeing.

Smith C.R., The Effect of Tapered Bolts on Structural Integrity, Assembly Engineering, paper 1/59.

Smith, B.S., Duxbury, E.J. and Moore, B.T. (1997) Atmospheric Corrosivity of Defence Bases in Northern and Eastern Australia, DSTO Tech. Report DSTO-GD-0123.

Spiedel, M.O. (1979) Stress Corrosion and Corrosion Fatigue Crack Growth in Aluminium Alloys, Stress corrosion Research, Ed. By Arup, H. and Parkins, R.N., NATO Advanced Study Institutes Series, Series E: Applied Science no. 30, 117-176.

Sprowls, D.O., Walsh, J.D., and Shumaker M.B. (1972) Simplified Exfoliation Testing of Aluminium Alloys, Localised Corrosion--Cause of Metal Failure, ASTM STP 516, 38-65.

Sprowls, D.O. et al. (1973), Evaluation of Stress Corrosion Cracking Susceptibility using Fracture Mechanics, Alcoa, Final Report Phase I.

Sprowls, D.O. (1987) Evaluation of Stress Corrosion Cracking, ASM Metals Handbook Vol. 13, 9th ed..

Stanzl, S.E., Mayer, H.R. and Tschegg, E.K. (1991) The Influence of Air Humidity on Near-Threshold Fatigue Crack Growth of 2024-T3 Aluminium Alloy, Material Science and Engineering, A147, 45-54.

Susans, G.R., Patching, C.A., and Beckett, R.C. (1982) Report of the Visit by an Australian Team to the US to Assess the Structural Airworthiness Implications of the Failure of A8-112 During Cold Proof Load Test, AED F-111 Database Reference AF1511/912/100 PT 3.

Sutherland, B.J. F-111 Service Experience—Use of High-strength Steel, Unknown Publication.

Swartz, D.D., Miller, M., and Hoeppner, D.W. (1995) Chemical Environments in Commercial Transport Aircraft and Their Effect on Corrosion Fatigue Crack Propagation, Presented at the International Committee on Aeronautical Fatigue, Melbourne, Australia.

Walker, K. (1999) Investigation of Bonded Repair Feasibility for RAAF F-111 Wings with Outer Lower Wing Skin Fatigue Cracks at Forward Auxiliary Spar Station 281.28, DSTO Letter Report, 20 December.

Wallace, W. and Hoeppner, D.W. (1985) Aircraft Corrosion: Causes and Case Histories, AGARD Corrosion Handbook.

Wanhill, R.J.H. (1988) Low Stress Intensity Fatigue Crack Growth in 2024-T3 and T351, Engineering Fracture Mechanics 30 (2), 233-260.

Wei, R.P. (1979) On Understanding Environment-Enhanced Fatigue Crack Growth-A Fundamental Approach, Fatigue Mechanisms, Proceedings of an ASTM-NBS-NSF symposium, Kansas City, Mo., May 1978, Fong, J.T. (ed.), ASTM STP 675, American Society for Testing and Materials, 816-840.

Wei, R.P. and Shim, G. (1983) Fracture Mechanics and Corrosion Fatigue, Corrosion Fatigue: Mechanics, Metallurgy, Electrochemistry, and Engineering, ASTM STP 801, Crooker, T.W. and Leis, B.N. (eds.), American Society for Testing and Materials, 5-25.
Wei, R.P. and Simmons, G.W. (1981) International Journal of Fracture 17.

Wilson, A.C. (1964) Steel Alloy Selection for F-111: Justification Data for D6ac Steel, FZM-12-408, General Dynamics.

Wilson, L. (1973) The Assessment of the Environment in the Bolt Holes of Australian F-111C Aircraft, ARL Metallurgy Note 92.

Appendix I: Summary of Corrosion Types

The information in this section, except where specifically referenced, is excerpt from *Defence Instruction (Air Force) AAP 7021.014-2: Aircraft Materials and Corrosion Protection Handbook* (1992) by Chin Quan.

As aircraft remain in service for extended periods of time, they are exposed to the effects of environment and repeated loading. The environmental attack may cause break down of the surface protective schemes and result in corrosion and together with the loading cycle may initiate and propagate cracks. However, the environment and loads interact in a very complicated manner, which generally leads to accelerated rates of crack propagation and, eventually, to a premature failure. Figure A1.1 schematically shows the possible interactions between loads and environment. The various damage mechanisms arising from the combined environmental attack and loading conditions are described in more detail in the following sections.

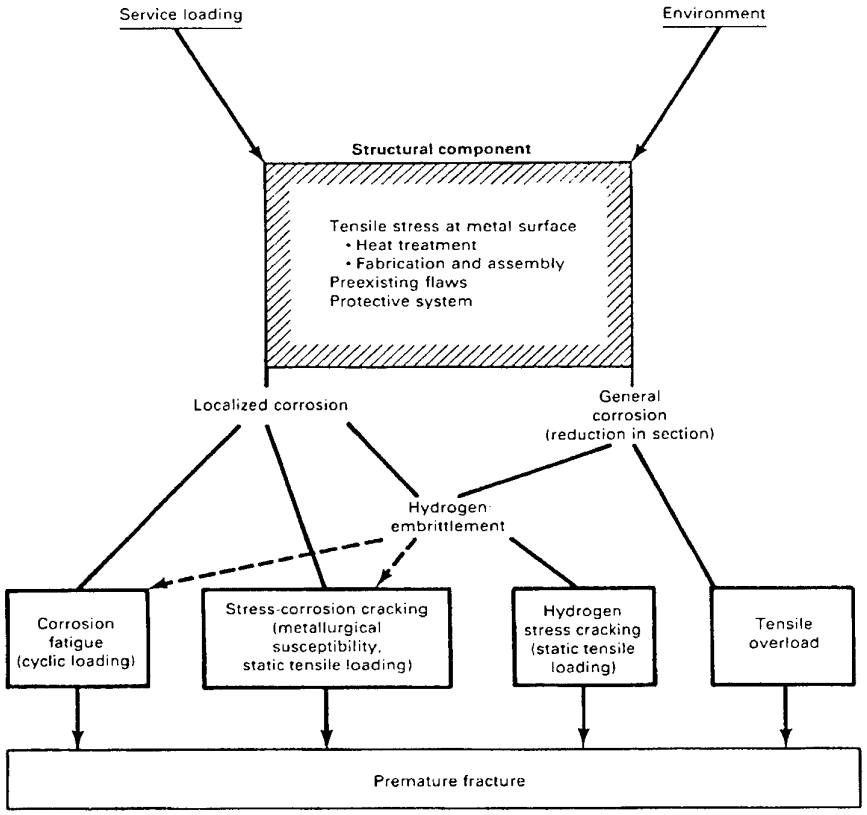

Figure A1.1. Causes of premature fracture influenced by the interaction between corrosive environment and service loading [Sprowls 1987].

Corrosion has several detrimental effects. Due to the loss of material, the load bearing capacities of the structural components are reduced. Corrosion also leads to degradation of the surface, creating stress raisers and potential fatigue crack initiation sites. For structure-critical items all forms of corrosion are initially important, as corrosion processes are complex, with one type frequently leading to another, (Fig. A1.2). The various forms of corrosion encountered in aircraft metallic components are outlined in the following sections.

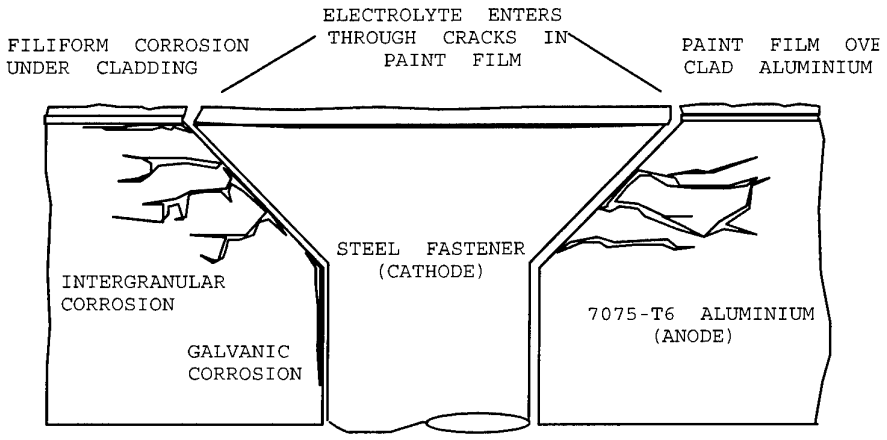

Figure A1.2. An example of possible types of corrosion at fastener locations.

In this section, details of corrosion appearance, corrosion effects on aircraft structure, and alloys, which are susceptible to corrosion, are addressed. This enables a ready comparison to be made of the important characteristics of corrosion types.

General or Surface Corrosion

Early visible signs of light corrosion may be termed general corrosion. General surface corrosion is a fairly uniform attack, which slowly reduces the cross-section of the metal. It may result from direct reaction of a metal surface with water, oxygen or sulphur in the air, e.g., the rusting of iron and steel, or the tarnishing of silver.

Initially, general corrosion appears as an etching of the surface, which becomes dull, rough or possibly frosted or lustreless.

General, or surface corrosion, is the least damaging form of corrosion, and equipment life, when based upon corrosion rates, can be accurately predicted from available data.

Most other forms of corrosion are more difficult to predict and more likely to cause unexpected or premature failure. Long term surface corrosion can develop if unchecked, into other forms of corrosion such as pitting corrosion, so it should be treated as soon as possible.

Aluminium alloys, magnesium alloys and non-stainless steels are susceptible whilst pure aluminium, stainless steel, copper and titanium alloys are generally resistant to surface corrosion.

Pitting Corrosion

Pitting is a form of localised corrosion, which occurs on the surface of metals. The pits may be shallow depressions or deep cavities. In its early stages, pitting may have the appearance of general corrosion. Pitting may be present under white or grey powdery deposits of corrosion product on the metal surface. Tiny holes or pits are seen after clearing the deposit.

Pitting is a particularly insidious and serious form of corrosion as it may lead to the perforation of thin component sections. In thicker sections, corrosion pits may initiate fatigue cracking by providing local stress concentrations.

Susceptible alloys include aluminium and magnesium alloys and stainless steels. Pitting results from localised breakdown of the natural protective surface films on the alloy surface, which can be accelerated in the presence of chloride-containing solutions, such as seawater.

Some causes of film breakdown are:

- Localised impurities in the alloy, which cause flaws in the surface structure and result in rough spots,
- Non-uniform alloy microstructure due to mechanical working or thermal treatment,
- Local contamination of the aircraft surfaces by heavy metal deposits from water or by a highly corrosive fluid, e.g., in a battery stowage area,
- Localised damage in applied protective coatings on highly finished or plated metal surfaces, e.g., electro-plated steels, and
- Accumulation of deposits such as dirt, dust or grease on unprotected metal surfaces.

Intergranular Corrosion

Microscopic corrosion penetration is along the grain boundaries of the metal microstructure. Intergranular corrosion occurs in certain susceptible alloys under highly specific conditions, due to the formation of corrosion cells on a microscopic scale. Metals and alloys have a granular microstructure and during heat-treatment, e.g., annealing, normalising, welding or the effects of heat damage, certain alloying elements may migrate to grain boundaries within the metal. Compounds are formed which differ electrochemically from the subsequent element-depleted regions adjacent to the grain boundaries. The grain boundary precipitate and adjacent element-depleted region usually constitute, respectively, cathodic and anodic areas.

In the presence of an electrolyte, rapid corrosion of the granular metal structure may occur adjacent to the grain boundaries, with relatively little attack within the grains. A less common situation can exist, as in magnesium alloys, where the element-depleted region is cathodic and the interior of grains may be attacked but there is no intergranular attack. This different mechanism is visible under low-power microscopic examination. The appearance of intergranular corrosion may be similar to pitting; however, the visual network of corrosion or surface cracks is accompanied by deep intergranular penetrations. Intergranular corrosion is a very serious form of corrosion; attack can penetrate deeply into the metal with little surface indication of the severity of damage. It is difficult to remove corrosion damage completely and, under conditions of internal or external stress, stress corrosion cracking is likely to occur.

Susceptible alloys are austenitic stainless steels and aluminium alloys containing copper. In some cases, the resistance of these alloys to intergranular corrosion can be increased by appropriate heat treatments.

Exfoliation Corrosion

In this type of corrosion damage, the metal tends to peel off in layers. Exfoliation corrosion is a form of intergranular corrosion specific to alloys with directional grain structures containing flattened elongated grains. Such grain structures, produced during rolling or extruding processes, are typically found in many aluminium alloy aircraft skins, spars and longerons.

The progression of intergranular attack along layered grain boundaries just below the metal surface causes visible bulging due to the force of expanding corrosion products, which occupy more volume than unaffected grain boundaries. This causes the metal to flake, layer and peel off.

High strength aluminium alloys in some heat-treated conditions are susceptible, particularly those with a directional microstructure and exposed end grain. Improper heat-treatment or heat damage, which promotes grain growth, also increases susceptibility.

It is essential to recognise this form of corrosion at an early stage, as extensive corrosion and serious structural weakening may occur before visible corrosion products accumulate at the surface.

Beyond structural weakening, exfoliation can also greatly effect fatigue performance of high strength alloys. Exfoliation, at its mechanical damage roots, is akin to pitting in that it violates surface integrity.

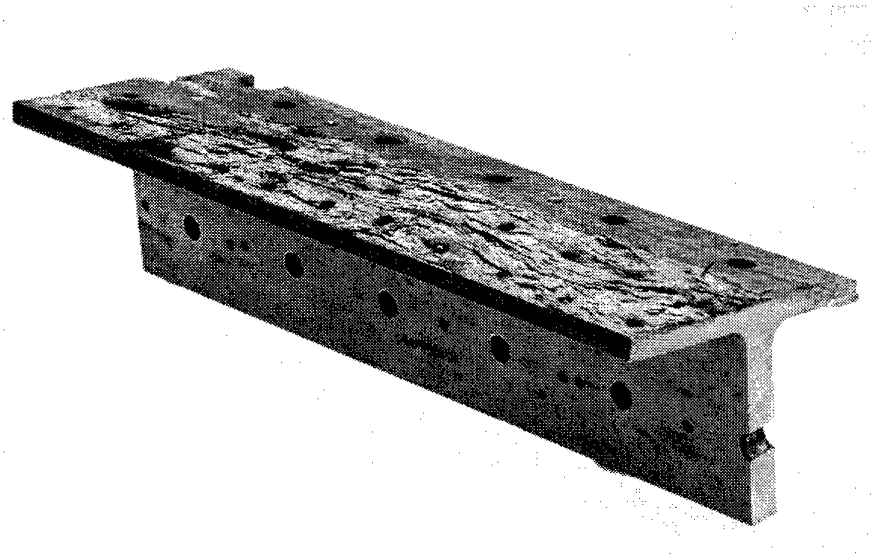

Figure A1.3. Extruded spar cap suffering from exfoliation corrosion on the top surface.

A whole host of projects from research institutions across the globe [Hubble and Chubb 1994, Mills 1995, Sharp *et al.* 2000] including AMRL lend ammunition to this hypothesis. As such, models are being developed to handle exfoliation damage from a fatigue perspective, and not just from a residual strength perspective.

Since the 1940s, several test methods have been developed to evaluate the susceptibility of copper-containing aluminium alloys (such as 2024, 7075, and 7178) to exfoliation corrosion. Because of the success of these test methods, the susceptibility of these alloys to exfoliation corrosion is now well documented, but the literature addressing the potential dangerous effects on structural integrity appears to be deficient.

Crevice Corrosion

Crevices in overlapping joints or around fasteners, or entrapment areas due to poor design or poor drainage, enable entrapped fluids, which form electrolytes, e.g., salt spray, to develop localised corrosion.

Crevice, or concentration-cell, corrosion is a type of pitting caused by variations in the concentration of the electrolytes. The variations can be attributed to the amount of oxygen dissolved in the electrolyte, (Fig. A1.4), or to metal ions, i.e., charged metal atoms (Fig. A1.5). For example, concentrations of electrolyte with a high metal ion content or low oxygen level can cause adjacent metal to become anodic and thus corrode.

Generally, this type of corrosion is not readily apparent as it occurs in concealed areas, in crevices and under faying surfaces. Investigation of crevices, especially near sealants and caulking compounds, surface deposits, scale, entrapped water or cleaning solutions can reveal corrosion products or intensified pitting.

Rates of crevice corrosion vary widely due to local conditions. Surface protective coatings may be significantly damaged causing accelerated corrosion of the underlying structure. Stainless steels and aluminium alloys are highly susceptible to accelerated crevice corrosion, particularly after initial corrosion breakdown of the natural oxide film has taken place.

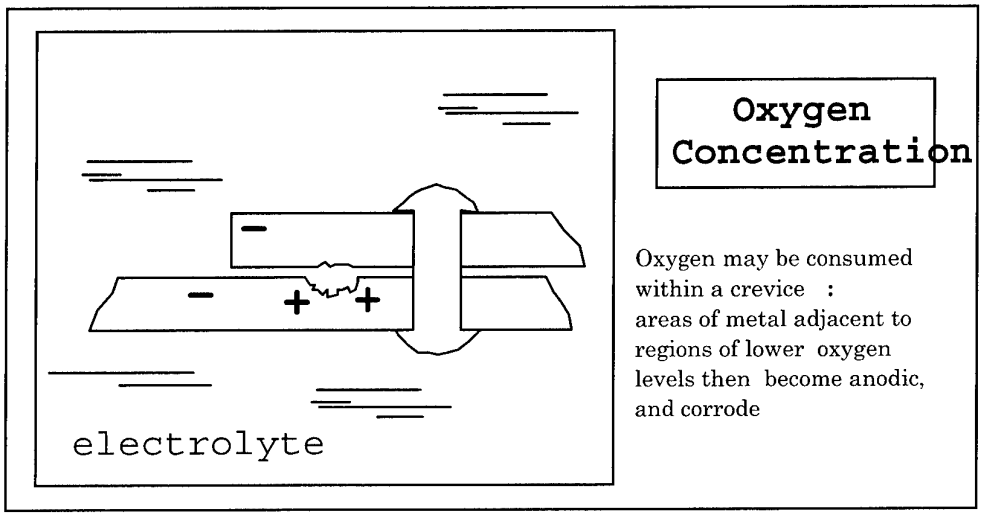

Figure A1.4. Crevice corrosion – internal to a crevice.

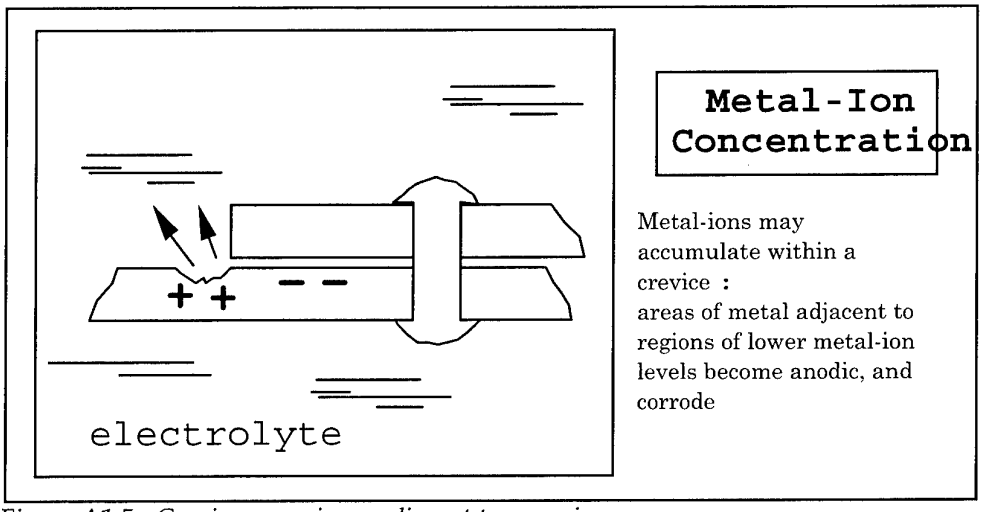

Figure A1.5. Crevice corrosion – adjacent to a crevice.

Filiform Corrosion

Filiform corrosion typically occurs under paint films and is caused by the diffusion of oxygen and water through the coating. The corrosion appears as numerous, meandering, threadlike-filaments. Filiform corrosion is shallow in depth and is not structurally damaging. However, it can be a significant precursor to more serious types of corrosion, e.g., exfoliation or intergranular corrosion.

Filiform corrosion can often occur on aircraft structures particularly around fastener heads where cracks through paint films develop and allow access of moisture. Clad aluminium alloys are highly susceptible particularly where a corrosion pit has penetrated the cladding and, instead of penetrating the core material, the attack spreads parallel to the surface to form the threadlike lines of corrosion. Filiform corrosion also occurs on steel, zinc, magnesium, and chromium-plated nickel.

Galvanic or Dissimilar Metal Corrosion

Galvanic corrosion is the accelerated corrosion of one metal in a corrosive medium due to electrical contact with a dissimilar metal. The corrosion rate is higher than that of the individual metals, when not connected, in the same corrosive medium. Galvanic corrosion is often seen at or near to the junction between two dissimilar metals, with a build-up of corrosion product at the joint. The anodic areas closer to the cathodic areas corrode most rapidly.

Galvanic corrosion may be a problem when fasteners used in a component are higher on the galvanic series, i.e., more anodic, than the component, or when protective metallic coatings such as cadmium on steel develop defects.

The severity of attack varies widely and depends on the electrochemical potential of the two metals, which are represented by the Galvanic Series, (Table A1.1). According to the Series, for any two dissimilar metals, one metal is anodic, i.e., it corrodes, and the other metal is cathodic and is protected. The further apart two metals are listed, the greater the extent of galvanic corrosion.

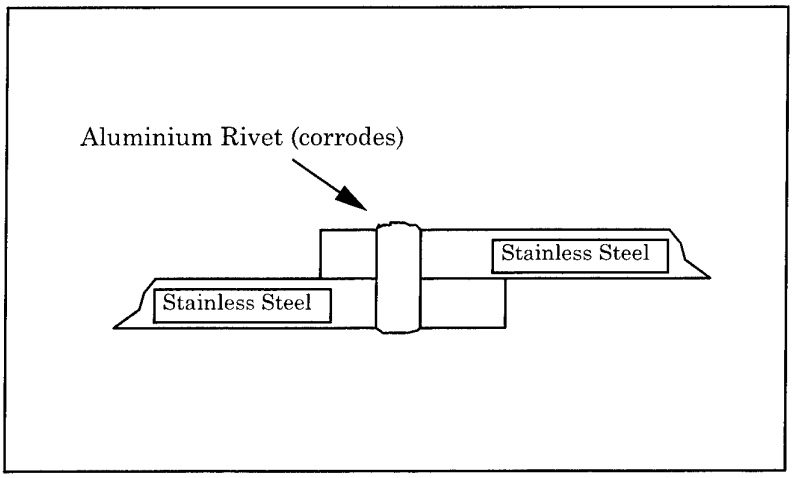

Figure A1.6. Galvanic corrosion – when the the anode area is much smaller than the cathode, the anode is rapidly attacked.

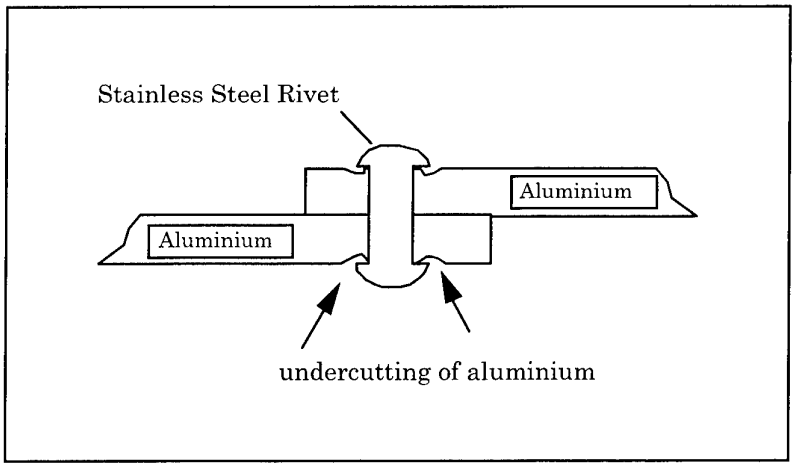

Figure A1.7. Galvanic corrosion – when the anodic material is has much greater area than the cathode, the attack to the anode is slower.

Table A1.1. Galvanic series for metals and alloys in seawater.

Anodic (most active)—corrodes	
GROUP 1	(Group 3 cont. from LH column)
Magnesium	Stainless steel 410 (passive)
Magnesium alloys	Stainless steel 17-7PH (active)
Zinc (plated)	Brasses
Al alloy 5052-0	Nickel-silver (18% Ni)
Al alloy 1100-0	Tin (plated)
Al alloy 6061-T6	Bronzes
Alclad	Stainless steel 347 (active)
Cadmium (plated)	Stainless steel 321 (active)
GROUP 2	Stainless steel 316 (active)
Al alloy 7075-T6	**GROUP 4**
Al alloy 2024-T4	Nickel alloys
Carbon/Low alloy steel	Stainless steel 17-7PH (passive)
Wrought iron	Stainless steel 304 (passive)
Cast iron	Stainless steel 347 (passive)
Stainless steel 430 (active)	Stainless steel 321 (passive)
Stainless steel 410 (active)	A286 (active)
Tin-lead solder	Stainless steel 316 (passive)
GROUP 3	A286 (passive)
Copper (plated, wrought cast)	**GROUP 5**
Nickel (plated)	Titanium Alloys
Stainless steel 304 (active)	Silver
Stainless steel 430 (passive)	Gold
	Graphite
(Group 3 Cont. RH Column)	Cathodic (least active)--protected

Division into five groups has simplified the Galvanic Series. Metal couples within one group are compatible, i.e., corrosion and/or protection effects are negligible. Couples from adjacent groups are less compatible and will require protection, such as coatings, whilst couples from widely separated groups should be avoided.

Stress Corrosion Cracking

Wallace and Hoeppner (1985) share that at one point in history, 90% of aluminium alloy stress corrosion failures could be traced to 2024-T3, 7075-T6, and 7079-T6. Do not let this estimate undermine the susceptibility of high-strength steels to stress-corrosion cracking. It merely represents the higher percentage of use of aluminium alloys in the aircraft industry.

Stress-corrosion cracking (SCC) is a synergism of three factors. If any factor is absent, so is SCC. The first ingredient is a (1) susceptible alloy, which in turn must be exposed to a (2) corrosive environment whilst (3) being held under tension at the same time.

SCC prevention and control is horribly problematic because it is often too difficult to control even one of the three factors. In aircraft sustainment, we are often forced to live with material choices made decades ago—decisions made largely on static strength margins.

To replace a susceptible part with a more corrosion resistant material is not always possible because the new material may not meet strength requirements, or in order to meet strength requirements, the component might need a major redesign. In short, somebody not only has to approve the substitution, they have to pay for this potentially very expensive option.

It is seldom possible to eliminate the environment responsible for a particular SCC problem. Instead, isolating the environment from the material may work by using traditional mitigation techniques such as maintenance of protective coatings and application of corrosion-inhibiting compounds.

The final factor, the sustained tensile stress, is typically the most difficult to control, or for that matter, to quantify. In some cases, the stress may be an externally applied service stress. Worse yet, the stress may be assembly induced through variations in tolerance, both machining tolerances and the tolerance of the person who had to assemble a bunch of components that did not quite fit at the time. Stresses may be internal as well, such as from unequal cooling rates from high temperature, non-uniform deformation during cold working; or neglect of post-weld stress relief.

Stress-corrosion cracking in metals originates at the surface. The cracking is often tight and difficult to detect, and though often intergranular, the cracking may also be transgranular with respect to the alloy microstructure. Development is characterised by a slow nucleation period, with protective film breakdown and the formation of a

stress-concentrating pit, prior to crack growth. SCC appearance is also often branching in nature.

As with fatigue, The total life to failure of a metal by SCC increases as the stress is reduced, and there is a minimum stress below which stress-corrosion cracking does not occur. These thresholds can change significantly depending on the environment. High strength aluminium alloys, high strength steels, and magnesium alloys undergo SCC in diverse environments such as seawater, moist air, organic solvents and acids. An appropriate heat-treatment process can significantly reduce the susceptibility of an alloy to SCC, as discussed in a later chapter.

Before moving on to other failure modes, it is interesting to note the relationship between stress corrosion cracking and intergranular attack. Intergranular attack has long been recognised as a precursor to stress corrosion cracking susceptibility in high-strength alloys, as stress corrosion cracks often propagated along grain boundaries. Artificially aged materials are particularly susceptible. For example, the expanded use of alloy 7075-T6 from sheet to heavy product forms, such as thick plate, extrusions, and forgings, saw the number of stress corrosion failures increase dramatically [ASM Handbook, Vol. 13 1985]. A recent finding by Lockheed showed that number of stress corrosion problems on an airframe correlated nicely with the number of pounds of 7075-T6 used in its construction [Bell 1999]. While this may sound anecdotal, it also happens to be accurate.

Because of the link between intergranular attack and SCC, researchers have developed methods to determine the susceptibility of high-strength aluminium alloys to intergranular attack, particularly exfoliation [Sprowls *et al.* 1972, Romans 1969]. One of the more successful methods, the EXCO test, was later adopted into *'ASTM Standard G34-72, Standard Test Method for Exfoliation Susceptibility in 7xxx-Series Copper Containing Alloys,'* later *'G34-90'* [ASTM G34 1990].

Corrosion Fatigue

Corrosion fatigue is so important to high strength materials it warrants a special discussion. Therefore, most of the information is located in later sections of this report dealing with specific materials. For now, the discussion is general and limited to some definitions.

The first definition is quoted from the *'Compilation of ASTM Standard Definitions'* (1986). The other definitions are non-standard.

Corrosion fatigue--the process in which a metal fractures prematurely under conditions of simultaneous corrosion and repeated cyclic loading at lower stress levels or fewer cycles than would be required in the absence of the corrosive environment.

Corrosion nucleated fatigue--the process in which physical corrosion damage (e.g., exfoliation, pitting) and/or chemical damage (e.g., embrittlement) accelerates the *formation* of fatigue cracks in a component or structure.

Prior-corrosion fatigue--occurs when a propagating fatigue crack encounters a prior-corroded region. A propagating fatigue crack in a prior-corroded region may be propagating by *corrosion fatigue* if an aggressive chemical environment is present and assists in further altering crack propagation in a synergistic manner.

Corrosion-induced fatigue via load transfer--occurs when corrosion damage or environmental degradation in a structure causes load to be transferred to nearby structure. The increased stresses or strains associated with the transfer may promote fatigue cracking.

The concepts surrounding this last definition may seem obscure, but the review of case studies, such as the Aloha accident [NTSB 1989], provide a good example of this failure mode.

The corrosion fatigue discussions in later chapters will focus on the mechanisms captured by the first three definitions.

Hydrogen Embrittlement

Hydrogen embrittlement is caused by the diffusion of hydrogen atoms into steel. The hydrogen assists in the formation of micro-cracks, and eventually to macroscopic, i.e., visible to the naked eye, cracking to rupture the steel. Atomic hydrogen may be introduced in a number of ways, namely:

- during steel melting or mill processes;
- as products of corrosion reactions; and
- during standard surface protective treatments, e.g., pickling, cleaning, electroplating processes or paint stripping.

Hydrogen embrittlement-cracking is difficult to detect, or even to identify as hydrogen embrittlement, without some knowledge of the previous processing history of the component.

Hydrogen embrittlement is extremely significant in relation to high-strength steels. The steels may suffer severe loss of ductility, toughness and strength resulting in fracture with very little warning, i.e., delayed failure. Ultra high-strength steels, such as D6ac, with tensile strengths above 180 000 psi (1240 MPa) are highly susceptible to hydrogen embrittlement (susceptibility of steels to hydrogen embrittlement increases with tensile strength).

Baking treatments, e.g., a minimum of six hours at 190-200°C, are required to remove any absorbed hydrogen. Longer baking times, up to 24 hours, are necessary for higher strength steels and thicker section sizes.

Appendix II: Data Representation

The crack growth rate data were scanned using software called DataThief from graphs contained in various sources. Feddersen et al. (1972) also provided all the raw data from which they calculated the rate of crack growth and stress intensity range, and the relevant equations. The accuracy of scanning of the data was determined by repeating Fedderesen's calculations and superimposing the data from the calculation onto the scanned data. The results are presented in Figure A2.1. There is very little difference between the individual scanned and calculated data points, and the scanning method provides a fast and convenient method to convert "paper copy" into electronic format. The missing data points from the scanned plot could not be imported into the software due to poor quality of the original.

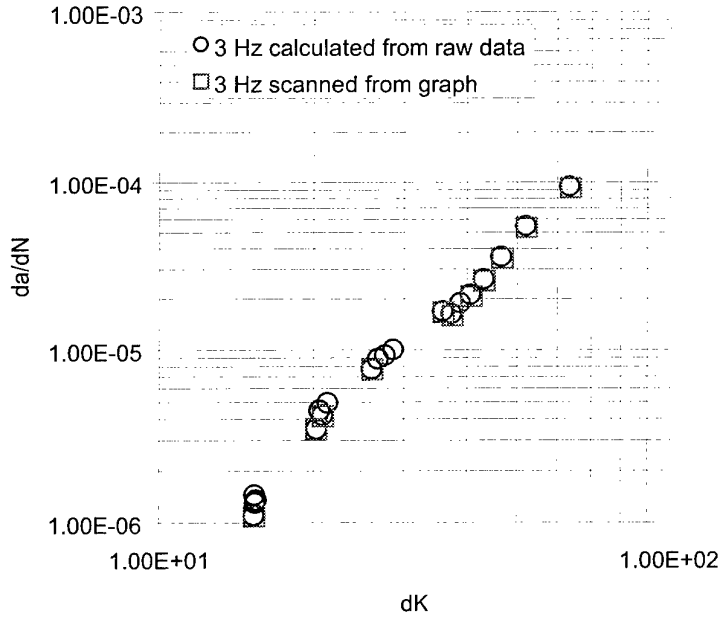

Figure A2.1. Comparison between scanned and calculated data points.

Appendix III: Changes in Stress Intensity Calculation

Most of the crack propagation data was determined in the early 1970s. However, the standard that Feddersen et al. (1972) used to calculate the stress intensity range is different from the standard in use today and the old standard yields somewhat different values than would be obtained today. Unfortunately, other publications do not list the standard or equations that were used in determining the stress intensity ranges, neither they include the raw data used in the calculation. Feddersen et al. (1972) used ASTM Standard E399-70T to calculate the stress intensity range for compact tension specimens, and the equation they used is listed below:

$$K = \frac{P}{BW^{1/2}}\left[29.6(a/W)^{1/2} - 185.5(a/W)^{3/2} + 655.7(a/W)^{5/2} - 1017.0(a/W)^{7/2} + 638.9(a/W)^{9/2}\right]$$

The present equation for stress intensity factors in compact tension specimens according to ASTM E647-95a (1995) is:

$$K = \frac{\Delta P}{B\sqrt{W}}\frac{2+\alpha}{(1-\alpha)^{3/2}}(0.886 + 4.64\alpha - 13.32\alpha^2 + 14.72\alpha^3 - 5.6\alpha^4)$$

These two equations yield different ΔK values when the same values are used. The results from these two equations are plotted in Figure A3.1. The data is for a constant amplitude test in desiccated air at frequency of three Hz and a compact tension specimen. The original equation predicts greater slope in the da/dN *versus* ΔK plot, and hence predicts faster rate of growth than would be calculated today.

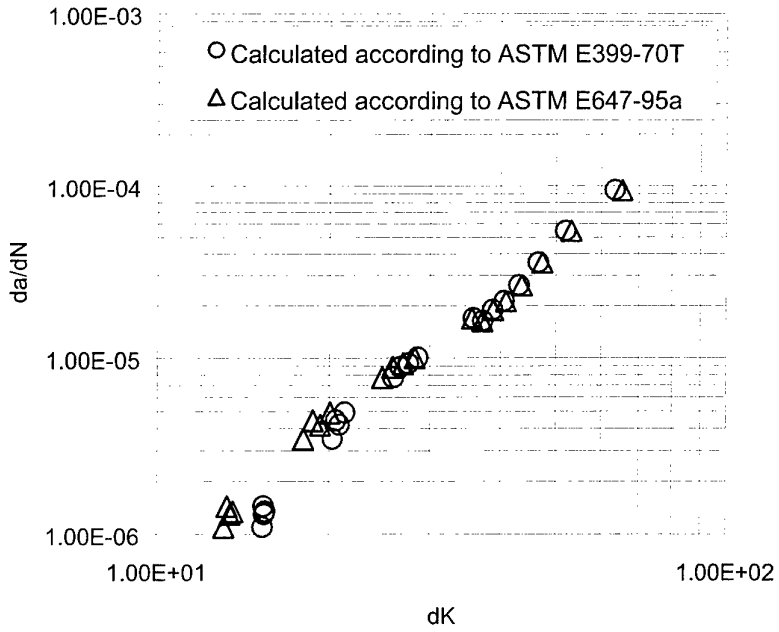

Figure A3.1. Comparison of ΔK calculated according to ASTM E399-T70 (from 1970) and E647-95a (present).

Appendix IV: Corrosion Environment at RAAF Amberley

Smith, Duxbury and Moore (1997) compared the corrosivity of the environment on a number of RAAF bases over a four-year period. Amberley air base, whose climate was classified as 'inland subtropical,' was included in the comparison. Copper-steel, Zinc, and 2090-T8E41 and 7075-T6 aluminium alloys were exposed to the environment during the trial. The copper-steel, Zinc and 7075 had a low corrosivity in the Amberley environment when examined according to ISO 9223 Standard. The 2090 alloy, which is an Al-Li alloy, had a high corrosivity. The average corrosion rates of the four materials examined are listed in Table 13.

Table A4.1. Average corrosion rates at the RAAF Air Base in Amberley [Smith et al. 1997].

Material	Ave. 4 Year Corr. Rate (μm)	Ave. 1 Year Corr. Rate(μm)
Copper-Steel	5.6	9.9
Zinc	0.22	0.23
7075-T6	0.11	0.16
2090-T8E41	0.3	0.9

Operational Environment

The F-111s flying missions around Amberley air base are exposed to the environment described in the previous section. The F-111s are occasionally flown from bases in the far north, where they are exposed to a tropical environment, which is more corrosive than the Amberley environment.

Furthermore, a certain percentage of the missions is flown at low altitudes above the ocean or along the coastline, where the aircraft is exposed to a marine environment. The maritime strike and reconnaissance role of the F-111 means it spends a fair amount of time over water, with up to 40% of the flying hours for the F-111C being dedicated to maritime mission types. Mission profiles for such a sortie, however, do not see the aircraft operating at low altitudes for extremely long periods of time, when the impact of chemical environment would be most severe (Russo, Turk, and Hinton 2000).

Fuel

Many of the D6ac components on the F-111 serve as fuel tanks or fuel flow conduits, where the fuel may come into a contact with the steel, especially if the protective coatings applied to the D6ac break down. Therefore, the fuel with its composition, additives and contaminants (especially water) provides yet another environment the steel is exposed to. USAF initially used JP-4 fuel [MIL-PRF-5624S] in their F-111 aircraft, and most of the initial corrosion fatigue testing in a water saturated fuel

environment was performed with this fuel. However, RAAF presently uses kerosene type JP-8 fuel [MIL-T-83133D] instead of the gasoline type JP-4 fuel, which has a different composition including different additives and inhibitors.

DISTRIBUTION LIST

Review of F-111 Structural Materials

T. Mills, G. Clark, C. Loader, P.K. Sharp and R. Schmidt

AUSTRALIA

DEFENCE ORGANISATION

Task Sponsor

ASI2-DGTA, SQNLDR P. Connor
ASI2D-DGTA, FLTLT J. Davern
CENGR-SRLMSQN, WGCDR M. Benfer

S&T Program

Chief Defence Scientist
FAS Science Policy
AS Science Corporate Management
} shared copy
Director General Science Policy Development
Counsellor Defence Science, London (Doc Data Sheet)
Counsellor Defence Science, Washington (Doc Data Sheet)
Scientific Adviser to MRDC Thailand (Doc Data Sheet)
Scientific Adviser Policy and Command
Navy Scientific Adviser (Doc Data Sheet and distribution list only)
Scientific Adviser - Army (Doc Data Sheet and distribution list only)
Air Force Scientific Adviser
Director Trials

Aeronautical and Maritime Research Laboratory

Director
Chief of Airframes & Engines Division
Research Leader (A.A. Baker)
K.C. Watters (AED)
Authors: T. Mills (Aerostructures Technologies, Pty., Ltd.)
G. Clark (AED)
P. K. Sharp (AED)
C. Loader (AED)
K. Walker (AED)
T. Van Blaricum (AED)
G. Swanton (AED)
R. Braemar (AED)
R. Chester (AED)
P. Callus (AED)

DSTO Library and Archives

Library Fishermans Bend (Doc Data Sheet)
Library Maribyrnong (Doc Data Sheet)
Library Salisbury
Australian Archives
Library, MOD, Pyrmont (Doc Data sheet only)
US Defense Technical Information Center, 2 copies
UK Defence Research Information Centre, 2 copies
Canada Defence Scientific Information Service, 1 copy
NZ Defence Information Centre, 1 copy
National Library of Australia, 1 copy

Capability Systems Staff

Director General Maritime Development (Doc Data Sheet only)
Director General Aerospace Development

Knowledge Staff

Director General Command, Control, Communications and Computers (DGC4) (Doc Data Sheet only)
Director General Intelligence, Surveillance, Reconnaissance, And Electronic Warfare (Dgisrew)R1-3-A142 Canberra Act 2600 (Doc Data Sheet Only)
Director General Defence Knowledge Improvement Team (Dgdknit) R1-5-A165, Canberra Act 2600 (Doc Data Sheet Only)

Army

STUART SCHNAARS, ABCA STANDARDISATION OFFICER, TOBRUCK BARRACKS, PUCKAPUNYAL, 3662(4 COPIES)
SO (Science), Deployable Joint Force Headquarters (DJFHQ) (L), MILPO Gallipoli Barracks, Enoggera QLD 4052 (Doc Data Sheet only)
NPOC QWG Engineer NBCD Combat Development Wing, Tobruk Barracks, Puckapunyal, 3662 (Doc Data Sheet relating to NBCD matters only)

Intelligence Program

DGSTA Defence Intelligence Organisation
Manager, Information Centre, Defence Intelligence Organisation

Corporate Support Program

Library Manager, DLS-Canberra

Aerostructures Technologies, Pty., Ltd.

R. Armitage, Manager AMRL

UNIVERSITIES AND COLLEGES

Australian Defence Force Academy
Library
Head of Aerospace and Mechanical Engineering
Serials Section (M list), Deakin University Library, Geelong, 3217

Hargrave Library, Monash University (Doc Data Sheet only)
Librarian, Flinders University

OTHER ORGANISATIONS
NASA (Canberra)
AusInfo

OUTSIDE AUSTRALIA

ABSTRACTING AND INFORMATION ORGANISATIONS
Library, Chemical Abstracts Reference Service
Engineering Societies Library, US
Materials Information, Cambridge Scientific Abstracts, US
Documents Librarian, The Center for Research Libraries, US

INFORMATION EXCHANGE AGREEMENT PARTNERS
Acquisitions Unit, Science Reference and Information Service, UK
Library - Exchange Desk, National Institute of Standards and Technology, US
National Aerospace Laboratory, Japan (
National Aerospace Laboratory, Netherlands

SPARES (5 copies)

Total number of copies: **60**

DEFENCE SCIENCE AND TECHNOLOGY ORGANISATION
DOCUMENT CONTROL DATA

1. PRIVACY MARKING/CAVEAT (OF DOCUMENT)

2. TITLE

Review of F-111 Structural Materials

3. SECURITY CLASSIFICATION (FOR UNCLASSIFIED REPORTS THAT ARE LIMITED RELEASE USE (L) NEXT TO DOCUMENT CLASSIFICATION)

Document (U)
Title (U)
Abstract (U)

4. AUTHOR(S)

T. Mills, G. Clark, C. Loader, P.K. Sharp, and R. Schmidt.

5. CORPORATE AUTHOR

Aeronautical and Maritime Research Laboratory
506 Lorimer St
Fishermans Bend Vic 3207 Australia

6a. DSTO NUMBER	6b. AR NUMBER	6c. TYPE OF REPORT	7. DOCUMENT DATE
DSTO-TR-1118	AR-011-800	Technical Report	March 2001

8. FILE NUMBER	9. TASK NUMBER	10. TASK SPONSOR	11. NO. OF PAGES	12. NO. OF REFERENCES
M1/9/786	AIR 00/139 A20926	RAAF ASI2-DGTA	114	123

13. URL on the World Wide Web

http://www.dsto.defence.gov.au/corporate/reports/DSTO-TR-1118.pdf

14. RELEASE AUTHORITY

Chief, Airframes and Engines Division

15. SECONDARY RELEASE STATEMENT OF THIS DOCUMENT

Approved for public release

OVERSEAS ENQUIRIES OUTSIDE STATED LIMITATIONS SHOULD BE REFERRED THROUGH DOCUMENT EXCHANGE, PO BOX 1500, SALISBURY, SA 5108

16. DELIBERATE ANNOUNCEMENT

No Limitations

17. CASUAL ANNOUNCEMENT Yes

18. DEFTEST DESCRIPTORS

F-111, material, fatigue crack growth, corrosion

19. ABSTRACT

The RAAF is now the sole operator of the F-111 and current plans for the fleet will keep the aircraft in service until 2020. The F-111 is a structurally complex aircraft, and its swing-wing geometry in particular requires materials of ultra high strength to handle expected loadings. In particular, the D6ac steel used in most of the critical components in the aircraft was subjected to rigorous research efforts in the early 1970s to better characterise material performance in fatigue. This report summarises many of these efforts to characterise the main alloys in the airframe, namely: D6ac steel and aluminium alloys 2024-T851, 7079-T651, and 7075-T6. The major goal is to study the available data for these critical F-111 materials, evaluate the completeness of the existing data sets and make recommendations for research efforts necessary to ensure that the F-111 fleet is operated as safely and economically as possible until retired. Particular attention is payed to the fact that the RAAF now uses JP-8 fuel rather than the original JP-4 fuel. Short crack behaviour from corrosion damage will likely be a concern for the F-111, particularly in the D6ac steel. Stress corrosion cracking is likely to continue to be the biggest problem for the 7xxx-series aluminium alloy components and will have to be monitored carefully.

DEPARTMENT OF DEFENCE
DEFENCE SCIENCE & TECHNOLOGY ORGANISATION
DSTO
AERONAUTICAL AND MARITIME RESEARCH LABORATORY
506 LORIMER STREET FISHERMANS BEND VICTORIA 3207 AUSTRALIA
TELEPHONE (03) 9626 7000